Targeted diagnostics and therapy in salivary gland adenoid cystic carcinoma

Thomas J.W. Klein Nulent

Targeted diagnostics and therapy in salivary gland adenoid cystic carcinoma

Thomas J.W. Klein Nulent

Targeted diagnostics and therapy in salivary gland adenoid cystic carcinoma
PhD thesis, Utrecht University, The Netherlands

ISBN: 978-94-6473-778-3
Cover based on a design & layout by: Esther Beekman (www.estherontwerpt.nl)
Printed by: Ipskamp printing

The research presented in this thesis was conducted at:

- University Medical Center Utrecht, Utrecht, The Netherlands
  Departments of Head and Neck Surgical Oncology, Oral and Maxillofacial Surgery, Pathology, Medical Oncology, and Radiology & Nuclear Medicine
- Netherlands Cancer Institute/Antoni van Leeuwenhoek, Amsterdam, The Netherlands
  Departments of Head and Neck Oncology and Surgery, Pathology, Radiation Oncology, and Nuclear Medicine

Financial support for the printing and distribution of this thesis was kindly provided by: Koninklijke Nederlandse Maatschappij tot bevordering der Tandheelkunde (KNMT); Nederlandse Vereniging voor Mondziekten, Kaak- en Aangezichtschirurgie (NVMKA); Utrechtse Stichting tot Bevordering der Mondziekten, Kaak- en Aangezichtschirurgie; Haaglanden Medisch Centrum; Haaglanden Clinics; Universitair Medisch Centrum Utrecht; ChipSoft; Dent-Med Materials; Dentsply Sirona; MedicoCare; Straumann.

Targeted diagnostics and therapy in salivary gland adenoid cystic carcinoma

Doelgerichte diagnostiek en therapie voor adenoïd cysteus carcinoom van de speekselklieren

(met een samenvatting in het Nederlands)

PROEFSCHRIFT

ter verkrijging van de graad van doctor aan de
Universiteit Utrecht
op gezag van de
rector magnificus, prof. dr. ir. W. Hazeleger,
ingevolge het besluit van het College voor Promoties
in het openbaar te verdedigen op

donderdag 26 juni 2025 des middags te 2.15 uur

door

Thomas Johannes Willem Klein Nulent

geboren op 19 oktober 1984
te Rotterdam

Promotoren:
Prof. dr. R. de Bree
Prof. dr. S.M. Willems

Copromotoren:
Dr. R.J.J. van Es
Dr. B. de Keizer

Beoordelingscommissie:
Prof. dr. P.J. van Diest (voorzitter)
Prof. dr. C.M.L. van Herpen
Prof. dr. B.F.A.M. van der Laan
Prof. dr. M.G.E.H. Lam
Prof. dr. A.J.W.P. Rosenberg

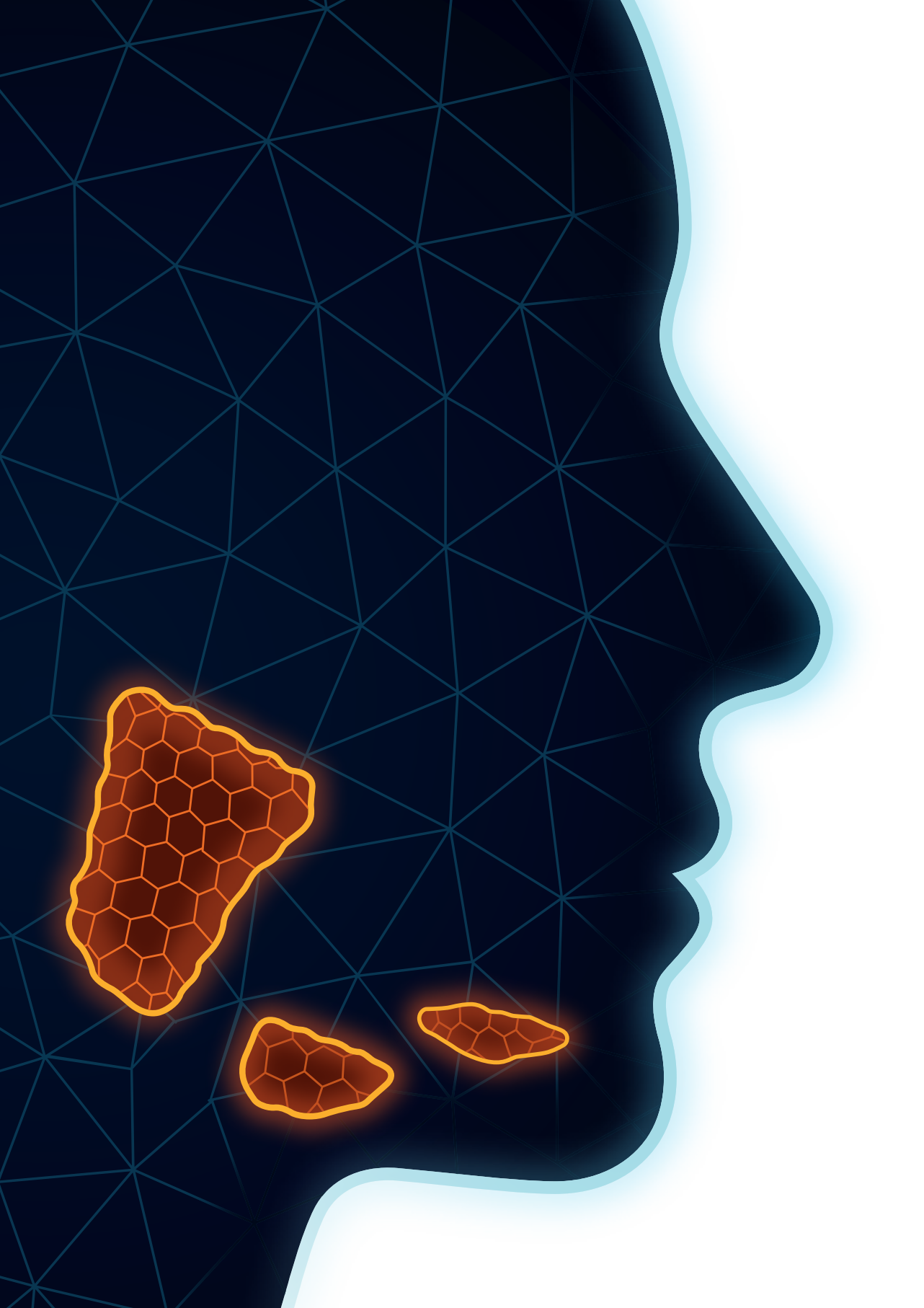

CONTENTS

General introduction, aims and thesis outline

Adenoid cystic carcinoma (AdCC) is one of the most malignant salivary gland cancers due to its aggressive nature and complex treatment aspects. It poses significant challenges not only in diagnosis but also in its (long-term) management, requiring new advances in diagnostics and therapy.[1–5] This thesis aims to address these challenges by focusing on three areas: **biomarkers**, **targeted diagnostics**, and **targeted therapy**.

SALIVARY GLAND TUMOURS

Malignancies of the head and neck originate in the oral cavity, pharynx, larynx, nasal cavity, paranasal sinuses, as well as in the salivary, seromucous, and lacrimal glands. The most common type of head and neck cancer is squamous cell carcinoma, which accounts for approximately 90% of all cases.[6] Salivary gland cancers are a heterogeneous group of neoplasms arising from the epithelial tissues of the salivary glands, including the major glands (parotid, submandibular, sublingual) and the minor salivary and seromucous glands dispersed throughout the upper aerodigestive tract. These represent about 3–10% of all head and neck cancers.[7]

Salivary gland cancer incidence is estimated around 1–2 per 100,000 inhabitants annually. These tumours are known for their histopathological diversity and unpredictable clinical behaviour, posing critical diagnostic and therapeutic challenges. They range from benign lesions to various malignant types, each requiring a tailored approach based on the specific characteristics of the tumour.[5,7,8] The most common malignant salivary gland tumour is mucoepidermoid carcinoma, followed by AdCC and adenocarcinoma, not otherwise specified. Mucoepidermoid carcinoma comprises approximately one-third of all salivary gland tumours. It consists of mucous-secreting, intermediate, and epidermoid (squamous) cells, with grades ranging from low to high. Low-grade tumours typically have a favourable prognosis, whereas high-grade tumours are more aggressive and prone to metastasis. The third-largest group, comprising 10–15% of the salivary gland tumours, includes a diverse range that does not fit into other specific histological types and is classified as adenocarcinoma, not otherwise specified. These tumours vary widely in behaviour and prognosis.[5,7]

ADENOID CYSTIC CARCINOMA

Adenoid cystic carcinoma (AdCC) accounts for approximately 20–35% of all malignant salivary gland tumours, with an annual incidence of 2 to 3 cases per 1,000,000 inhabitants. The incidence peaks in the fifth and sixth decades of life, though it can occur across all age groups, with a slight predominance in women. After initial treatment, patients with advanced disease often face locoregional recurrence, which is challenging to manage due to prior surgical interventions and radiotherapy limitations. Additionally, up to 40% of the patients develop slowly progressing pulmonary or osseous metastases within five years of diagnosis. Poor prognostic factors include advanced tumour stage, origin from minor salivary glands, inadequate surgical margins, a solid growth pattern, and (peri)neural invasion.[1–3,5,9,10]

Diagnosing AdCC involves a multifaceted approach that combines clinical evaluation, histopathological examination and imaging. AdCC is identified by its distinctive tubular, cribriform and solid growth patterns on histopathology, which reflect a degree of differentiation and crucial for determining tumour prognosis. Tubular growth (Perzin grade 1) is the best differentiated, characterized by small nests of cells surrounding well-formed lumens, and is linked to a favourable prognosis, slow progression, and few recurrences. The cribriform pattern (Perzin grade 2) shows moderate differentiation, with cells arranged in a mesh-like structure, and carries an intermediate prognosis. Solid tumours (Perzin grade 3) are the least differentiated, lacking lumens, and demonstrate aggressive growth. When more than 30% of the tumour is solid, it is linked to poor outcome in terms of disease recurrence, metastasis, and survival.[11,12] Due to its complex presentation, molecular diagnostics play an increasingly important role by the identification of specific genetic alterations, such as the *MYB::NFIB* fusion which is found in approximately half of AdCC cases.[1,13] In recurrent or metastatic AdCC, the *NOTCH1* gene is predominantly mutated, with an incidence of 26.3%, compared to 8.5% in non-recurrent tumours. *NOTCH1* plays a role in regulating cell differentiation, proliferation, and apoptosis, and its mutation is associated with a solid growth pattern.[14,15]

MRI and CT scans are crucial for determining the (locoregional) extent of the disease and its anatomical alignment, while PET/CT scans, particularly with fluorodeoxyglucose (FDG), play a vital role in detecting distant metastases. Because AdCC typically exhibits lower FDG uptake in relation to other epithelial tumours, the assessment of suspected locoregional recurrence and/or metastatic disease may be complicated.[16,17] Therefore, there is a need to develop new targeted imaging modalities with high sensitivity to better map and evaluate these sites.

The primary treatment for AdCC involves surgical resection with the aim of achieving clear margins, often followed by radiation therapy to manage residual microscopic disease and reduce the risk of local recurrence. However, the invasive nature of AdCC and especially its tendency for extensive perineural invasion, makes achieving clear margins challenging.[1,2] Chemotherapy is generally reserved for cases of unresectable or metastatic disease, though its efficacy in boosting survival remains limited. Similarly, recent developments in targeted therapies, immunotherapy, and hormonal therapies offer new treatment possibilities, but their benefits may be restricted to a subset of patients. These approaches require further clinical validation to determine their efficacy and potential role in the management of AdCC.[8,18,19] Nevertheless, survival rates have shown significant progress over the past decades, with existing management strategies contributing to meaningful gains in patient outcomes. Locoregional control rates have advanced from approximately 36% to over 80% at 5 years, and from 25% to nearly 60% at 10 years. Disease-free survival has improved from around 31% to more than 65% at 5 years, and from 16% to close to 50% at 10 years. Disease-specific survival has increased from the mid-60% range to above 80% at 5 years, and from just over 50% to beyond 80% at 10 years. Overall survival has risen from the mid-60% range to over 80% at 5 years, and from around 37% to more than 60% at 10 years.[2,3,9,10]

BIOMARKERS

Cellular myeloblastosis gene

The majority of AdCC cases involve a fusion of the cellular myeloblastosis gene (*c-MYB* or *MYB*) with the nuclear factor I B-type (*NFIB*) gene due to translocation t(6;9)(q22–23;p23–24). This fusion leads to the upregulation of a fusion protein containing the aminoterminal of 90% of the MYB protein. Under normal conditions, the *MYB* gene regulates cell proliferation and differentiation, but when abnormally activated by this fusion it drives oncogenic processes such as increased cell survival, uncontrolled proliferation, and reduced apoptosis. Consequently, the *MYB::NFIB* fusion is considered a key oncogenic driver in AdCC and serves as an important marker for this tumour, regardless of its site of origin.[1,13] MYB protein overexpression can also occur in the absence of this fusion, possibly due to other *MYB* rearrangements or alternative pathways.[20,21] The *MYB::NFIB* fusion also functions as an oncogene in various other cancers, including leukaemia, breast cancer, colorectal cancer, pancreatic cancer, seminoma, and thymoma.[22,23]

In challenging diagnostic cases where salivary gland adenocarcinomas cannot be further specified histologically, fluorescence in situ hybridization (FISH) is applied to detect this specific translocation pathognomonic for AdCC, using a break-apart probe.[24] While FISH is highly specific, it is complex and expensive. Immunohistochemistry, on the other hand, may provide a quicker and more cost-effective alternative.[25]

To intervene in disease progression, several *MYB*-targeting agents are under investigation. For instance, the *MYB::NFIB* fusion is regulated by the AKT-dependent IGF1R signalling pathway, and several inhibitors, such as linsitinib, have demonstrated encouraging therapeutic effects. In contrast, targeting the proto-oncogene *C-KIT* with imatinib, which is regulated by *MYB* and shows elevated expression in solid pattern AdCC, has yielded limited efficacy.[26–28]

Chemokine receptor type 4

Chemokines, or chemotactic cytokines, are viable therapeutic targets due to their critical roles in the immune system. They are involved in various functions including apoptosis, mitogenesis, and angiogenesis, and play crucial roles in embryogenesis, haematopoiesis, tumour growth, and metastasis.[29,30] Chemokines act as ligands for G protein-coupled receptors, such as chemokine receptor type 4 (CXCR4), which specifically binds to chemokine ligand 12 (CXCL12), also known as stromal cell-derived factor 1 alpha (SDF-1α). This receptor-ligand interaction is crucial for several physiological processes, such as embryonic development and immune cell trafficking.[31] Additionally, it plays a pivotal role in tumourigenesis, with CXCR4 overexpression detected in over 20 tumour types, including AdCC, highlighting its role in tumour progression.[32,33] Increased CXCR4 expression in tumours is often associated with a higher risk of local recurrence and distant metastases, as it promotes angiogenesis and tumour cell migration to metastatic sites expressing high levels of CXCL12 such as lymph nodes, lungs, and liver.[30,32–34]

Furthermore, CXCR4 may act as a specific target for diagnostic and therapeutic purposes in AdCC. Antagonist drugs like AMD3100, along with various anti-CXCR4 peptides, antibodies, and low-molecular-weight agents, have been investigated and proven to inhibit or delay cancer progression in several tumour types. These agents have also enhanced tumour cell sensitization to conventional chemotherapy, improving outcomes with combined treatment.[33–36] Radiolabelled CXCR4 ligands have recently been developed for PET-specific imaging, making CXCR4 also a promising target for radioligand treatment in the future.[37,38]

Prostate-specific membrane antigen

Prostate-specific membrane antigen (PSMA) has revolutionized the approach to diagnosing and managing prostate cancer since its discovery in the late 20th century.[39] PSMA was first described by Horoszewicz in 1987 using a prostate-specific monoclonal antibody against the LNCaP human prostate cancer cell line.[40] It was successfully cloned and characterized in 1993, setting the stage for its extensive use in both diagnostic imaging and therapeutic applications for prostate cancer.[41]

PSMA is a type II transmembrane glycoprotein predominantly expressed in prostate tissue, both benign and malignant. Under normal conditions, PSMA is primarily localized in the cytoplasm and on the apical surface of epithelial cells lining the prostatic ducts, but it is absent in basal epithelial cells and stromal cells.[40,41] During dysplastic and neoplastic transformation of prostate tissue, PSMA may relocate from the apical membrane to the luminal surface.[42,43] Its expression is notably upregulated in prostate carcinoma and correlates with tumour grade, advanced stage, and poor prognosis.[42,44,45] The gene encoding PSMA is mapped on the short arm of chromosome 11.[46]

The initial perception of PSMA as a prostate-specific antigen has evolved, as subsequent studies revealed its expression in various other tissues, including the kidneys (proximal tubules); nervous system (astrocytes and Schwann cells); the small bowel (jejunal brush border) and ductal epithelium of normal breasts.[44,47] The expression of PSMA on salivary gland cell membranes was first reported in 1995, and later refined to be predominantly cytoplasmic in secretory acinar cells, with no expression in excretory duct cells.[48,49]

The precise role of PSMA in the prostate and kidneys remains unclear; however, it is thought to be involved in folate metabolism.[50] In the nervous system, PSMA, also known as glutamate carboxypeptidase II, functions by hydrolyzing N-acetylaspartylglutamate into N-acetylaspartate and glutamate, thereby increasing glutamate levels at synaptic sites. In the small intestine, a PSMA homolog folate hydrolase 1, plays a critical role in the absorption of folate.[44,51] Unlike prostate-specific antigen (PSA), which is used as a tumour marker for monitoring treatment responses due to its leakage into the bloodstream in prostate carcinoma, PSMA cannot be used as a serum-based diagnostic or screening marker.[52,53]

In neoplasms, PSMA has been identified in subtypes of schwannoma and bladder carcinoma.[51] Subsequently, it has been found in the neovascular capillary endothelium of a wide spectrum of solid tumours, i.e., epithelial tumours (carcinomas); neuroendocrine tumours; mesenchymal tumours (soft tissue sarcomas); as well as malignant melanoma and glioma. This pattern of expression suggests that PSMA may play a role in tumour-

associated angiogenesis.[47,54] More recently, evidence has emerged suggesting the possible expression of PSMA in AdCC, expanding the applications of PSMA-targeted diagnostics and therapies beyond prostate cancer.[55]

TARGETED DIAGNOSTICS

Although each of the aforementioned markers is relevant, PSMA stands out due to its well-established role in theranostics —combining both diagnostics and targeted therapies— particularly in prostate cancer, where it has been extensively validated. Building on this success and the identification of PSMA expression in AdCC, PSMA was selected as the primary focus due to its potential for precise imaging using PET/CT and its promise for targeted therapy.

The anatomy of salivary glands presents unique challenges for diagnostic imaging, particularly when assessing tumour involvement. The three paired major glands and 600–1,000 minor salivary glands consist predominantly of mucous cells, clustered in areas such as the palate, lips, buccal mucosa, tongue, and floor of the mouth. Additionally, numerous seromucous glands are scattered throughout the pharynx, paranasal sinuses, larynx, trachea, and oesophagus.[56,57] While CT and MRI are effective in visualizing the parotid and submandibular glands, these techniques struggle with smaller structures like the sublingual and minor salivary glands, which are often indistinguishable due to their size and low contrast with surrounding tissues. Previously, minor glands were only detectable when affected by tumour growth.[58,59]

The initial use of PSMA in diagnostic imaging involved radio-immunoscintigraphy techniques, utilizing radiolabelled monoclonal antibodies such as CYT-356 labelled with 111-Indium. Known as ProstaScint™, this method had limitations due to its specificity only for the intracellular domain of PSMA, making it suitable only for imaging viable tumour cells following internalization or apoptotic cells with disrupted cell membranes.[60–63]

Imaging typically occurred four to six days after intravenous administration of the conjugate, necessitating hydration and cathartics to manage excretion of the conjugate into the bowel and bladder. Interpreting the local extent of the tumour was difficult without concurrent SPECT/CT.[51] Antibodies targeting the extracellular epitope of PSMA were later developed, but the use of radiolabelled monoclonal antibodies comes with several limitations, including a prolonged circulatory half-life of 3–4 days, suboptimal tumour penetration, and low tumour-to-normal tissue uptake ratios.[62]

The development of PSMA PET/CT using small-molecule inhibitors labelled with radionuclides like Gallium-68 (^{68}Ga) and Fluorine-18 (^{18}F) significantly enhanced the accuracy of diagnostic imaging, allowing for better staging and monitoring of disease progression.[51] These agents, such as ^{68}Ga-PSMA-HBED-CC provide rapid blood clearance, low hepatic uptake, and high specific uptake in PSMA-expressing tissues and tumours shortly after administration, greatly augmenting the imaging contrast of malignant tissues. This is particularly advantageous in medical imaging, as the physical properties of ^{68}Ga are well-matched with the pharmacokinetics of PSMA-targeting peptides.[62] Clinical evaluation of the biodistribution of ^{68}Ga-HBED-CC has depicted uptake in the salivary and lacrimal glands, liver, spleen, intestines, and kidneys, whereas no noteworthy radioactivity has been reported in the bladder.[64] Furthermore, the availability of ^{68}Ga from in-house generators offers a convenient and cost-effective alternative to cyclotron-produced isotopes.[65]

TARGETED THERAPY

Lutetium-177-labelled PSMA-617 therapy for AdCC

Radiolabelled ligands targeting PSMA offer a promising approach for treating tumours that express this antigen by guiding radiation specifically to cancer cells. Lutetium-177 (^{177}Lu) is a key isotope in these theranostic treatments. It emits beta radiation with moderate penetration depth, which effectively destroys cancer cells while minimizing damage to surrounding healthy tissues. Moreover, it releases gamma radiation, enabling real-time imaging and precise tracking of the isotope within the body, enhancing the accuracy and effectiveness of the treatment.[66] In prostate cancer, palliative treatment with ^{177}Lu-PSMA in patients with high PSMA-ligand uptake on PET/CT scans has demonstrated a biochemical response in up to 97% of cases. The therapy is generally considered safe and well-tolerated, with minimal side effects.[67,68] Meta-analysis data of 175 patients indicate that 37% of patients experienced a partial response, 38% had stable disease, and 25% exhibited disease progression.[69]

Additionally, integrating ^{177}Lu-PSMA therapy with standard care has been associated with an increase in median progression-free survival from 3.4 to 8.7 months and overall survival from 11.3 to 15.3 months.[68]

Initial studies have also evaluated radionuclide therapy for other solid tumours expressing PSMA. Tumours such as glioblastoma, thyroid carcinoma, renal cell carcinoma, and hepatocellular carcinoma express PSMA in the tumour neovasculature rather than intracellularly.[70] Given the presence of PSMA protein in salivary gland

tumour cells and PSMA uptake in salivary glands on PET/CT scans, there is growing interest in exploring the feasibility of ^{177}Lu-PSMA as a palliative therapy for AdCC, especially when other treatment options fail.

AIMS AND OUTLINE OF THIS THESIS

The general aim of this thesis is to explore and validate novel targets for diagnostic and therapeutic strategies in AdCC of the salivary glands. By integrating histopathology, advanced imaging techniques, and targeted therapies, this thesis seeks new insights into the pathogenesis, diagnosis, and treatment of AdCC, ultimately contributing to improved clinical outcomes and enhanced patient quality of life.

Part A (Chapters 2, 3, and 4) presents three biomarkers in AdCC —MYB, CXCR4, and PSMA— highlighting their roles in tumour identification, disease progression, and therapeutic potential.

Part B (Chapters 5 and 6) focuses on PSMA in diagnostics, aiming to refine AdCC staging by first mapping PSMA-ligand's normal uptake pattern on PET/CT, followed by its initial use in AdCC in combination with immunohistochemistry.

Part C (Chapter 7) introduces PSMA-targeted radioligand therapy, offering promising new avenues for treatment in patients with salivary gland cancers for whom conventional options have failed.

Chapter 2 describes the biomarker *MYB*, which when fused to *NFIB* and typically detected by fluorescence in situ hybridization (FISH), is pathognomonic for AdCC. The chapter assesses the diagnostic value of MYB protein expression by immunohistochemistry as an alternative to FISH for predicting this translocation. Additionally, it studies MYB expression levels in relation to the presence or absence of the *MYB::NFIB* translocation and correlates these levels with clinicopathological parameters.

CXCR4, a biomarker known for driving tumour progression and metastasis, is examined in **Chapter 3** for its immunohistochemical expression in a large cohort of AdCC cases. The study investigates its associations with clinicopathological prognosticators and survival, with particular focus on the occurrence of a locoregional recurrence and distant metastases.

Continuing on the findings of a case report that identified the presence of the prostate marker PSMA in metastatic AdCC, **Chapter 4** explores PSMA protein expression in primary, recurrent, and metastatic AdCC tissues.[71] It analyzes the correlation between PSMA expression levels, clinical outcomes, and tumour characteristics to assess its diagnostic and prognostic significance, aiming to expand the clinical applications of PSMA beyond prostate cancer.

Chapter 5 quantifies and illustrates the physiological distribution of PSMA-ligand in normal salivary and seromucous glands in the head and neck to enhance PSMA PET/CT interpretation and identify innovative clinical applications.

The first clinical study to evaluate the capability of visualizing local recurrent and distant metastatic AdCC using PSMA PET/CT is described in **Chapter 6**. This study correlates PSMA-ligand uptake with immunohistochemistry results and compares standardized uptake values (SUV) with those from FDG PET/CT when available.

Finally, **Chapter 7** describes the first series of patients with advanced or metastatic salivary gland cancer who received palliative treatment using ^{177}Lu-PSMA therapy, after all other treatments had failed. The chapter evaluates the feasibility, efficacy, safety, and clinical outcome/benefits of this PSMA-targeted radioligand therapy in six patients.

REFERENCES

1. Coca-Pelaz A, Rodrigo JP, Bradley PJ, et al. Adenoid cystic carcinoma of the head and neck - An update. Oral Oncol. 2015;51(7):652-661.
2. Jang S, Patel PN, Kimple RJ, McCulloch TM. Clinical Outcomes and Prognostic Factors of Adenoid Cystic Carcinoma of the Head and Neck. Anticancer Res. 2017;37(6):3045-3052.
3. Spiro RH, Huvos AG, Strong EW. Adenoid cystic carcinoma of salivary origin. A clinicopathologic study of 242 cases. Am J Surg. 1974;128(4):512-520.
4. Bradley PJ. Adenoid cystic carcinoma of the head and neck: a review. Curr Opin Otolaryngol Head Neck Surg. 2004;12(2):127-132.
5. Bjørndal K, Krogdahl A, Therkildsen MH, et al. Salivary gland carcinoma in Denmark 1990-2005: A national study of incidence, site and histology. Results of the Danish Head and Neck Cancer Group (DAHANCA). Oral Oncol. 2011;47(7):677-682.
6. Gupta B, Johnson NW, Kumar N. Global Epidemiology of Head and Neck Cancers: A Continuing Challenge. Oncology. 2016;91(1):13-23.
7. WHO. Classification of Head and Neck Tumours. In: "Tumours of salivary glands," El-Naggar A.K., Chan J.K.C., Grandis J.R., Takata T., Slootweg P.J, eds. Classification of Head and Neck Tumors. Vol 9. 4th ed. ; 2017.
8. Alfieri S, Granata R, Bergamini C, et al. Systemic therapy in metastatic salivary gland carcinomas: A pathology-driven paradigm? Oral Oncol. 2017;66:58-63.
9. Huang M, Ma D, Sun K, Yu G, Guo C, Gao F. Factors influencing survival rate in adenoid cystic carcinoma of the salivary glands. Int J Oral Maxillofac Surg. 1997;26(6):435-439.
10. Van Weert S, Bloemena E, Van Der Waal I, et al. Adenoid cystic carcinoma of the head and neck: a single-center analysis of 105 consecutive cases over a 30-year period. Oral Oncol. 2013;49(8):824-829.
11. Hellquist H, Skalova A. Adenoid Cystic Carcinoma. In: Histopathology of the Salivary Glands. Springer Berlin Heidelberg; 2014:221-260.
12. Perzin KH, Gullane P, Clairmont AC. Adenoid cystic carcinomas arising in salivary glands: a correlation of histologic features and clinical course. Cancer. 1978;42(1):265-282.
13. West RB, Kong C, Clarke N, et al. MYB expression and translocation in adenoid cystic carcinomas and other salivary gland tumors with clinicopathologic correlation. Am J Surg Pathol. 2011;35(1):92-99.
14. Ho AS, Ochoa A, Jayakumaran G, et al. Genetic hallmarks of recurrent/metastatic adenoid cystic carcinoma. J Clin Invest. 2019;129(10):4276-4289.
15. de Sousa LG, Jovanovic K, Ferrarotto R. Metastatic Adenoid Cystic Carcinoma: Genomic Landscape and Emerging Treatments. Curr Treat Options Oncol. 2022;23(8):1135-1150.
16. Freling N, Crippa F, Maroldi R. Staging and follow-up of high-grade malignant salivary gland tumours: The role of traditional versus functional imaging approaches - A review. Oral Oncol. 2016;60:157-166.
17. Jung JH, Lee SW, Son SH, et al. Clinical impact of (18) F-FDG positron emission tomography/CT on adenoid cystic carcinoma of the head and neck. Head Neck. 2017;39(3):447-455.
18. Laurie SA, Ho AL, Fury MG, Sherman E, Pfister DG. Systemic therapy in the management of metastatic or locally recurrent adenoid cystic carcinoma of the salivary glands: a systematic review. Lancet Oncol. 2011;12(8):815-824.
19. Locati LD, Perrone F, Losa M, et al. Treatment relevant target immunophenotyping of 139 salivary gland carcinomas (SGCs). Oral Oncol. 2009;45(11):986-990.

20. Persson M, Andersson MK, Mitani Y, et al. Rearrangements, Expression, and Clinical Significance of MYB and MYBL1 in Adenoid Cystic Carcinoma: A Multi-Institutional Study. Cancers (Basel). 2022;14(15):3691.
21. Mitani Y, Li J, Rao PH, et al. Comprehensive analysis of the MYB-NFIB gene fusion in salivary adenoid cystic carcinoma: Incidence, variability, and clinicopathologic significance. Clin Cancer Res. 2010;16(19):4722-4731.
22. Drier Y, Cotton MJ, Williamson KE, et al. An oncogenic MYB feedback loop drives alternate cell fates in adenoid cystic carcinoma. Nat Genet. 2016;48(3):265-272.
23. Ramsay RG, Gonda TJ. MYB function in normal and cancer cells. Nat Rev Cancer. 2008;8(7):523-534.
24. Rettig EM, Tan M, Ling S, et al. MYB rearrangement and clinicopathologic characteristics in head and neck adenoid cystic carcinoma. Laryngoscope. 2015;125(9):E292-E299.
25. Jacobs TW, Gown AM, Yaziji H, Barnes MJ, Schnitt SJ. Comparison of fluorescence in situ hybridization and immunohistochemistry for the evaluation of HER-2/neu in breast cancer. J Clin Oncol. 1999;17(7):1974-1982.
26. Holst VA, Marshall CE, Moskaluk CA, Frierson HF. KIT protein expression and analysis of c-kit gene mutation in adenoid cystic carcinoma. Mod Pathol. 1999;12(10):956-960.
27. Pfeffer MR, Talmi Y, Catane R, Symon Z, Yosepovitch A, Levitt M. A phase II study of Imatinib for advanced adenoid cystic carcinoma of head and neck salivary glands. Oral Oncol. 2007;43(1):33-36.
28. Andersson MK, Afshari MK, Andrén Y, Wick MJ, Stenman G. Targeting the Oncogenic Transcriptional Regulator MYB in Adenoid Cystic Carcinoma by Inhibition of IGF1R/AKT Signaling. J Natl Cancer Inst. 2017;109(9).
29. Zlotnik A, Yoshie O. The Chemokine Superfamily Revisited. Immunity. 2012;36(5):705-712.
30. Wang Z, Sun J, Feng Y, Tian X, Wang B, Zhou Y. Oncogenic roles and drug target of CXCR4/CXCL12 axis in lung cancer and cancer stem cell. Tumour Biol. 2016;37(7):8515-8528.
31. Oberlin E, Amara A, Bachelerie F, et al. The CXC chemokine SDF-1 is the ligand for LESTR/fusin and prevents infection by T-cell-line-adapted HIV-1. Nature. 1996;382(6594):833-835.
32. Zushi Y, Noguchi K, Hashitani S, et al. Relations among expression of CXCR4, histological patterns, and metastatic potential in adenoid cystic carcinoma of the head and neck. Int J Oncol. 2008;33(6):1133-1139.
33. Domanska UM, Kruizinga RC, Nagengast WB, et al. A review on CXCR4/CXCL12 axis in oncology: No place to hide. Eur J Cancer. 2013;49(1):219-230.
34. Vandercappellen J, Van Damme J, Struyf S. The role of CXC chemokines and their receptors in cancer. Cancer Lett. 2008;267(2):226-244.
35. Chatterjee S, Behnam Azad B, Nimmagadda S. The intricate role of CXCR4 in cancer. Adv Cancer Res. 2014;124:31-82.
36. Muller A, Sonkoly E, Eulert C, et al. Chemokine receptors in head and neck cancer: Association with metastatic spread and regulation during chemotherapy. Int J Cancer. 2006;118(9):2147-2157.
37. Gourni E, Demmer O, Schottelius M, et al. PET of CXCR4 Expression by a 68Ga-Labeled Highly Specific Targeted Contrast Agent. J Nucl Med. 2011;52(11):1803-1810.
38. Schottelius M, Osl T, Poschenrieder A, et al. [177Lu]pentixather: Comprehensive preclinical characterization of a first CXCR4-directed endoradiotherapeutic agent. Theranostics. 2017;7(9):2350-2362.
39. Velonas V, Woo H, Remedios C, Assinder S. Current Status of Biomarkers for Prostate Cancer. Int J Mol Sci. 2013;14(6):11034-11060.

40. Horoszewicz JS, Kawinsky E MG. Monoclonal antibodies to a new antigenic marker in epithelial prostatic cells and serum of prostatic cancer patients. Anticancer Res. 1987;7(5B):927-935.
41. Israeli RS, Powell CT, Fair WR, Heston WD. Molecular cloning of a complementary DNA encoding a prostate-specific membrane antigen. Cancer Res. 1993;53(2):227-230.
42. Wright GL, Haley C, Beckett M Lou, Schellhammer PF. Expression of prostate-specific membrane antigen in normal, benign, and malignant prostate tissues. Urol Oncol Semin Orig Investig. 1995;1(1):18-28.
43. Madu CO, Lu Y. Novel diagnostic biomarkers for prostate cancer. J Cancer. 2010;1:150-177.
44. Ristau BT, O'Keefe DS, Bacich DJ. The prostate-specific membrane antigen: Lessons and current clinical implications from 20 years of research. Urol Oncol Semin Orig Investig. 2014;32(3):272-279.
45. Ross JS, Sheehan CE, Fisher H a G, et al. Correlation of primary tumor prostate-specific membrane antigen expression with disease recurrence in prostate cancer. Clin Cancer Res. 2003;9(17):6357-6362.
46. O'Keefe DS, Su SL, Bacich DJ, et al. Mapping, genomic organization and promoter analysis of the human prostate-specific membrane antigen gene. Biochim Biophys Acta. 1998;1443(1-2):113-127.
47. Chang SS, Reuter VE, Heston WDW, Bander NH, Grauer LS, Gaudin PB. Five Different Anti-Prostate-specific Membrane Antigen (PSMA) Antibodies Confirm PSMA Expression in Tumor-associated Neovasculature. Cancer Res. 1999;59(13):3192-3198.
48. Troyer JK, Beckett ML, Wright GL. Detection and characterization of the prostate-specific membrane antigen (PSMA) in tissue extracts and body fluids. Int J Cancer. 1995;62(5):552-558.
49. Wolf P, Freudenberg N, Bühler P, et al. Three conformational antibodies specific for different PSMA epitopes are promising diagnostic and therapeutic tools for prostate cancer. Prostate. 2010;70(5):562-569.
50. Pinto JT, Suffoletto BP, Berzin TM, et al. Prostate-specific membrane antigen: a novel folate hydrolase in human prostatic carcinoma cells. Am Assoc Cancer Res. 1996;2(9):1445-1451.
51. Mease RC, Foss CA, Pomper MG. PET imaging in prostate cancer: focus on prostate-specific membrane antigen. Curr Top Med Chem. 2013;13(8):951-962.
52. Levesque M, Hu H, D'Costa M, Diamandis EP. Prostate-specific antigen expression by various tumors. J Clin Lab Anal. 1995;9(2):123-128.
53. Chang SS. Overview of prostate-specific membrane antigen. Rev Urol. 2004;6(Suppl 10):S13-S18.
54. Silver DA, Pellicer I, Fair WR, Heston WD, Cordon-Cardo C. Prostate-specific membrane antigen expression in normal and malignant human tissues. Am Assoc Cancer Res. 1997;3(1):81-85.
55. Lütje S, Sauerwein W, Lauenstein T, Bockisch A, Poeppel TD. In Vivo Visualization of Prostate-Specific Membrane Antigen in Adenoid Cystic Carcinoma of the Salivary Gland. Clin Nucl Med. 2016;41(6):476-477.
56. Bailey B, Calhoun K. Head and Neck Surgery Otolaryngology, Vol 1. 3rd ed. Lippincot Williams&Wilkins.; 2001.
57. Hand AR, Pathmanathan D, Field RB. Morphological features of the minor salivary glands. Arch Oral Biol. 1999;44(Suppl 1):S3-S10.
58. Afzelius P, Nielsen MY, Ewertsen C, Bloch KP. Imaging of the major salivary glands. Clin Physiol Funct Imaging. 2016;36(1):1-10.

59. Wang X dong, Meng L jiao, Hou T ting, Zheng C, Huang S hui. Frequency and Distribution Pattern of Minor Salivary Gland Tumors in a Northeastern Chinese Population: A Retrospective Study of 485 Patients. J Oral Maxillofac Surg. 2015;73(1):81-91.
60. Lopes AD, Davis WL, Rosenstraus MJ, Uveges AJ, Gilman SC. Immunohistochemical and Pharmacokinetic Characterization of the Site-specific Immunoconjugate CYT-356 Derived from Antiprostate Monoclonal Antibody 7E11-C5. Cancer Res. 1990;50(19):6423-6429.
61. Babaian RJ, Sayer J, Podoloff DA, Steelhammer LC, Bhadkamkar VA, Gulfo J V. Radioimmunoscintigraphy of pelvic lymph nodes with 111indium-labeled monoclonal antibody CYT-356. J Urol. 1994;152(6 Pt 1):1952-1955.
62. Lütje S, Heskamp S, Cornelissen AS, et al. PSMA Ligands for Radionuclide Imaging and Therapy of Prostate Cancer: Clinical Status. Theranostics. 2015;5(12):1388-1401.
63. Troyer JK, Beckett ML, Wright GL. Location of prostate-specific membrane antigen in the LNCaP prostate carcinoma cell line. Prostate. 1997;30(4):232-242.
64. Afshar-Oromieh A, Hetzheim H, Kratochwil C, et al. The novel theranostic PSMA-ligand PSMA-617 in the diagnosis of prostate cancer by PET/CT: biodistribution in humans, radiation dosimetry and first evaluation of tumor lesions. J Nucl Med. 2015;56(11):1697-1705.
65. Banerjee SR, Pomper MG. Clinical applications of Gallium-68. Appl Radiat Isot. 2013;76:2-13.
66. Parlak Y, Mutevellzade G, Sezgln C, Goksoy D, Gumuser G, Saylt E. EFFECTIVE HALF-LIFE, EXCRETION AND RADIATION EXPOSURE OF 177LU-PSMA. Radiat Prot Dosimetry. 2023;199(10):1090-1095.
67. Hofman MS, Violet J, Hicks RJ, et al. [177Lu]-PSMA-617 radionuclide treatment in patients with metastatic castration-resistant prostate cancer (LuPSMA trial): a single-centre, single-arm, phase 2 study. Lancet Oncol. 2018;19(6):825-833.
68. Sartor O, de Bono J, Chi KN, et al. Lutetium-177–PSMA-617 for Metastatic Castration-Resistant Prostate Cancer. N Engl J Med. 2021;385(12):1091-1103.
69. Yadav MP, Ballal S, Sahoo RK, Dwivedi SN, Bal C. Radioligand therapy with 177Lu-PSMA for metastatic castration-resistant prostate cancer: A systematic review and meta-analysis. Am J Roentgenol. 2019;213(2):275-285.
70. Uijen MJM, Derks YHW, Merkx RIJ, et al. PSMA radioligand therapy for solid tumors other than prostate cancer: background, opportunities, challenges, and first clinical reports. Eur J Nucl Med Mol Imaging. 2021;48(13):4350-4368.
71. de Keizer B, Krijger GC, Ververs FT, van Es RJJ, de Bree R, Willems S. 68Ga-PSMA PET-CT Imaging of Metastatic Adenoid Cystic Carcinoma. Nucl Med Mol Imaging. 2017;51(4):360-361.

1

PART A

Biomarkers

MYB immunohistochemistry as a predictor of *MYB::NFIB* fusion in the diagnosis of adenoid cystic carcinoma of the head and neck

Thomas J.W. Klein Nulent
Robert J.J. van Es
Gerben E. Breimer
Matthijs H. Valstar
Laura A. Smit
Caroline M. Speksnijder
Remco de Bree
Stefan M. Willems

Chapter as published in:
Oral Surgery, Oral Medicine, Oral Pathology and Oral Radiology. 2024; 138(6): 772–780

doi: 10.1016/j.oooo.2024.08.006

ABSTRACT

Objectives

Diagnosing adenoid cystic carcinoma (AdCC) is challenging due to histopathological variability and similarities with other tumours. In AdCC pathogenesis, the cellular myeloblastosis gene (*c-MYB*) often exhibits a *MYB::NFIB* fusion from a reciprocal translocation. This study aimed to assess the predictive accuracy of MYB immunohistochemistry for detecting this translocation compared to fluorescence in situ hybridization (FISH).

Study design

This study included 110 AdCC patients (1999–2017) from two Dutch head and neck centres using tissue microarrays and full slides. Median MYB expression levels by immunohistochemistry were compared based on translocation status by FISH, and differences within clinicopathological parameters were examined. An immunohistochemical cut-off was established to estimate the translocation.

Results

MYB immunohistochemistry was available in 90/110 patients, with a median expression of 27%. FISH was interpretable in 79/108 tumours, identifying *MYB::NFIB* fusion in 44 (56%). Among 62 patients with both MYB expression and translocation data, the fusion was present in 38 (61%). These tumours had higher MYB expression (30%) than non-translocated tumours (6%); p=0.02. A 60% MYB expression cut-off yielded 100% specificity for detecting the translocation but had no prognostic value.

Conclusion

Although MYB protein expression alone lacks diagnostic precision, protein expression >60% predicted the *MYB::NFIB* fusion in all tumours.

INTRODUCTION

Adenoid cystic carcinoma (AdCC) is a rare epithelial malignancy of the secretory glands. It comprises around 20% to 35% of all salivary gland malignancies in the head and neck region, with an annual incidence of 2 to 3 cases per 1,000,000 inhabitants. Its incidence peaks in the fifth and sixth decade, but it arises in all age groups with a slight predominance in women.[1-4] It consists of ductal (luminal) and basal/myoepithelial (abluminal) cells arranged in a glandular (cribriform), tubular, or solid growth pattern.[5] Histopathological diagnosis of salivary gland cancers, in general, is challenging on small biopsies and cytological specimens. In case of AdCC, the cribriform pattern is well recognized, while other patterns are less clear, reflected by the high reclassification rate of 14% to 29% on the surgical specimens after definitive treatment.[1]

The predominant gene mutated in recurrent or metastatic AdCC is *NOTCH1*, with an incidence of 26.3%, contrasting to 8.5% in non-recurrent tumours, and is associated with a solid growth pattern.[6,7]

Ten-year rates of disease-free survival have significantly increased over the last decades, from approximately 16% in older studies to 48% in more recent publications.[2,3] Local recurrences are difficult to cure due to previous surgical procedures and radiotherapy limitations. Negative prognosticators are advanced tumour stage, AdCC originating from the minor salivary glands, inadequate resection margins, solid growth pattern, and (peri)neural invasion.[1-4,8-10]

The cellular myeloblastosis gene (*c-MYB* or *MYB*) is a proto-oncogene that encodes a transcription factor involved in cellular differentiation and proliferation. It functions as an oncogene in a variety of cancers, including leukaemia, breast-, colorectal- and pancreatic cancer, seminoma, and thymoma.[11-13] Fusion of *MYB* to the transcription factor gene *NFIB* by a translocation t(6;9)(q22–23;p23–24) is present in the majority of AdCC cases. This *MYB::NFIB* fusion results in the upregulation of a fusion protein that contains the aminoterminal of 90% of the MYB protein, which is believed to be an oncogenic driver of this tumour.[1,12] However, overexpression of the MYB protein is also observed in fusion-negative AdCC and, to a lesser extent, in non-AdCC salivary gland tumours, indicating the existence of additional mechanisms for MYB overexpression.[12] Nonetheless, the *MYB::NFIB* translocation, or rearrangements such as multiple variant fusions, have consistently emerged as AdCC-specific abnormalities, distinguishing it from other salivary gland tumours.[14,15] Disease-specific survival is not affected by the *MYB::NFIB* fusion specifically, while *MYB* rearrangements are frequently found to negatively influence prognosis.[16]

Fluorescence in situ hybridization (FISH) is applied to detect this translocation using a break-apart probe that hybridizes respectively the 5′ and 3′ end of the *MYB* gene, labelled with different fluorophores.[17] The *MYB::NFIB* fusion is present in AdCCs irrespective of their derived tumour site, i.e., the major and minor salivary glands, lacrimal glands, ceruminous glands, or breasts.[14] In challenging diagnostic cases where salivary gland adenocarcinomas cannot be further specified histologically, FISH can be used to visualize *MYB* rearrangements pathognomonic for AdCC. Immunohistochemistry is deemed faster and more cost-effective than FISH.[18] This study aims to investigate MYB protein expression levels in AdCC, depending on the presence of the *MYB::NFIB* translocation by FISH, and to correlate these levels with clinicopathological parameters and patient survival. Additionally, it aims to assess the diagnostic value of MYB immunohistochemistry in the predictability of the *MYB::NFIB* translocation.

MATERIALS AND METHODS

Patient selection

A previously fabricated tissue microarray (TMA) and tissue blocks of the resection specimens of patients diagnosed with AdCC of the head and neck between 1990 and 2017 in the University Medical Center Utrecht and Antoni van Leeuwenhoek Hospital/ The Netherlands Cancer Institute were used.[9]

The following clinicopathological parameters were available from the matching data files: histopathological diagnosis, sex, age at diagnosis, tumour site, treatment regimen, (time to) recurrence or metastasis, date of last follow-up, survival status, type and diameter of the tumour, pathological T- and N-stage (AJCC Cancer Staging Manual 7th edition), histopathological growth pattern and associated grade according to the differentiation of Perzin et al.[19], surgical resection margins, and the presence of perineural, vascular, and bone invasion. All data were handled according to the European Union General Data Protection Regulation. Studies on AdCC residual tissue did not require formal consent. Approval was received from both institutional Medical and Biobank Research Ethics Committees, protocol numbers UMCU 16–564 and 17–073, respectively. The study is in accordance with the 1964 Helsinki declaration and its later amendments or comparable ethical standards.

MYB translocation analysis by FISH

The Zytolight *MYB* break-apart FISH probe, a mixture of two directly labelled probes hybridizing to the 6q23.2–q23.3 band, was used to determine *MYB* gene

rearrangements. The orange fluorochrome direct labelled probe hybridizes distal, and the green fluorochrome direct labelled probe hybridizes proximal to the *MYB* breakpoint cluster region. TMA slides (4 mm) were deparaffinized and pre-treated with citrate and protease buffers. Next, they were dehydrated and hybridized with 15 ml FISH probes in a ThermoBrite System (Abbott Laboratories, Chicago, Ill., USA) at 37˚C overnight. The next day, slides were washed in salinesodium citrate buffers, counterstained and mounted with Vectashield containing 4',6-diamidino-2-phenylindole (DAPI) dihydrochloride. *MYB* probe signals were analyzed in 100 random tumour cells from different areas at a 100x magnification using a Leica DM5500 B microscope system with Application Suite Advanced Fluorescence Software (Leica Microsystems, Rijswijk, NL).
A tumour was defined as translocated when a break apart signal was seen in >10% of the tumour cells of at least two arrayed cores or a whole slide. The mean percentage of cells showing the translocation was noted, as well as other *MYB* rearrangements that were seen within the tumour.

MYB expression analysis by immunohistochemistry

The slides were deparaffinized and rehydrated. Heat induced antigen retrieval was applied by boiling the sections in a sodium citrate buffer (10 mM, pH 6.0) for 20 minutes. After cooling down for 15 minutes, the sections were washed in PBS-Tween twice. An UltraVision protein block buffer was added to the sections prior to primary antibody administration (Clone EP769Y (Abcam, Cambridge, UK)), dilution 1:200 in a BSA blocking buffer PBS with sodium azide. Sections were incubated overnight. Before adding the secondary antibody (BrightVision Poly-HRP-Anti-Rabbit (ImmunoLogic, Duiven, NL)), slides were incubated in hydrogen peroxidase 0.3% in PBS for 15 minutes. Finally, the slides were counterstained using haematoxylin, dehydrated, and fixed.
Blinded semiquantitative scoring of the tumour cores or whole slides was done until a consensus was reached by a head and neck pathologist and a head and neck surgeon (S.W. and T.K.N.). Per core or whole slide, the percentage of MYB-positive tumour cells was scored in increments of five percent. For the arrayed cores, MYB expression was defined by the mean percentage of MYB-positive tumour cells in the cores that contained >5% tumour tissue. When less than two adequate cores were available, a whole slide was subsequently stained and scored.

Statistical analysis

A two-way random model intraclass correlation coefficient (ICC) was employed to validate the consistency of a single core's MYB expression within the arrayed cores per tumour by assessing the degree of resemblance among different quantitative

measurements.[20] The median MYB expression with interquartile range (IQR) within the clinical and pathological characteristics was compared using the Independent Samples Kruskal-Wallis (KW) test. An optimal cut-off value for MYB tissue expression to estimate a *MYB::NFIB* fusion was computed by plotting a receiver operating characteristic (ROC) curve, and sensitivity, specificity, predictive values, and likelihood ratios were calculated for the selected cut-off points. Pearson's chi-square or Fisher's exact test (N<5) was used to analyze the number of translocated tumours within the dichotomized parameters. Survival rates were determined and compared across the groups using Fisher's exact test, and the univariate prognostic value of MYB expression was analyzed by the log-rank test for overall, disease-specific, disease-free, recurrence-free, and metastasis-free survival.

RESULTS

The medical records of 110 patients diagnosed with adenoid cystic carcinoma (AdCC) of the secretory glands, who underwent surgery between 1990 and 2017 at the head and neck oncology departments of the University Medical Center Utrecht or the Antoni van Leeuwenhoek Hospital / The Netherlands Cancer Institute, were available. The clinical and pathological data are outlined in Table 1.

Fluorescence in situ hybridization

Due to the retrospective nature of the study, it was not possible to gather additional tissue from two patients. As a result, FISH was carried out on 108 tumour specimens, of which 79 (73%) could be successfully interpreted for technical reasons. A *MYB::NFIB* fusion was identified in 44 of these 79 tumours (56%) and not detected in 26 tumours (33%). *MYB* rearrangements, other than a break apart signal, were present in the other 9 tumours (11%) and are of unclear significance. This led to exclusion from further analysis: one inversion, one single red signal, and seven specimens depicted a single green signal.

MYB immunohistochemistry

The average percentage of MYB positive tumour cells by immunohistochemistry could be successfully scored in the primary tumour samples of 90 out of all 110 patients. Core biopsies of 77 of these were previously incorporated in TMAs: results were based on three cores of 49, and on two cores of 12 tumours. Sixteen tumours were excluded due to insufficient (i.e., <2) cores, however whole slides could be obtained from these 16

and another 13 tumours. From the 20 remaining patients, tumour tissue could not be requested from different (referring) hospital archives, or there was insufficient tissue left for reliable diagnostics. Staining and scoring were done according to the study protocol in the UMC Utrecht pathology laboratory.

MYB expression was predominantly nuclear, tended to concentrate in the abluminal cells, and was homogenously distributed as reflected by a substantial single measurement ICC of 0.68 ($p<0.01$). Eighty out of the 90 tumours (89%) showed positive MYB expression with a median expression of 27% (IQR 8–46%).

MYB immunohistochemistry vs FISH

Ultimately, both MYB expression and translocation status were accessible for 62 primary tumours. Clinical and pathological parameters of these patients were extracted from medical records and outlined in Table 1; Figure 1 illustrates different immunostaining and fluorescence patterns. Out of these 62 patients, a *MYB::NFIB* fusion was detected in 38 tumours (61%). Four out of 62 tumours (6%) were negative for MYB expression on immunohistochemistry. The median MYB expression was 25% (IQR 5–42%). In the 38 translocated tumours, 37 showed MYB expression with a median staining of 30% (IQR 12–56%), significantly higher ($p=0.02$) than the median 6% (IQR 4–30%) in non-translocated tumours.

Within the clinical and pathological parameters, there was an equal distribution of translocated and non-translocated tumours. Although there was a rise in median MYB expression with increasing solid growth, no association was found between the growth pattern, MYB immunohistochemistry, or translocation status. This lack of association applied to all other differences within the clinicopathological (sub)groups as well.

The area under the ROC curve was 0.71 (95% confidence interval 0.58–0.84). Given the moderate diagnostic predictability of the *MYB::NFIB* fusion by MYB expression, the optimal cut-off value of 5% has no clinical relevance for daily practice. It was determined that MYB expression of 60% or higher accurately indicates the presence of the translocation in this cohort (N=9; specificity 100%; positive predictive value 100%). Conversely, the absence of MYB expression indicates the absence of the translocation (N=4; sensitivity 97%; negative predictive value 75%), as shown in Table 2. A proposed diagnostic workflow based on these findings is presented in Figure 2. Table 3 presents the five and ten-year survival rates regarding both *MYB::NFIB* fusion status and dichotomized MYB expression. Disease recurrence occurred with equal frequency in all groups; no statistical difference was found. Furthermore, the current data revealed no univariate prognostic value for either variable in terms of overall survival, disease-specific survival, disease-free survival, recurrence-free survival, and metastasis-free survival (data not shown).

Table 1. Cohort characteristics

	N (%)	Median % MYB	Translocated (%)	MYB ≤60%	MYB >60%
PATIENTS	62	29%		53	9
Sex					
Male	19 (31%)	28%	12 (63%)	15 (79%)	4 (21%)
Female	43 (69%)	23%	26 (60%)	38 (88%)	5 (12%)
Age at diagnosis					
Median (IQR)	57 (44–67)			57 (43–67)	52 (47–65)
Range	20–89			20–83	37–89
Site and subsite					
Major salivary gland	38 (61%)	23%	23 (61%)	34 (89%)	4 (11%)
Minor salivary and seromucous gland	24 (39%)	30%	15 (63%)	19 (79%)	5 (21%)
Parotid gland	17	17%	9 (53%)	16 (94%)	1 (6%)
Submandibular gland	19	23%	12 (63%)	17 (90%)	2 (10%)
Sublingual gland	2	50%	2 (100%)	1 (50%)	1 (50%)
Oral cavity (lip/buccal mucosa/ hard palate/gingival	8	5%	3 (38%)	7 (88%)	1 (12%)
Oropharynx (soft palate/base of tongue)	7	17%	6 (86%)	7 (100%)	0
Nasal cavity/nasopharynx/maxillary sinus	3	42%	3 (100%)	2 (67%)	1(33%)
Larynx/trachea	3	43%	1 (33%)	2 (67%)	1 (33%)
Lacrimal gland	1	77%	1 (100%)	0	1 (100%)
External auditory canal	2	55%	1 (50%)	1 (50%)	1 (50%)
TUMOUR					
pT-stage (TNM 7th ed.)					
pT1	23	25%	13 (57%)	19 (83%)	4 (17%)
pT2	23	23%	15 (65%)	21 (91%)	2 (9%)
pT3	3	30%	3 (100%)	3 (100%)	0
pT4a	9	30%	4 (44%)	7 (78%)	2 (22%)
pT4b	4	21%	3 (75%)	3 (75%)	1 (25%)
Nodal status					
pN0	56 (90%)	27%	36 (64%)	47 (84%)	9 (16%)
pN+	6 (10%)	12%	2 (33%)	6 (100%)	0
Distant metastasis					
cM0	61 (98%)	25%	37 (61%)	52 (85%)	9 (15%)
cM1	1 (2%)	1%	1 (100%)	1 (100%)	0
Resection margins					
Clear (≥5 mm)	9 (15%)	17%	5 (56%)	8 (89%)	1 (11%)
Close or positive (<5 mm)	53 (85%)	25%	33 (62%)	45 (85%)	8 (15%)
Perineural growth					
Present	43 (69%)	30%	24 (56%)	39 (91%)	4 (9%)
Absent	18 (29%)	12%	14 (78%)	13 (72%)	5 (28%)

Vaso-invasive growth					
Present	9 (15%)	5%	5 (56%)	9 (100%)	0
Absent	52 (84%)	30%	33 (63%)	43 (83%)	9 (17%)
Bone invasion					
Present	10 (16%)	33%	7 (70%)	7 (70%)	3 (30%)
Absent	52 (84%)	23%	31 (60%)	46 (89%)	6 (11%)
Growth pattern (Perzin grade[19])					
Tubular (grade 1)	25 (40%)	17%	14 (56%)	23 (92%)	2 (8%)
Cribriform; <30% solid (grade 2)	27 (44%)	25%	19 (70%)	22 (82%)	5 (18%)
Solid (grade 3)	10 (16%)	34%	5 (50%)	8 (80%)	2 (20%)
**MYB::NFIB* fusion					
Present	38 (61%)	*30%		†29 (76%)	9 (24%)
Absent	24 (39%)	6%		24 (100%)	0
TREATMENT					
Adjuvant radiotherapy					
Yes	60 (97%)		36 (58%)	9 (15%)	9 (15%)
No	2 (3%)		2 (100%)	2 (100%)	0

*Kruskal-Wallis analysis p=0.02. †Pearson's chi-square test p<0.01.

Figure 1. MYB immunohistochemistry and MYB FISH patterns

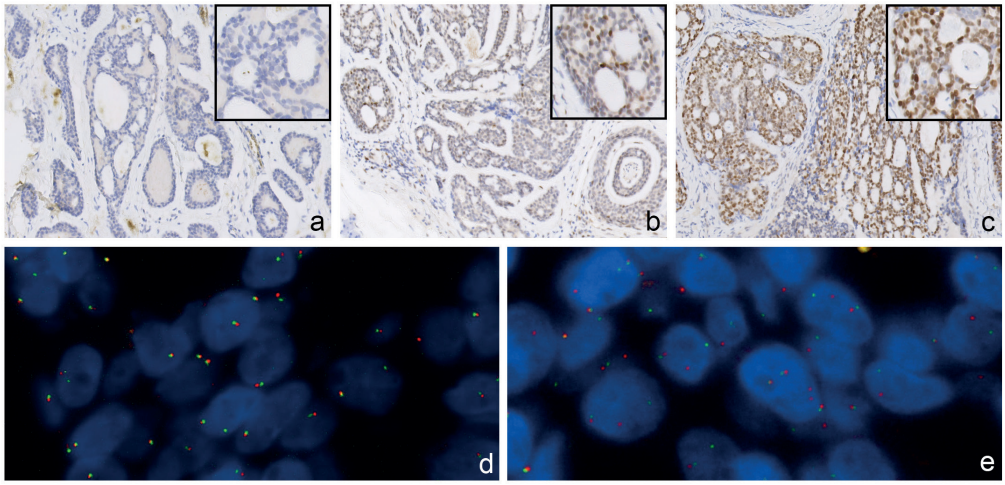

MYB immunohistochemistry. (**a**) 2% expression; (**b**) 40% expression; (**c**) 70% expression. *Magnification: 100x, with insets at 200x.*
MYB FISH. (**d**) no translocation; (**e**) *MYB::NFIB* translocation >10% break apart signal.

Table 2. Predictability results for the presence of *MYB::NFIB* fusion / translocation (6;9)(q22–23;p23–24) using immunohistochemistry

	MYB cut-off 0%			MYB cut-off >60%		
		FISH+	FISH-		FISH+	FISH-
N = 62	MYB >0%	37	21	MYB >60%	9	0
	MYB 0%	1	3	MYB ≤60%	29	24
Sensitivity	97.4%			23.7%		
Specificity	12.5%			100%		
Positive predictive value	63.8%			100%		
Negative predictive value	75.0%			45.3%		
Likelihood ratio +	1.11			∞		
Likelihood ratio -	0.03			0.76		

Figure 2. Proposed diagnostic workflow

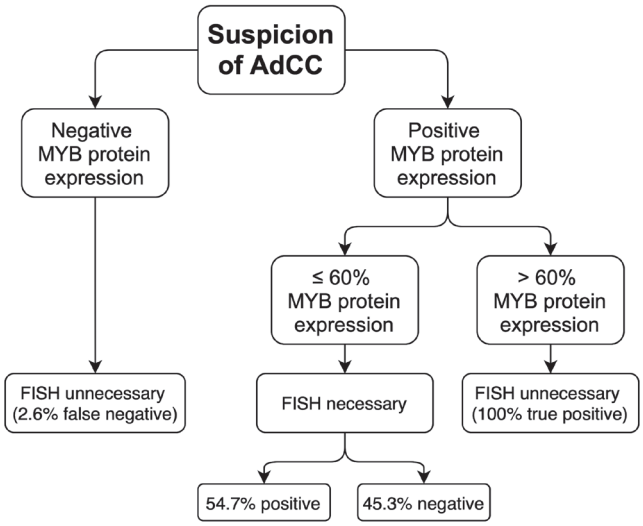

Table 3. Survival data

	MYB::NFIB Negative	*MYB::NFIB* Positive	MYB ≤60%	MYB >60%
Overall survival (OS)				
5-year OS	79%	84%	83%	78%
10-year OS	75%	82%	79%	78%
Disease-specific survival (DSS)				
5-year DSS	88%	87%	89%	78%
10-year DSS	75%	82%	79%	78%
Disease-free survival (DFS)				
5-year DFS	63%	68%	68%	56%
10-year DFS	50%	63%	59%	56%
Locoregional recurrence-free survival (RFS)				
5-year RFS	88%	76%	83%	67%
10-year RFS	79%	71%	76%	67%
Metastatis-free survival (MFS)				
5-year MFS	71%	79%	77%	67%
10-year MFS	63%	74%	70%	67%

DISCUSSION

This study demonstrates that 58/62 tumour samples showed substantial homogenous MYB protein expression and that overexpression >60% corresponds to a *MYB::NFIB* fusion in all tested samples (9/9). Therefore, we suggest a 60% immunohistochemical expression of MYB as a reliable cut-off point to predict *MYB::NFIB* fusion in AdCC. Furthermore, negative MYB expression by immunohistochemistry may be used to rule out the translocation as only one out of the 38 translocated tumours did not show any MYB expression, reflected by a high sensitivity of 97.4%. This then enables a shift from secretory gland translocation analysis, such as by FISH, towards immunohistochemistry in future diagnostic screening (see Figure 2). In this study, the test has proven to be reliably applicable in 13 patients (23%). It provides a fast and accurate diagnosis against reduced costs in 9 patients and raises a strong suspicion of the absence of AdCC in 4 cases.

Several studies on the same subject, as elaborated below, have concluded that *MYB::NFIB* fusion is absent in salivary gland neoplasms other than AdCC, thereby establishing its pathognomonic association with this specific entity. Furthermore, West et al.[12] suggest that strong MYB protein expression, defined by positivity in more than 50% of the tumour cells, is highly specific to AdCC, as all other salivary gland neoplasms in their study either stained negative or showed weak and focal expression at most.

The gene fusion and immunostaining results presented in this paper align with the common findings of similar studies despite variations in staining protocols and interpretation thresholds. West et al.[12] reported a *MYB::NFIB* translocation in 49% of the 37 AdCCs out of a group of 149 salivary gland tumours. All 112 non-AdCC samples were fusion negative, although *MYB* rearrangements were seen in 16%. Negative FISH results in all tested non-AdCC salivary gland tumours were concordantly reported by Mitani et al.[15] (N=34) and all non-AdCC lacrimal tumours by Holstein et al.[21] (N=19). In their AdCCs, the translocation was identified in 28% and 50% respectively. Xu et al.[22] identified the translocation in 59% of its AdCCs. The current study identified comparable results, with the translocation detected in 56% and rearrangements in 11% of the tumours. Additionally, immunohistochemistry results from these studies consistently demonstrate predominant nuclear expression of MYB.

West et al.[12] described positive (>5%) nuclear MYB expression in 24/37 (65%) of all AdCCs, 14/18 (78%) of the translocated AdCCs and 6/13 (46%) of the non-translocated AdCCs. The suggested trend of higher recurrence rates in translocated AdCCs was concordantly seen in our study, although it was not statistically significant. Increased perineural invasion related to the translocation was not observed (see Tables 1 and

3). The immunohistochemical analysis by Mitani et al.[15] described positive nuclear expression (10%) in 85% of the translocated tumours (17/20), in contrast to 61% (25/41) of the non-translocated tumours. They found an association between translocation status and age above 50 years, which is not supported by our data. Lacrimal AdCCs all showed strong nuclear expression of the MYB protein.[21]

Xu et al.[22] reported positive (>5% nuclear staining) MYB expression in 72% of the samples (57/79), and peripheral staining was described in 39%. Five out of 56 (9%) of the non-salivary gland tumours were MYB positive. Sensitivity and specificity indicating the translocation by immunostaining were 78% and 50% respectively.

MYB overexpression in *MYB::NFIB* negative tumours is probably caused by alternative genomic rearrangements, such as different fusion partners that involve the *MYB* locus or the loss of genetic materials at the same location, denoting the presence of a tumour suppressor gene. Furthermore, epigenetic modifications affecting the transcriptional activity of the *MYB* promoter can lead to a positive-feedback loop that upregulates the MYB protein expression.[11,12,15]

Xu et al.[23] investigated *MYB* gene expression by (m)RNA analysis. They concluded that high expression was significantly associated with solid growth pattern (known as a negative prognosticator) and lung metastases.[2] In contrast, the study by Park et al.[24] found a higher risk of developing distant metastases in tumours without MYB protein expression and argued that MYB acts protectively. Our results reflected neither of these findings.

A recent and large study unravelled the different *MYB* rearrangements and identified the specific loss of the 3' part of the *MYB* gene to be associated with diminished overall survival in AdCC. It was more common in grade 3 tumours (>30% solid growth pattern) but remained a significant independent prognosticator in multivariate analysis. Again, *MYB* rearrangements demonstrated no association with age, sex, perineural invasion, or other clinicopathological characteristics, consistent with our findings.[25]

Patients with advanced recurrent or metastatic AdCC face limited treatment options, prompting research into targeted therapies.[26] The *MYB::NFIB* fusion in AdCC is regulated by the AKT-dependent IGF1R signalling pathway, and inhibitors like linsitinib demonstrate potential therapeutic effects.[27] The polyether ionophore monensin and proteasome inhibitor oprozomib exhibit *MYB* inhibition, but require further investigation for clinical use.[28] The proto-oncogene *C-KIT*, a target gene of *MYB*, shows increased expression in solid pattern AdCC, indicating its role in disease progression, although its inhibitor imatinib has limited efficacy. Various markers and immunotherapeutic agents are under study, emphasizing the need for a personalized approach based on patient-specific expression patterns.[29-31] The histopathologic differential diagnosis for

head and neck AdCC encompasses various salivary gland neoplasms that may show reactivity to the MYB antibody. Furthermore, interpreting MYB immunohistochemistry on cytology samples may raise a challenge due to the presence of strong lymphocyte positivity, although lymphocytes should not typically constitute the majority of the cells.[32] In addition to the AdCC cases, West et al.[12] conducted MYB immunohistochemistry on 112 other salivary gland neoplasms. Among these, 9% showed weak and focal expression: 2/4 myoepithelial carcinomas; 4/12 polymorphous adenocarcinomas; 1/5 myoepithelioma; 2/35 (cellular) pleomorphic adenomas; and 1/23 mucoepidermoid carcinoma. All negative were 9 basal cell adenomas; 9 oncocytomas; 5 adenosquamous carcinomas; 7 acinic cell carcinomas; and 3 salivary duct carcinomas.

Similarly, Brill et al.[33] studied a cohort of 133 non-AdCC salivary gland neoplasms for both *MYB::NFIB* fusion status using PCR and immunohistochemical expression. Intense MYB expression in more than 5% of cell nuclei was defined as positive. They observed a total positive immunohistochemistry rate of 14%: 4/5 basaloid squamous cell carcinomas; 3/9 monomorphic/basal cell adenomas; 2/15 polymorphous adenocarcinomas; 2/18 salivary duct carcinomas; and one of each acinic cell carcinoma, basal cell adenocarcinoma, mucoepidermoid carcinoma, epithelial-myoepithelial carcinoma, and pleomorphic adenoma. However, the specific percentage of positive cells was not provided despite the knowledge that MYB immunohistochemistry results do not strictly categorize as positive or negative. It is emphasized that it is crucial to assess both the quality and quantity of MYB protein expression.[32] Additionally, all non-AdCC samples that showed MYB protein expression in both studies were *MYB::NFIB* fusion negative.[12,33]

A diagnostic dilemma lies in distinguishing cribriform AdCC and cribriform basal cell adenomas and -carcinomas. A direct comparison analyzing MYB yielded incongruent results in protein expression between the studies by Tian et al. and the study by Rooney et al. Positive gene splitting was observed by Tian et al.[34] in 9/20 (45%) cases in the AdCC group, and positive MYB immunostaining in 11/20 (55%). All basal cell adenomas and carcinomas tested negative for both FISH and immunohistochemistry. In contrast, Rooney et al.[35] described MYB overexpression in 17/ 30 (57%) of basal cell adenomas and 9/17 (53%) of basal cell adenocarcinomas, utilizing the same protein. However, the specific percentage of MYB-positive nuclei was again not provided, except for the 10% threshold. Another histopathological diagnosis that shares similarities with AdCC and basal cell adeno(carcino)mas is Human Papillomavirus-Related Multiphenotypic Sinonasal Carcinoma, which exhibits a salivary gland tumour-like appearance. This carcinoma demonstrates a variable spectrum of MYB expression on immunohistochemistry, ranging from moderate to strong intensity.[36]

It is challenging to conclude from the aforementioned studies whether a high percentage of diffuse MYB nuclear staining is restricted to AdCC, as several studies do not specifically mention the staining pattern. Relying solely on MYB immunohistochemistry in diagnosing AdCC can still pose a diagnostic pitfall. The sensitivity and specificity values provided by this study might be lower in typical clinical settings, where other entities besides AdCC are present.
In summary, despite consistent and substantially homogenous protein expression in AdCC, future investigations into the clinical significance of various *MYB* rearrangements and their impact on associated protein expression, clinicopathological prognosticators and survival will be relevant for a more comprehensive understanding in the context of daily clinical practice.

CONCLUSION

Identification of the *MYB::NFIB* fusion is relevant for diagnosing AdCC. This fusion was present in the majority of AdCC cases (61%), exhibiting significantly higher MYB expression compared to non-translocated tumours. A MYB expression assessed by immunohistochemistry using a cut-off value of 60% accurately predicted the presence of *MYB::NFIB* fusion in all cases of this cohort. Negative MYB expression served as a strong indicator for the absence of the translocation. The study did not identify a correlation between MYB expression, prognostic parameters and survival. Further research is necessary to clarify whether this high percentage of MYB-positive cell nuclei is specific enough for diagnosing AdCC in routine clinical practice.

REFERENCES

1. Coca-Pelaz A, Rodrigo JP, Bradley PJ, et al. Adenoid cystic carcinoma of the head and neck - An update. Oral Oncol 2015;51:652–61.
2. Jang S, Patel PN, Kimple RJ, McCulloch TM. Clinical Outcomes and Prognostic Factors of Adenoid Cystic Carcinoma of the Head and Neck. Anticancer Res 2017;37:3045–52.
3. Spiro RH, Huvos AG, Strong EW. Adenoid cystic carcinoma of salivary origin. A clinicopathologic study of 242 cases. Am J Surg. 1974;128:512–20.
4. Bjørndal K, Krogdahl A, Therkildsen MH, et al. Salivary gland carcinoma in Denmark 1990-2005: A national study of incidence, site and histology. Results of the Danish Head and Neck Cancer Group (DAHANCA). Oral Oncol 2011;47:677–82.
5. Hellquist H, Skalova A. Adenoid Cystic Carcinoma. Histopathology of the Salivary Glands, Springer Berlin Heidelberg; 2014, p. 221–60.
6. Ho AS, Ochoa A, Jayakumaran G, et al. Genetic hallmarks of recurrent/metastatic adenoid cystic carcinoma. J Clin Invest 2019;129:4276–89.
7. de Sousa LG, Jovanovic K, Ferrarotto R. Metastatic Adenoid Cystic Carcinoma: Genomic Landscape and Emerging Treatments. Curr Treat Options Oncol 2022;23:1135–50.
8. Huang M, Ma D, Sun K, Yu G, Guo C, Gao F. Factors influencing survival rate in adenoid cystic carcinoma of the salivary glands. Int J Oral Maxillofac Surg 1997;26:435–9.
9. Klein Nulent TJW, Valstar MH, Smit LA, et al. Prostate-specific membrane antigen (PSMA) expression in adenoid cystic carcinoma of the head and neck. BMC Cancer 2020;20:519.
10. Van Weert S, Bloemena E, Van Der Waal I, et al. Adenoid cystic carcinoma of the head and neck: a single-center analysis of 105 consecutive cases over a 30-year period. Oral Oncol 2013;49:824–9.
11. Drier Y, Cotton MJ, Williamson KE, et al. An oncogenic MYB feedback loop drives alternate cell fates in adenoid cystic carcinoma. Nat Genet 2016;48:265–72.
12. West RB, Kong C, Clarke N, et al. MYB expression and translocation in adenoid cystic carcinomas and other salivary gland tumors with clinicopathologic correlation. Am J Surg Pathol 2011;35:92–9.
13. Ramsay RG, Gonda TJ. MYB function in normal and cancer cells. Nat Rev Cancer 2008;8:523–34.
14. Persson M, Andren Y, Mark J, Horlings HM, Persson F, Stenman G. Recurrent fusion of MYB and NFIB transcription factor genes in carcinomas of the breast and head and neck. Proc Natl Acad Sci U S A 2009;106:18740–4.
15. Mitani Y, Li J, Rao PH, et al. Comprehensive analysis of the MYB-NFIB gene fusion in salivary adenoid cystic carcinoma: Incidence, variability, and clinicopathologic significance. Clin Cancer Res 2010;16:4722–31.
16. Wagner VP, Bingle CD, Bingle L. MYB-NFIB fusion transcript in adenoid cystic carcinoma: Current state of knowledge and future directions. Crit Rev Oncol Hematol 2022;176:103745.
17. Rettig EM, Tan M, Ling S, et al. MYB rearrangement and clinicopathologic characteristics in head and neck adenoid cystic carcinoma. Laryngoscope 2015;125:E292–9.
18. Jacobs TW, Gown AM, Yaziji H, Barnes MJ, Schnitt SJ. Comparison of fluorescence in situ hybridization and immunohistochemistry for the evaluation of HER-2/neu in breast cancer. J Clin Oncol 1999;17:1974–82.
19. Perzin KH, Gullane P, Clairmont AC. Adenoid cystic carcinomas arising in salivary glands: a correlation of histologic features and clinical course. Cancer 1978;42:265–82.

20. Noorlag R, van Es RJJ, de Bree R, Willems SM. Cytokeratin 19 expression in early oral squamous cell carcinoma and their metastasis: Inadequate biomarker for one-step nucleic acid amplification implementation in sentinel lymph node biopsy procedure. Head Neck 2017;39:1864–8.
21. von Holstein SL, Fehr A, Persson M, et al. Adenoid cystic carcinoma of the lacrimal gland: MYB gene activation, genomic imbalances, and clinical characteristics. Ophthalmology 2013;120:2130–8.
22. Xu B, Drill E, Ho A, et al. Predictors of Outcome in Adenoid Cystic Carcinoma of Salivary Glands: A Clinicopathologic Study With Correlation Between MYB Fusion and Protein Expression. Am J Surg Pathol 2017;41:1422–32.
23. Xu LH, Zhao F, Yang WW, et al. MYB promotes the growth and metastasis of salivary adenoid cystic carcinoma. Int J Oncol 2019;54:1579–90.
24. Park S, Vora M, Van Zante A, et al. Clinicopathologic implications of Myb and Beta-catenin expression in adenoid cystic carcinoma. J Otolaryngol Head Neck Surg 2020;49.
25. Persson M, Andersson MK, Mitani Y, et al. Rearrangements, Expression, and Clinical Significance of MYB and MYBL1 in Adenoid Cystic Carcinoma: A Multi-Institutional Study. Cancers (Basel) 2022;14:3691.
26. Alfieri S, Granata R, Bergamini C, et al. Systemic therapy in metastatic salivary gland carcinomas: A pathology-driven paradigm? Oral Oncol 2017;66:58–63.
27. Andersson MK, Afshari MK, Andrén Y, Wick MJ, Stenman G. Targeting the Oncogenic Transcriptional Regulator MYB in Adenoid Cystic Carcinoma by Inhibition of IGF1R/AKT Signaling. J Natl Cancer Inst 2017;109
28. Yusenko M V., Biyanee A, Andersson MK, et al. Proteasome inhibitors suppress MYB oncogenic activity in a p300-dependent manner. Cancer Lett 2021;520:132–42.
29. da Silva FJ, Carvalho de Azevedo J, Ralph ACL, Pinheiro J de JV, Freitas VM, Calcagno DQ. Salivary glands adenoid cystic carcinoma: a molecular profile update and potential implications. Front Oncol 2023;13:1191218.
30. Holst VA, Marshall CE, Moskaluk CA, Frierson HF. KIT protein expression and analysis of c-kit gene mutation in adenoid cystic carcinoma. Mod Pathol 1999;12:956–60.
31. Pfeffer MR, Talmi Y, Catane R, Symon Z, Yosepovitch A, Levitt M. A phase II study of Imatinib for advanced adenoid cystic carcinoma of head and neck salivary glands. Oral Oncol 2007;43:33–6.
32. Griffith CC, Schmitt AC, Little JL, Magliocca KR. New Developments in Salivary Gland Pathology: Clinically Useful Ancillary Testing and New Potentially Targetable Molecular Alterations. Arch Pathol Lab Med 2017;141:381–95.
33. Brill LB, Kanner WA, Fehr A, et al. Analysis of MYB expression and MYB-NFIB gene fusions in adenoid cystic carcinoma and other salivary neoplasms. Mod Pathol 2011;24:1169–76.
34. Tian Z, Li L, Zhang C ye, Gu T, Li J. Differences in MYB expression and gene abnormalities further confirm that salivary cribriform basal cell tumors and adenoid cystic carcinoma are two distinct tumor entities. J Oral Pathol Med 2016;45:698–703.
35. Rooney SL, Robinson RA. Immunohistochemical expression of MYB in salivary gland basal cell adenocarcinoma and basal cell adenoma. J Oral Pathol Med 2017;46:798–802.
36. Shah AA, Bahram ·, Oliai R, Bishop JA. Consistent LEF-1 and MYB Immunohistochemical Expression in Human Papillomavirus-Related Multiphenotypic Sinonasal Carcinoma: A Potential Diagnostic Pitfall 2019;13:220–4.

High CXCR4 expression in adenoid cystic carcinoma of the head and neck is associated with increased risk of locoregional recurrence

Thomas J.W. Klein Nulent
Robert J.J. van Es
Matthijs H. Valstar
Raquel Klein Gunnewiek
Laura A. Smit
Ludwig E. Smeele
Nicolaas P.A. Zuithoff
Bart de Keizer
Remco de Bree
Stefan M. Willems

Chapter as published in:
Journal of Clinical Pathology 2020; 73(8): 476–482

doi: 10.1136/jclinpath-2019-206273

ABSTRACT

Aim

Treatment options for head and neck adenoid cystic carcinoma (AdCC) are limited in advanced disease. Chemokine receptor type 4 (CXCR4) is present in various tumour types, including AdCC. Upregulation is associated with tumour recurrence and metastasis. New CXCR4-specific diagnostic and therapeutic target agents have recently been available. This study aimed to analyze CXCR4 expression in a cohort of primary head and neck AdCC.

Methods

After histopathological revision, tumour tissues of 73 consecutive patients with AdCC over 1990–2016 were sampled on a tissue microarray. Slides were immunohistochemically stained for CXCR4 and semiquantitatively scored. Associations between protein expression and clinicopathological parameters were tested. HRs were calculated using a Cox proportional hazards model.

Results

Sixty-six tumours could be analyzed. CXCR4 expression was present in 81% of the tumours with a median of 29% (IQR 1–70) positive cells. Expression was univariately correlated to perineural growth (Spearman ρ 0.26, p=0.04) and bone invasion (Spearman ρ 0.32, p=0.01), but not with tumour grade. CXCR4 expression in the primary tumour was significantly higher in tumours that recurred as compared with those that did not recur (median 60%, IQR 33–72 vs 12%, IQR 1–70, Kruskal-Wallis p=0.01). After dichotomization, >25% of CXCR4 expressions proved an independent prognosticator for a reduced recurrence-free survival (RFS) (HR 7.2, 95% CI 1.5 to 72.4, p=0.04).

Conclusion

CXCR4 is expressed in the majority of primary AdCCs and independently correlated to worse RFS, suggesting CXCR4 as a target for imaging and therapy purposes in patients with advanced AdCC.

INTRODUCTION

Adenoid cystic carcinoma (AdCC) is an uncommon malignant epithelial tumour of the secretory glands in the head and neck region. It comprises approximately 10% of all salivary gland neoplasms and 20–35% of all salivary gland malignancies, and is the most common malignancy of the minor salivary glands. The major and minor salivary glands are equally affected, although reports are contradictory.[1–5] It arises in all age groups, with a peak incidence in the fifth and sixth decades, and women are slightly more affected.[1–3,5] AdCC originates from ductal (luminal) and basal/myoepithelial (abluminal) cells arranged in a glandular (cribriform), tubular or solid growth pattern.[6] Diagnosis can be enhanced by detecting fusion of the cellular *Myeloblastosis Gene (MYB)* to the transcription factor gene *NFIB*, which is present in the majority of AdCC cases.[1]

After surgery, adjuvant radiotherapy is usually indicated due to involved tumour margins and its typical perineural spread. A tendency for locoregional recurrence and late onset of indolent, slowly growing multiple distant metastases is reflected by local control rates of 58% and poor disease-specific survival of 54% after 10 years.[1,2,7,8]

Other negative prognosticators are advanced tumour stage, solid growth pattern, involvement of the skull base and perineural spread.[1-3] Local recurrences are difficult to cure due to previous surgical procedures and exceeded radiotherapy limits. There is only limited evidence on the efficacy of systemic chemotherapy or immunotherapy, and there is a need for alternative strategies.[9]

Chemokines (chemotactic cytokines) could have that potential. They play an important role in the immune system by chemotaxis of leucocytes during inflammatory response. Furthermore, chemokines perform a variety of functions, such as apoptosis and mitogenic and angiogenic activities and are therewith involved in embryogenesis, hematopoiesis, as well as tumour growth and metastasis.[10,11] Chemokines typically act as ligands to the G protein-coupled seven-transmembrane receptor domain. The chemokine receptor type 4 (CXCR4) is such a transmembrane receptor. The *CXCR4* gene is localized on chromosome 2 and was originally called leucocyte-expressed seven-transmembrane domain receptor (fusin). It was renamed CXCR4 when the homeostatic chemokine "stromal cell-derived factor 1 alpha", also known as CXC-chemokine ligand 12 (CXCL12), was identified as its natural ligand.[10,12,13] During embryonic development, CXCR4 is expressed on progenitor cells, and in the 1990s, it was discovered to serve as a co-entry receptor for HIV.[14] CXCL12 is expressed in different tissues and organs, including skin, lymph nodes, lung, intestine, liver, stromal cells and endothelial cells.[11,15,16]

Besides trafficking and homeostasis of immune cells and homing and retention of hematopoietic stem cells within the bone marrow, the CXCR4/CXCL12 receptor-ligand interaction plays a prominent role in tumourigenesis. CXCR4 overexpression is present in more than 20 human tumour types, including AdCC.[15–17] In addition, increased CXCR4 expression is in most tumours directly associated with an increased risk of local recurrence and distant metastases by promoting angiogenesis and migration of tumour cells, preferentially into metastatic sites that highly express CXCL12.[13] In the present study, we aimed to analyze CXCR4 expression in a large cohort of primary AdCC of the head and neck and the association with the above-mentioned prognosticators and outcome, that is, locoregional recurrence, distant metastases and survival.

PATIENTS AND METHODS

Patient selection

All consecutive patients diagnosed with AdCC in the University Medical Center Utrecht and Netherlands Cancer Institute-Antoni van Leeuwenhoek Hospital between 1990 and 2016 were retrospectively reviewed. Patients were selected if they had a histology-proven primary AdCC in the head and neck region and if their primary tumour tissue cores were incorporated in a previously fabricated tissue microarray (TMA). Patients with previous salivary gland disease and/or radiotherapy to the head or neck were excluded.

CXCR4 immunohistochemistry and expression analysis

Representative TMA paraffin sections 4 μm thick were immunohistochemically stained using fully automated protocols on the Benchmark XT (Ventana Medical Systems, Tucson, Arizona, USA). For the primary antibody, a mouse antihuman CXCR4 monoclonal antibody (LEAF Purified Mouse IgG2a, κ Isotype Ctrl, Biolegend) of the IgD2a isotype was used (dilution 1/800). The tissue sections were deparaffinized with ethanol and xylene, followed by pre-treatment with protease 1 (8 min) and subsequent primary antibody incubation for 32 min. Antigen antibody reactions were visualized using Ventana OptiView™ Universal DAB Detection Kit. Finally, the slides were counterstained with haematoxylin, dehydrated and mounted.

Semiquantitative scoring of the primary AdCC tumour samples was done in a blinded fashion by a dedicated head and neck pathologist (S.W.) and two researchers (T.K.N. and R.K.G.). Discrepant cases were discussed to reach consensus. The percentage of CXCR4-positive tumour cells per tumour core was scored in increments of 5%. Total

tumour CXCR4 expression of the arrayed cores was defined by the mean percentage of positive tumour cells out of the three cores. A core was considered inadequate when it contained <5% tumour tissue. Patients with less than two adequate cores were excluded to minimize tumour heterogeneity.[18]

Clinical parameters and tumour characteristics

The following clinical parameters were retrieved from the medical files: patient's gender, age at diagnosis, tumour site, treatment regimen, (time to) recurrence or metastasis, vital status (cause of death) and date of last follow-up until 1 January 2018. Recurrence-free survival (RFS) was defined as the interval from the operation to the detection of a locoregional disease recurrence. Two dedicated head and neck pathologists (S.W. and L.S.) re-examined all H&E-stained slides for the following parameters: type and diameter of the tumour, pathological T and N stages, histopathological growth pattern and associated grade (according to the differentiation of Perzin et al.[19]), surgical resection margins and the presence of perineural, vascular and bone invasion. When fluorescence in situ hybridization (FISH) had been applied to detect the *MYB::NFIB* fusion, the tumour was defined translocated when a break-apart signal was seen in >10% of the tumour cells of at least two arrayed cores.

Statistical analysis

Consistency of CXCR4 expression within the tumour was analyzed using the intraclass correlation coefficient (ICC), as earlier described.[20] Associations between CXCR4 expression and tumour characteristics were tested by calculating Spearman's rank correlation coefficient. The independent samples Kruskal-Wallis (KW) test was used to compare CXCR4 expression median between the primary tumours that did and did not recur or metastasize. CXCR4 expression was dichotomized by plotting receiver operating characteristic (ROC) curves. Differences in baseline characteristics of the groups divided by dichotomization were compared using Pearson's chi-square or Fisher's exact test with appropriate Bonferroni correction; KW was used in case of a continuous dependent parameter. Statistical analyses were performed using SPSS Statistics version 22.0 for Windows. Both univariate and multivariate survival analyses were carried out to calculate HRs with 95% CI. A Cox proportional hazards regression model was performed with SAS version 9.4. Firth's correction was applied to reduce bias of maximum likelihood estimation and, if needed, to deal with the occurrence of monotone likelihood in small-sample studies.[21] Discriminative ability of the model was assessed by computing Harrell's C-statistic.[22] A two-tailed p value of <0.05 was considered statistically significant for all analyses.

RESULTS

Patients, clinical parameters and tumour characteristics

Within the defined study period of 27 years, in total, 122 patients were diagnosed with AdCC of the head and neck. Seventy-three of them were previously randomly incorporated in a TMA. CXCR4 expression could be analyzed of 66 patients: one patient was excluded because of inadequate cores; six patients were excluded because they only had one available core. Close or positive resection margins were merged because only three tumours had close margins and the treatment regimen for these two groups is equal. Cohort characteristics are summarized in Table 1.

CXCR4 immunohistochemistry and expression analysis

CXCR4 expression in primary AdCC ranged from 0% to 100% (median 29%, IQR 1–70). Fourteen patients (19%) were CXCR4-negative and seven tumours (9%) showed 100% expression. In general, CXCR4 staining intensity of the matched cores per tumour was homogenous with limited spatial variability, which is reflected by a high single-core ICC of 0.89 ($p<0.01$). Different percentages of immunohistochemical staining are visualized in Figure 1. Spearman's rho correlation coefficients and CXCR4 medians for clinical parameters and pathological characteristics of the primary tumour were calculated and listed in Table 1. A significant correlation was found between high CXCR4 expression and perineural growth (Spearman ρ 0.26, $p=0.04$) and bone invasion (Spearman ρ 0.32, $p=0.01$).

Follow-up and survival analysis

Median follow-up (from diagnosis until 1 January 2018) was 55 months (IQR 32–98). Thirteen patients (20%) developed a locoregional recurrence, at a median of 42 months (IQR 21–95) after diagnosis. Distant metastases occurred in 18 patients (27%), at a median of 31 months (IQR 13–49). Metastatic sites were the lungs in 17 patients and isolated liver metastasis in 1 patient. Besides the lungs, bone metastases were found in four patients and liver metastases in three patients. Cohort and subgroup follow-up and survival data are summarized in Tables 2 and 3.

CXCR4 expression in the primary tumour was significantly higher in tumours that recurred compared with those that did not recur (median 60%, IQR 33–72 vs 12%, IQR 1–70, KW $p=0.01$). There was no difference in expression between primary tumours that did or did not metastasize to (the different) distant sites. Given the higher CXCR4 expression in tumours that recurred, dichotomization was carried out by plotting an ROC curve (Supplementary Figure 1) for CXCR4 expression by RFS.

The cut-off was defined at 25% (area under the curve 0.73), the dichotomized population characteristics (0–25% and >25%) were added to Tables 1 and 2. The >25% expression group was dominated by perineural growth and bone invading tumours (Pearson χ^2 p=0.02 and p=0.03, respectively). The difference in oral cavity tumour subsite did not reach statistical significance after Bonferroni correction for multiple comparisons.

Univariate RFS analyses were carried out for relevant prognosticators using the log-rank test as shown in Table 4. The multivariate Cox proportional hazards model showed a significant relation between >25% CXCR4 expression and worse RFS (HR 7.2, 95% CI 1.5 to 72.4, p=0.04). Postoperative radiotherapy extended RFS significantly (HR 25.1, 95% CI 1.9 to 339.9, p=0.03). The model incorporated growth pattern, bone invasion, perineural growth and resection margins, which were no individual predictors of RFS. Harrell's C-statistic of the predictive Cox proportional hazards model was 0.80, and that without CXCR4 expression was 0.73. Multivariate RFS survival graph is plotted in Figure 2A. CXCR4 expression was in multivariate analysis no prognosticator for overall survival (OS), disease-specific survival (DSS) and metastasis-free survival (MFS). Although statistical significance is not reached, the univariate MFS survival graph (Figure 2B) shows a clear divergent pattern starting 100 months after diagnosis in favour of the 0–25% CXCR4-expressing tumours. When other prognosticators are added to this model, the possible long-term relation between high CXCR4 expression and distant metastasis can, however, no longer be demonstrated.

Table 1. Cohort characteristics

	N (%)	Median (%) CXCR4	Associations (Spearman's ρ)	CXCR4 0–25%	CXCR4 >25%	χ^2 CXCR4 ≤25% vs >25%
PATIENTS	66	29		32 (48%)	34 (52%)	
Gender						
Male	24 (36%)	34	-0.10, p=0.43	11 (46%)	13 (54%)	p=0.75
Female	42 (64%)	27		21 (50%)	21 (50%)	
Age at diagnosis (years)						
Median (IQR)	59 (44–71)		-0.01, p=0.92	58 (42–71)	61 (49–71)	p=0.78
Range	20–89			20–89	29–83	
Site and subsite						
Major salivary gland	36 (55%)	17	0.21, p=0.10	21 (58%)	15 (42%)	p=0.08
Parotid gland	15	12		8	7	p=0.67
Submandibular gland	20	22		12	8	p=0.22
Sublingual gland	1	0		1	0	p=0.30
Minor salivary and seromucous gland	30 (45%)	58	0.21, p=0.10	11 (37%)	19 (63%)	p=0.08
Oral cavity (lip/buccal mucosa/ hard palate/gingival	11	83		2	9	p=0.03*
Oropharynx (soft palate/base of tongue)	6	19		3	3	p=0.94
Nasal cavity/nasopharynx/maxillary sinus	7	85		2	5	p=0.26
Larynx/trachea	3	0		3	0	p=0.07
Lacrimal gland	2	72		0	2	p=0.16
External auditory canal	1	0		1	0	p=0.30
TUMOUR						
pT-stage (TNM 7th ed.)						
pT1	19	21	0.14, p=0.26	11	8	p=0.33
pT2	24	39		9	15	p=0.18
pT3	3	12		3	0	p=0.07
pT4a	14	49		6	8	p=0.64
pT4b	6	30		3	3	p=0.94
Nodal status						
pN0	59 (89%)	23	0.07, p=0.59	30 (51%)	29 (49%)	p=0.27
pN+	7 (11%)	60		2 (29%)	5 (71%)	
Distant metastasis						
cM0	65 (98%)	30				
cM1	1 (2%)	8				
Resection margins						
Clear (≥5 mm)	13 (20%)	38	-0.02, p=0.89	5 (38%)	8 (62%)	p=0.54
Close or positive (<5 mm)	53 (80%)	23		27 (51%)	26 (49%)	
Perineural growth†						
Present	47 (71%)	38	0.26, p=0.04	19 (40%)	28 (60%)	p=0.02
Absent	18 (27%)	3		13 (72%)	5 (28%)	

Vaso-invasive growth						
Present	10 (15%)	49	0.15, p=0.23	4 (40%)	6 (60%)	p=0.53
Absent	55 (83%)	23		28 (51%)	27 (49%)	
Bone invasion†						
Present	16 (24%)	74	0.32, p=0.01	4 (25%)	12 (75%)	p=0.03
Absent	50 (76%)	20		28 (56%)	22 (44%)	
Growth pattern (Perzin grade[19])						
Tubular (grade 1)	30 (46%)	35	-0.02, p=0.89	14 (47%)	16 (53%)	p=0.79
Cribriform; <30% solid (grade 2)	26 (39%)	10		15 (58%)	11 (42%)	p=0.23
Solid (grade 3)	10 (15%)	38		3 (30%)	7 (70%)	p=0.20
***MYB::NFIB* fusion**						
Present	28 (42%)	11	-0.09, p=0.53	17 (61%)	11 (39%)	p=0.33
Absent	20 (30%)	27		10 (51%)	10 (49%)	
TREATMENT						
Adjuvant radiotherapy						
Yes	63 (96%)	23	-0.14, p=0.27	32 (51%)	31 (49%)	p=0.09
No	3 (4%)	53		0	3 (100%)	

*Statistically not significant due to multiple comparisons. †Association is considered statistically significant.

Figure 1. Immunohistochemical CXCR4 expression in AdCC. *Magnification: 200x.*

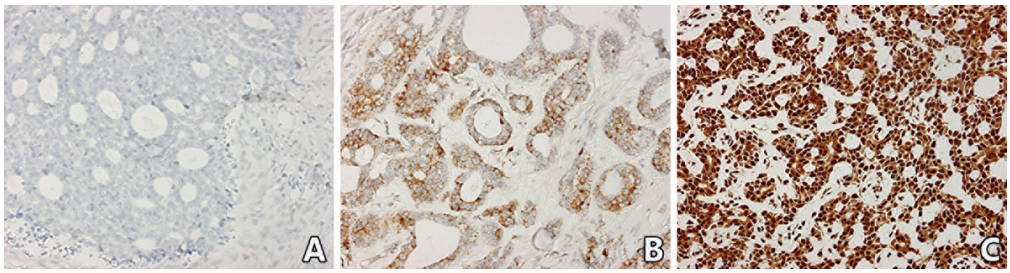

(**A**) negative; (**B**) 30% positive; (**C**) 100% positive.

Table 2. Survival data

Survival by disease recurrence	N	DOD (%)	Median months
Locoregional recurrence only	6	2 (33%)	140
Distant metastases only	11	6 (55%)	51
Locoregional recurrence and distant metastases	7	6 (86%)	62
Cohort survival	**N affected**	**Median months**	**% survival**
Overall survival			
5-year	16	34	76%
10-year	18	37	73%
Disease-specific survival			
5-year	10	38	85%
10-year	12	51	82%
Locoregional recurrence-free survival			
5-year	9	35	86%
10-year	11	37	83%
Metastasis-free survival			
5-year MFS	14	20	79%
10-year MFS	17	28	74%

DOD: died of disease

DISCUSSION

The present study demonstrates CXCR4 expression in 81% of primary AdCC samples with a median of 29% (IQR 1–70) positive cells. Interpretation of the used TMA was reliable with a high single-core ICC of 0.89 ($p<0.01$), indicating that one single-core is sufficiently reliable to determine the CXCR4 expression status of the whole tumour. CXCR4 expression of the primary tumour is significantly higher in tumours that recur (KW $p=0.01$) and is significantly associated with perineural spread and bone invasion. Tumour expression >25% is independently correlated with reduced RFS (HR 7.2, 95% CI 1.5 to 72.4, $p=0.04$).

The reported high expression by immunohistochemistry and present intracellular localization of CXCR4 in primary AdCC corresponds to the results of other smaller studies on this rare topic.[16,17,23]

A solid growth pattern is associated with a worse OS and DSS (data not shown) and is in accordance with the literature.[2,3] Various studies, however, report differently regarding an increased risk of locoregional recurrence in case of a more solid growth pattern (Perzin grade 2 or 3), which is not observed in the present results.[1,2,24] A (linear) correlation between increased CXCR4 expression and AdCC growth pattern as reported by Zushi et al.[16] in a small series was disputed by Phattarataratip and Dhanuthai[23] and also not confirmed in this study. Interestingly, only one out of the present 14 CXCR4-negative tumours was classified Perzin grade 3 (solid growth pattern) and none of these 14 patients developed a locoregional recurrence during a median follow-up of 55 months. An increased metastatic potential by increase of CXCR4 expression could additionally not be confirmed by our results, although primary tumours that metastasized showed a higher (but statistically not significant) median CXCR4 expression (49% vs 23%). The metastatic spread of tumours is thought to be the result of a process critically regulated by chemokines and their receptors. CXCR4 has been shown to play an essential role in the metastatic spread of tumour cells to distant organs, as cells migrate along the gradient of the CXCR4-ligand CXCL12. This has also been confirmed in AdCC.[13,15,17] Moreover, an important mechanism that alters the metastatic behaviour of tumour cells in vivo is hypoxia, which enhances angiogenesis and upregulation of CXCR4 via the hypoxia-inducible factor-1α (HIF-1α).[13,15] Opposite AdCC inhibitory effects by downregulation of HIF-1α in AdCC have recently been described.[25]

The typical AdCC distant metastatic sites (lungs, liver and bone) show peak levels of CXCL12 expression and as a consequence one could have expected a significant correlation between high expression and metastatic spread.[11]

Table 3. Follow-up

	N (%)	Primary tumour median % CXCR4	CXCR4 0–25%	CXCR4 >25%	χ^2 CXCR4 ≤25% vs >25%
Patients	66		32	34	
Follow-up (median months; IQR)	55; 32–98		57; 42–83	53; 31–137	p=0.63
Locoregional recurrence					
Yes	13 (20%)	60 % *	1 (3%)	12 (35%)	p<0.01
No	53 (80%)	12 % *	31 (97%)	22 (65%)	
Distant metastasis					
Yes	18 (27%)	49 %	7 (22%)	11 (32%)	p=0.33
No	48 (73%)	23 %	25 (78%)	23 (68%)	

* difference is considered statistically significant (KW p=0.01)

In this study, distant metastases were identified median after 31 months and were equally distributed between the high and low expression groups (Table 2). However, Figure 2B depicts a (non-significant) divergent pattern starting 100 months after diagnosis indicating a worsened long-term MFS for the >25% CXCR4-expressing tumours. Significance might not have been reached due to the relatively small study population and short median follow-up time of 55 months, which are possibly insufficient to evaluate the (very) late onset of clinically irrelevant small and indolent distant AdCC metastases.[3]

In contrast to the frequent hematogenous dissemination, AdCC lymph node metastases are less common despite the high CXCL12 expression of lymph node stromal cells. One explanatory theory states that CXCL12 is involved in homing of memory T-cells via the bloodstream, and not via the lymphatic veins.[17] Studies on different (adeno-) carcinomas, however, did report an increased risk of both nodal metastases and local disease recurrence in case of high primary tumour CXCR4 expression.[26,28] This is not reflected by the present results as eventually only in 20% of patients' lymph nodes were involved: seven at diagnosis and six more cases during follow-up, of which five also developed distant metastases. It was subsequently argued that high tumour CXCR4 expression is associated with worse biological parameters and aggressive behaviour, resulting in an increased risk of disease progression, eventually leading to a worsened survival.[28]

Table 4. Recurrence-free survival analysis

	Locoregional recurrences / N (%)	RFS Univariate log-rank	RFS Multivariate Hazard Ratio ; 95% CI
CXCR4			
0–25%	1 / 32 (3%)	7.9 (p<0.01)	7.2 ; 1.5–72.4 (p=0.04)
>25%	12 / 22 (55%)		
Adjuvant radiotherapy			
Yes	12 / 63 (19%)	19.0 (p<0.01)	25.1 ; 1.9–339.9 (p=0.03)
No	1 / 3 (33%)		
Resection margins			
Clear (≥5 mm)	1 / 13 (8%)	0.5 (p=0.49)	2.0 ; 0.4–20.6 (p=0.49)
Close or positive (<5 mm)	12 / 53 (23%)		
Perineural growth			
Present	11 / 47 (23%)	1.8 (p=0.18)	1.0 ; 0.2–6.3 (p=0.97)
Absent	2 / 18 (11%)		
Bone invasion			
Present	4 / 16 (25%)	0.3 (p=0.59)	0.7 ; 0.2–2.7 (p=0.68)
Absent	9 / 50 (18%)		
Growth pattern			
Tubular	5 / 30 (17%)	3.2 (p=0.20)	2.6 ; 0.5–12.1 (p=0.26)
Cribriform	5 / 26 (19%)		
Solid	3 / 10 (30%)		

In a study on colon carcinoma, it was specifically hypothesized that by tumour alteration to a migratory phenotype, CXCL12-producing normal intestine epithelial cells would become at high risk of recurrence. Normal salivary gland cells, however, do not or at most weakly express CXCR4, but interestingly, CXCL12 was found to be expressed in areas of inflamed reactive salivary gland ductal epithelial cells and surrounding vessels in Sjögren's syndrome.[16,29,30] Inflammation around the AdCC tumour border with possible associated upregulation of CXCL12 may therefore play a role in the development of a recurrence in high CXCR4-expressing AdCCs.

CXCR4 is correlated to perineural growth and bone invasion, Spearman ρ 0.26 (p=0.04) and 0.32 (p=0.01), respectively. The latter could possibly be explained by involvement of the CXCL12/CXCR4 axis in mediating osteolysis by the tumour as CXCL12 has been recognized to stimulate migration of osteoclast precursors and upregulation of several pro-osteoclastic genes.[31] Both perineural growth and bone invasion are not associated

with locoregional recurrence as shown in multivariate analysis and in accordance with the literature.[2] Perineural invasion is not correlated to involved resection margins and postoperative radiotherapy, which are mutually strongly correlated (Spearman ρ 0.37, p=0.01). Remarkably also, other patient and tumour characteristics as pT stage, tumour site and adjuvant radiotherapy did not differ significantly between free, close and positive resection margins (data not shown). Merging the patients with close and positive margins was therefore considered reliable.

A deep locoregional recurrence is a relevant problem in the management of AdCC in the case of functional irresectability or exceeding radiation limits. Conventional treatment options are no longer applicable and the results of (combinations of) chemotherapeutic or new targeted agents are limited.[9] Remarkably, cisplatin, a chemotherapeutic agent frequently used in head and neck malignancies, induces chemotherapy resistance itself by directly providing survival signals to tumour cells and indirectly by upregulation of CXCR4, which again promotes so-called "prosurvival" pathways. In addition, CXCL12 reduces apoptosis induced by cisplatin in AdCC cells.[17] The current study presents CXCR4 as a new independent prognosticator for AdCC and may advocate comprehensive and aggressive treatment combined with stringent follow-up in CXCR4-positive tumours. Furthermore, CXCR4 may act as specific target for diagnostic and therapeutic purposes in AdCC. Antagonist drug AMD3100 and multiple other anti-CXCR4 peptides, antibodies and low-molecular-weight agents have been investigated and proven to inhibit or delay cancer progression in various tumour sites, and furthermore improved sensitization of tumour cells to conventional

Figure 2. Impact of CXCR4 expression on survival.

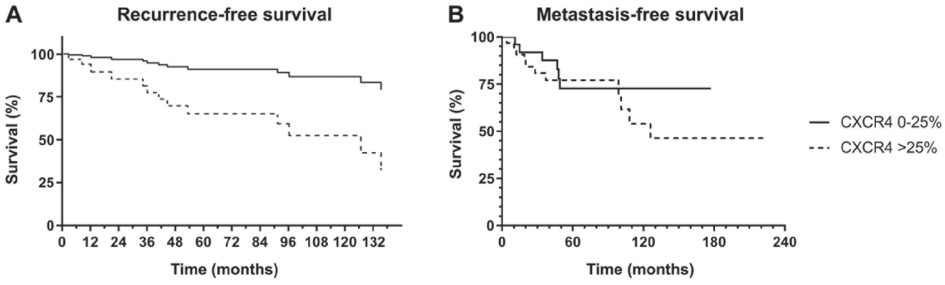

(A) Multivariate Cox regression survival graph showing a worsened recurrence-free survival regarding high (>25%) versus low (0–25%) CXCR4 expression (HR 7.2, 95% CI 1.5–72.4, p=0.04). (B) Univariate survival graph showing a non-significant diverging pattern indicating a worsened long-term MFS in high (>25%) CXCR4-expressing tumours.

chemotherapy for combined treatment.[13,15,28] Radiolabelled CXCR4 ligands have now been developed for positron emission tomography (PET)-specific imaging, which also makes these targets suitable for potential radionuclide treatment in the future.[32,33] Further research is necessary to delineate whether CXCR4 expression in AdCC is preserved in recurrent and distant tissues, and whether primary, recurrent and/or distant AdCC tumour sites are depicted on CXCR4-targeted PET/CT.

CONCLUSION

CXCR4 expression is present on 81% of primary head and neck AdCC samples in a retrospective cohort of 66 cases. High primary tumour CXCR4 expression of >25% is independently associated with worse RFS. Based on the expression levels provided by the present study, CXCR4 is a potential target for targeted imaging and possibly radionuclide therapy in AdCC.

Supplementary Figure 1. ROC curve showing the association between CXCR4 expression and RFS.

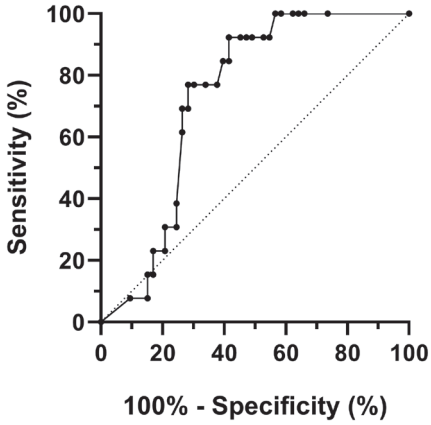

REFERENCES

1. Coca-Pelaz A, Rodrigo JP, Bradley PJ, et al. Adenoid cystic carcinoma of the head and neck - An update. Oral Oncol. 2015;51(7):652-661.
2. Jang S, Patel PN, Kimple RJ, McCulloch TM. Clinical Outcomes and Prognostic Factors of Adenoid Cystic Carcinoma of the Head and Neck. Anticancer Res. 2017;37(6):3045-3052.
3. Spiro RH, Huvos AG, Strong EW. Adenoid cystic carcinoma of salivary origin. A clinicopathologic study of 242 cases. Am J Surg. 1974;128(4):512-520.
4. Bradley PJ. Adenoid cystic carcinoma of the head and neck: a review. Curr Opin Otolaryngol Head Neck Surg. 2004;12(2):127-132.
5. Bjørndal K, Krogdahl A, Therkildsen MH, et al. Salivary gland carcinoma in Denmark 1990-2005: A national study of incidence, site and histology. Results of the Danish Head and Neck Cancer Group (DAHANCA). Oral Oncol. 2011;47(7):677-682
6. Hellquist H, Skalova A. Adenoid Cystic Carcinoma. In: Histopathology of the Salivary Glands. Springer Berlin Heidelberg; 2014:221-260.
7. Huang M, Ma D, Sun K, Yu G, Guo C, Gao F. Factors influencing survival rate in adenoid cystic carcinoma of the salivary glands. Int J Oral Maxillofac Surg. 1997;26(6):435-439.
8. van Weert S, Reinhard R, Bloemena E, et al. Differences in patterns of survival in metastatic adenoid cystic carcinoma of the head and neck. Head Neck. 2017;39(3):456-463.
9. Alfieri S, Granata R, Bergamini C, et al. Systemic therapy in metastatic salivary gland carcinomas: A pathology-driven paradigm? Oral Oncol. 2017;66:58-63.
10. Zlotnik A, Yoshie O. The Chemokine Superfamily Revisited. Immunity. 2012;36(5):705-712.
11. Wang Z, Sun J, Feng Y, Tian X, Wang B, Zhou Y. Oncogenic roles and drug target of CXCR4/CXCL12 axis in lung cancer and cancer stem cell. Tumor Biol. 2016;37(7):8515-8528.
12. Oberlin E, Amara A, Bachelerie F, et al. The CXC chemokine SDF-1 is the ligand for LESTR/fusin and prevents infection by T-cell-line-adapted HIV-1. Nature. 1996;382(6594):833-835.
13. Vandercappellen J, Van Damme J, Struyf S. The role of CXC chemokines and their receptors in cancer. Cancer Lett. 2008;267(2):226-244.
14. Feng Y, Broder CC, Kennedy PE, Berger EA. HIV-1 entry cofactor: functional cDNA cloning of a seven-transmembrane, G protein-coupled receptor. Science. 1996;272(5263):872-877.
15. Domanska UM, Kruizinga RC, Nagengast WB, et al. A review on CXCR4/CXCL12 axis in oncology: No place to hide. Eur J Cancer. 2013;49(1):219-230.
16. Zushi Y, Noguchi K, Hashitani S, et al. Relations among expression of CXCR4, histological patterns, and metastatic potential in adenoid cystic carcinoma of the head and neck. Int J Oncol. 2008;33(6):1133-1139.
17. Muller A, Sonkoly E, Eulert C, et al. Chemokine receptors in head and neck cancer: Association with metastatic spread and regulation during chemotherapy. Int J Cancer. 2006;118(9):2147-2157.
18. Goethals L, Perneel C, Debucquoy A, et al. A new approach to the validation of tissue microarrays. J Pathol. 2006;208(5):607-614.
19. Perzin KH, Gullane P, Clairmont AC. Adenoid cystic carcinomas arising in salivary glands: a correlation of histologic features and clinical course. Cancer. 1978;42(1):265-282.
20. Noorlag R, van Es RJJ, de Bree R, Willems SM. Cytokeratin 19 expression in early oral squamous cell carcinoma and their metastasis: Inadequate biomarker for one-step nucleic acid amplification implementation in sentinel lymph node biopsy procedure. Head Neck. 2017;39(9):1864-1868.

21. Heinze G, Dunkler D. Avoiding infinite estimates of time-dependent effects in small-sample survival studies. Stat Med. 2008;27(30):6455-6469.
22. Harrell FEH, Lee KL, Mark DB. Multivariable prognostic models: issues in developing models, evaluating assumptions and adequacy, and measurin and reducing errors. Stat Med. 1996;15(4):361-387.
23. Phattarataratip E, Dhanuthai K. Expression of C-X-C motif chemokine receptors 4 and 7 in salivary gland neoplasms. Arch Oral Biol. 2017;83:136-144.
24. Zhang CY, Xia RH, Han J, et al. Adenoid cystic carcinoma of the head and neck: Clinicopathologic analysis of 218 cases in a Chinese population. Oral Surg Oral Med Oral Pathol Oral Radiol. 2013;115(3):368-375.
25. Xiao C, Pan Y, Zeng X, et al. Downregulation of hypoxia-inducible factor-1α inhibits growth, invasion, and angiogenesis of human salivary adenoid cystic carcinoma cells under hypoxia. Oncol Rep. 2018;40(3):1675-1683.
26. Kato M, Kitayama J, Kazama S, Nagawa H. Expression pattern of CXC chemokine receptor-4 is correlated with lymph node metastasis in human invasive ductal carcinoma. Breast Cancer 2003;5(5):R144–R150.
27. Yoshitake N, Fukui H, Yamagishi H, et al. Expression of SDF-1α and nuclear CXCR4 predicts lymph node metastasis in colorectal cancer. Br J Cancer. 2008;98(10):1682-1689.
28. Chatterjee S, Behnam Azad B, Nimmagadda S. The intricate role of CXCR4 in cancer. Adv Cancer Res. 2014;124:31-82.
29. Yopp AC, Shia J, Butte JM, et al. CXCR4 expression predicts patient outcome and recurrence patterns after hepatic resection for colorectal liver metastases. Ann Surg Oncol. 219(Suppl 3);339–346.
30. Barone F, Bombardieri M, Rosado MM, et al. CXCL13, CCL21, and CXCL12 Expression in Salivary Glands of Patients with Sjogren's Syndrome and MALT Lymphoma: Association with Reactive and Malignant Areas of Lymphoid Organization. J Immunol. 2008;180(7):5130-5140.
31. Coniglio SJ. Role of tumor-derived chemokines in osteolytic bone metastasis. Front Endocrinol (Lausanne). 2018;9:313.
32. Gourni E, Demmer O, Schottelius M, et al. PET of CXCR4 Expression by a 68Ga-Labeled Highly Specific Targeted Contrast Agent. J Nucl Med. 2011;52(11):1803-1810.
33. Schottelius M, Osl T, Poschenrieder A, et al. [177Lu]pentixather: Comprehensive preclinical characterization of a first CXCR4-directed endoradiotherapeutic agent. Theranostics. 2017;7(9):2350-2362.

Prostate-specific membrane antigen (PSMA) expression in adenoid cystic carcinoma of the head and neck

Thomas J.W. Klein Nulent
Matthijs H. Valstar
Laura A. Smit
Ludwig E. Smeele
Nicolaas P.A. Zuithoff
Bart de Keizer
Remco de Bree
Robert J.J. van Es
Stefan M. Willems

Chapter as published in:
BMC Cancer 2020; 20(1): 519

doi: 10.1186/s12885-020-06847-9

ABSTRACT

Background

Treatment options for advanced head and neck adenoid cystic carcinoma (AdCC) are limited. Prostate-specific membrane antigen (PSMA), a transmembrane protein that is known for its use in diagnostics and targeted therapy in prostate cancer, is also expressed by AdCC. This study aimed to analyze PSMA expression in a large cohort of primary, recurrent and metastasized AdCC of the head and neck.

Methods

One hundred ten consecutive patients with histologically confirmed AdCC in the period 1990–2017 were included. An analysis was made of clinical details, revised pathology and semiquantitative immunohistochemical expression of PSMA on tissue microarray and whole slides. Associations of PSMA expression with clinicopathological parameters were explored and survival was analyzed by multivariate Cox proportional hazards analysis.

Results

PSMA expression was present in 94% of the 110 primary tumours, with a median of 31% positive cells (IQR 15–60%). Primary tumours (N=18) that recurred (N=15) and/or had metastases (N=10) demonstrated 40, 60 and 23% expression respectively. Expression was not independently related to increased pathological stage, tumour grade, and the occurrence of locoregional recurrence or metastasis. After dichotomization, only primary tumour PSMA expression ≤10% appeared to be associated with reduced 10-years recurrence-free survival (HR 3.0, 95% CI 1.1–8.5, p=0.04).

Conclusion

PSMA is highly expressed in primary, recurrent and metastatic AdCC of the salivary and seromucous glands. PSMA expression has no value in predicting clinical behaviour of AdCC although low expression may indicate a reduced recurrence-free survival. This study provides supporting results to consider using PSMA as target for imaging and therapy when other diagnostic and palliative treatment options fail.

BACKGROUND

The prostate-specific membrane antigen (PSMA) is a transmembrane glycoprotein of the prostate secretory acinar epithelium that is upregulated in prostate cancer (PC) and known from its use in diagnostics and targeted therapy in metastatic PC.[1,4] Besides tracer accumulation in prostate tissue, PSMA PET/CT depicts physiological uptake in the salivary and lacrimal glands, liver and kidneys, but also in benign and malignant neoplasms, mostly adenomas and (adeno)carcinomas, of glandular or epithelial origin.[5,6] In PC, increased intracellular PSMA expression by immunohistochemistry is related to increased pathological grade, and subsequently correlated with disease-related mortality.[1,4] Malignancies other than PC also express PSMA but in endothelial cells of tumours' neovasculature, which suggests PSMA involvement in tumour angiogenesis. In salivary glands PSMA was identified on the acinar cells in the epithelium.[3,7,9] Recently, PSMA PET/CT analysis in a series of patients with head and neck adenoid cystic carcinoma (AdCC) showed tracer uptake in areas of locoregional recurrent and distant metastatic AdCC, and expression was confirmed immunohistochemically.[10] AdCC is the most common malignant secretory gland tumour in the head and neck region. Incidence peaks in the fifth and sixth decade and has a female predominance.[11,15] AdCC originates from ductal (luminal) and basal/myoepithelial (abluminal) cells and typically arises in the major salivary glands, the minor salivary and seromucous glands of the lip and upper aerodigestive tract, but also in the lacrimal and ceruminous glands. The tumour is characterized by an indolent but persistent growth rate, frequent locoregional recurrence and a delayed silent onset of distant metastasis, mainly in the lungs.[11,15,17] Surgery is the primary treatment, frequently followed by adjuvant radiation therapy because of positive resection margins and typical perineural growth. Although radiotherapy has probably no benefit to survival, it is reported to improve local and regional control.[15,16] Disease-specific survival (DSS) is moderate, with five and 10 year survival rates of 68–78% and 54–65% respectively.[18,19] Survival is negatively affected by the occurrence of an irresectable locoregional recurrence, which is considered clinically more relevant than the occurrence of slowly growing —often pulmonary and osseous— distant metastases that develop in almost half of the patients within 5 years after diagnosis.[11,16,18] Other negative prognostic factors are advanced tumour stage, inadequate resection margins, skull base involvement and a solid growth pattern on histopathology. Perineural invasion does not directly affect mortality, but is significantly correlated with metastatic disease.[11,15] Regular treatment options are limited in advanced recurrent or metastasized disease.[16] Given the positive results of PSMA-targeted diagnostic and treatment modalities in PC, this study aimed to analyze PSMA expression in a large cohort of primary and corresponding recurrent

and metastatic AdCC tissues of the head and neck.[20] Secondly, we aimed to explore associations with patient- and tumour characteristics and outcome, analogous to PC.

METHODS

Patient selection

All patients diagnosed with AdCC in the University Medical Center Utrecht and Netherlands Cancer Institute-Antoni van Leeuwenhoek Hospital between 1990 and 2017 were analyzed in a retrospective cohort study. Patients were selected in case of a histology-proven primary AdCC in the head and neck region with available representative formaldehyde-fixed paraffin embedded tissue blocks of the resection specimen. Tumour samples of available corresponding locoregional recurrences or distant metastases were collected. Patients with previous (non-AdCC) salivary gland disease, radiotherapy to the head or neck, or incomplete data were excluded. All data and samples were handled according to the GDPR.

Clinical parameters and tumour characteristics

The following clinical parameters were retrieved from the medical files: patient's gender, age at diagnosis, tumour site, treatment regimen, (time to) recurrence or metastasis, vital status (cause of death) and date of last follow-up until January 1st 2018. Two dedicated head and neck pathologists (S.W. and L.S.) re-examined all haematoxylin- and eosin-stained slides for the following parameters: type and diameter of the tumour, pathological T- and N-stage, histopathological growth pattern and associated grade according to the differentiation of Perzin et al.[21], surgical resection margins and the presence of perineural, vascular and bone invasion.

PSMA immunohistochemistry

A tissue microarray (TMA) was used to assess PSMA expression. From each tumour, three central 0.6 mm tissue cylinders from vital tumour were incorporated and covered the different aspects of this tumour morphology. Tumour whole-slides were analyzed when patient's tissue was not incorporated in the microarray, as well as whole-slides of all available recurrent and distant tissues. Representative TMA or whole slide paraffin sections 4 µm thick were immunohistochemically stained using fully automated protocols on the Benchmark XT (Ventana Medical Systems, Tucson, AZ, USA), validated for diagnostic purposes. Incorporated as control tissues were prostate cancer, normal salivary gland and duct tissue.

For the primary antibody, a mouse antihuman PSMA monoclonal antibody was used (3E6; DAKO, Carpinteria, CA) of the IgG1 isotype directed against the internal domain of the PSMA antigen (DAKO, cat. no. M3620, Carpinteria, CA, dilution 1/80). The tissue sections were deparaffinized with xylene and ethanol followed by Heat Induced Epitope Retrieval in Ventana Cell Conditioning 1 for 24 min and subsequently incubated with the primary antibody for 60 min. Antigen-antibody reactions were visualized using Ventana OptiView™ Amplification kit, followed by Ventana OptiView™ Universal DAB Detection Kit (Optiview HQ Linker 8 min, Optiview HRP Multimer 8 min, Optiview Amplifier H2O2/Amplifier 4 min, Optiview Amplifier Multimer 4 min). Finally the slides were counterstained with haematoxylin, dehydrated and mounted.

PSMA expression analysis

Blinded semiquantitative scoring of all selected primary, recurrent and distant AdCC tumour samples was done until consensus was reached by two head and neck pathologists and two researchers (S.W., L.S., T.K.N. and M.V.). Per tumour core or whole slide the localization of PSMA-positive tumour cells was noted, followed by scoring the percentage of positive tumour cells in increments of 5%. Total tumour PSMA expression of the arrayed cores was defined by the mean percentage of PSMA-positive tumour cells of the three tissue cores. A core was considered inadequate when it contained <5% tumour tissue. In case of a mean PSMA expression below 10% or in case of more than 1 inadequate core on microarray, one representative tumour whole slide was subsequently stained and scored in order to exclude false-negative results.

Statistical evaluation

Continuous and ordinal variables were reported as medians with interquartile ranges (IQR), categorical variables were reported as the number of patients and percentages. Associations between PSMA expression and all clinical parameters and tumour characteristics, except when categorical with more than 3 categories, were estimated with Spearman's rho correlation coefficient with corresponding p-values. The Independent Samples Kruskal-Wallis test (KW) was used to compare expression distribution between patients' primary tumours, which recurred or metastasized and those that did not. Subsequently, the median expression of corresponding primary, recurrent and distant samples was compared. A cut-off level for the prediction of overall survival (OS), DSS, locoregional recurrence-free survival (RFS), and metastasis-free survival (MFS) was determined by dichotomizing PSMA expression and plotting receiver operating characteristic (ROC) curves. Differences in baseline characteristics of the groups divided by dichotomization were compared using Pearson's chi-square

test with appropriate Bonferroni correction. Statistics were performed using SPSS Statistics (version 22.0, IBM Corp., Armonk, NY, USA) for Windows. Multivariate OS, DSS, RFS and MFS survival analyses were carried out to calculate hazard ratios with 95% confidence interval (CI). A Cox proportional hazards regression model was created by using SAS software (version 9.4, SAS Institute Inc., Cary, NC, USA) for Windows. Firth's correction was applied to reduce bias of maximum likelihood estimation, as it deals with the occurrence of monotone likelihood in small-sample studies with time-dependent effects.[22] Discriminative ability of the model was assessed by computing Harrell's C-statistic.[23] A two-tailed p-value <0.05 was considered statistically significant for all analyses.

RESULTS

Patients, clinical parameters and tumour characteristics

In total 122 newly diagnosed patients with AdCC of the head and neck were identified within the 27-year period, of whom 12 were excluded because of incomplete data. From 110 patients the clinical history and histopathological samples of the primary tumour were available for analysis and summarized in Table 1.

PSMA immunohistochemistry

Samples of 73 out of 110 patients were available for TMA immunohistochemistry. Of the remaining 37 primary tumours and available locoregional (N=15) and distant (N=10) tumour samples whole-slides were separately stained and scored. Expression was seen intracellular in a granular fashion, mainly cytoplasmic, or concentrated at the luminal side of the cell membrane. No conclusive staining pattern within the cells was observed. The staining intensity was consistent and there was limited spatial variability. Staining of the whole slides and microarray cores were comparable and therefore usage of this TMA was considered reliable. TMA analysis of 14 tumours was unsuccessful due to inadequate cores, and 21 tumours initially scored 0–10% expression. Matched whole slides of these 35 tumours were subsequently stained and PSMA expression was adjusted in six cases with conflicting (>10% difference) results. Different immunohistochemistry examples are visualized in Figure 1.

PSMA expression analysis in primary AdCC

In 103 out of 110 primary tumours (94%) PSMA was expressed with median 31% positive tumour cells (IQR 15–60%). Median PSMA expression and Spearman's rho correlation coefficients for all clinical parameters and pathological characteristics are listed in Table 1. Although no strong associations were found, Spearman's rho analysis revealed a significant association between PSMA expression and both tumour subsite and bone invasion. The minor salivary glands demonstrated less PSMA expression than the major salivary glands (21 vs 50% median expression; $p<0.01$) and tumours invading bone showed less PSMA expression (17 vs 39% median expression; $p=0.04$). However, tumour subsite and bone invasion are mutually strongly correlated (Pearson's chi-square test $p<0.01$) as all except one of the tumours invading bone originated from the minor salivary glands. Median PSMA expression did not differ between the subgroups of tumour site, pathological tumour stage (pT-stage) and Perzin grade. Furthermore, primary tumour PSMA expression medians of distant metastasis seem higher, but did not differ statistically from the distribution of those who remained disease-free (Table 2).

PSMA expression analysis in recurrent and distant metastatic AdCC

Fifteen locoregional recurrent and 10 distant metastatic tissue samples could be retrieved from 18 patients. Nine of these 18 patients developed only locoregional recurrence(s), 6 patients developed only distant metastases and 3 patients developed both a recurrence and metastases. Distant metastatic tissues were lung (3 cases), leptomeningeal (3 cases), bone (1 case), liver (1 case), peritoneum (1 case) and skin (1 case). Positive PSMA expression was seen in 12/15 (80%) recurrent and 9/10 (90%) distant samples that ranged from 5 to 100%. All together, the median PSMA expression of the recurrent samples was 60% (IQR 30–90%) and of all metastatic samples 23% (IQR 10–55%). When these were compared to the expression of their corresponding 18 primary tumours (40% median expression; IQR 15–70%), there was a (non-significant) tendency of increased expression in recurrences and decreased expression in distant metastases. Expression patterns of corresponding tumour samples are visualized in Supplementary Figure 1.

Table 1. Cohort characteristics

	N (%)	Median % PSMA	Spearman's ρ; p-value	PSMA ≤10%	PSMA >10%	χ^2 PSMA ≤10% vs >10%
PATIENTS	110	31%		23 (21%)	87 (79%)	
Gender						
Male	36 (33%)	30%	0.11; p=0.24	7 (19%)	29 (81%)	p=0.79
Female	74 (67%)	45%		16 (22%)	58 (78%)	
Age at diagnosis						
Median (IQR)	57 (45–68)		0.08; p=0.42	56 (50–70)	58 (43–68)	p=0.45
Range	20–90			34–87	20–90	
Site and subsite						
*Major salivary gland	59 (54%)	50%	-0.25; p<0.01	7 (12%)	52 (88%)	p=0.01
*Minor salivary and seromucous gland	51 (46%)	21%		16 (31%)	35 (69%)	
Parotid gland	26	50%		2	24	p=0.06
Submandibular gland	30	35%		5	25	p=0.50
Sublingual gland	3	57%		0	3	p=0.37
Oral cavity (lip/buccal mucosa/hard palate/gum)	21	19%		7	14	p=0.12
Oropharynx (soft palate/base of tongue)	8	21%		1	7	p=0.54
Nasal cavity/nasopharynx/maxillary sinus	15	10%		8	7	p<0.01
Larynx/trachea	3	42%		0	3	p=0.37
Lacrimal gland	2	35%		0	2	p=0.46
External auditory canal	2	40%		0	2	p=0.46
TUMOUR						
pT-stage (TNM 7th ed.)						
pT1	35	50%		5	30	p=0.24
pT2	39	33%		7	32	p=0.57
pT3	5	20%	-0.18; p=0.06	1	4	p=0.96
pT4a	23	30%		6	17	p=0.49
pT4b	8	13%		4	4	p=0.04
Nodal status						
pN0	99 (90%)	33%	-0.09; p=0.37	20 (20%)	79 (80%)	p=0.58
pN+	11 (10%)	25%		3 (27%)	8 (73%)	
Distant metastasis						
cM0	108	31%	-0.01; p=0.90	23 (21%)	85 (79%)	p=0.62
cM1	2	36%		0 (0%)	2 (100%)	
Resection margin						
clear (≥5 mm)	20 (18%)	50%		2 (10%)	18 (90%)	p=0.18
close (1–5 mm)	4 (4%)	20%	-0.08; p=0.43	2 (50%)	2 (50%)	p=0.14
positive (<1 mm)	86 (78%)	30%		19 (22%)	67 (78%)	p=0.56
Perineural growth						
Present	76 (69%)	30%	-0.02; p=0.86	14 (18%)	62 (82%)	p=0.44
Absent	32 (31%)	45%		8 (25%)	24 (75%)	

Vaso-invasive growth						
Present	17 (15%)	30%	-0.05; p=0.64	5 (29%)	12 (71%)	p=0.33
Absent	90 (82%)	33%		17 (19%)	73 (81%)	
***Bone invasion**						
Present	27 (25%)	17%	-0.20; p=0.04	10 (37%)	17 (63%)	p=0.02
Absent	82 (75%)	39%		13 (16%)	69 (84%)	
Growth pattern (Perzin grade[21])						
Tubular (grade 1)	46 (42%)	30%		10 (22%)	36 (78%)	p=0.89
Cribriform; <30% solid (grade 2)	43 (39%)	33%	0.12; p=0.21	7 (16%)	36 (84%)	p=0.32
Solid (grade 3)	20 (18%)	46%		6 (30%)	14 (70%)	p=0.28
TREATMENT						
Adjuvant radiotherapy						
Yes	102 (93%)	33%	0.14; p=0.15	20 (20%)	82 (80%)	p=0.23
No	8 (7%)	26%		3 (38%)	5 (62%)	

* difference is considered statistically significant

Figure 1. Representative immunohistochemical PSMA expression in primary and metastatic AdCC showing variation in the number of positive staining tumour cells.

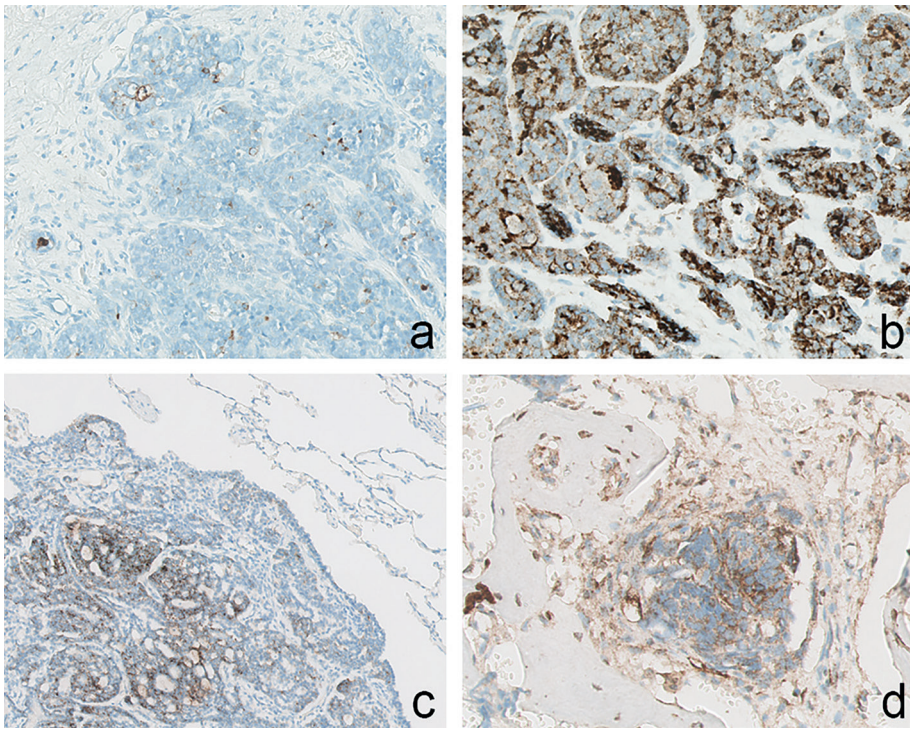

(a) nasal cavity, 5%; *magnification 200x*. **(b)** submandibular gland, 90%; *magnification 400x*. **(c)** pulmonary metastasis, 70%; *magnification 200x*. **(d)** bone metastasis, 5%; *magnification 200x*.

Follow-up and survival analysis

Details of follow-up and survival rates are summarized in Tables 2 and 3. Dichotomization of PSMA expression was carried out by plotting different ROC curves for prediction of OS, DSS, RFS and MFS, which showed optimal cut-off points in a range of 8–12%. Although the area under these curves was not sufficient to assume high sensitivity and specificity, for practical reasons a merged cut-off point of 10% PSMA expression was defined (graphs not shown). The 0–10% expression group was dominated by patients whose tumour was located in the minor salivary glands and, more specifically, in the nasal cavity, nasopharynx or maxillary sinus as revealed by post-hoc analysis ($p=0.01$ and $p<0.01$ respectively). Furthermore, in this group, relatively more tumours showed bone

Table 2. Follow-up

	N (%)	Median months; IQR	Median % PSMA primary tumour	PSMA 0–10%	PSMA >10%	χ^2 PSMA ≤10% vs >10%
Patients	110			23	87	
Follow-up (median months; IQR)		57; 26–100		50; 13–96	63; 27–110	
Locoregional recurrence						
Yes	29 (26%)	39; 20–91	40%	9	20	p=0.12
No	81 (74%)		30%	14	67	
Distant metastasis						
Yes	36 (33%)	33; 12–77	38%	7	29	p=0.79
No	74 (67%)		30%	16	58	
*Locoregional recurrence-free @ 10 years						
Yes	84 (76%)		35%	14	70	p=0.05
No	26 (24%)		31%	9	17	

* difference is considered statistically significant

Table 3. Survival data

	N affected	Median months	% survival
Overall survival			
5-year OS	25	36	77%
10-year OS	29	41	74%
Disease-specific survival			
5-year DSS	17	41	85%
10-year DSS	21	47	81%
Disease-free survival			
5-year DFS	36	20	67%
10-year DFS	49	31	55%
Locoregional recurrence-free survival			
5-year RFS	19	27	83%
10-year RFS	26	36	76%
Metastasis-free survival			
5-year MFS	26	22	76%
10-year MFS	33	28	70%

invasion (p=0.02) and relatively more patients were not recurrence-free 10 years after diagnosis (p=0.05). Despite half of the pT4b tumours expressed 0–10% PSMA, this distribution did not reach statistical significance due to multiple testing (p=0.04), see Table 1. A multivariate Cox proportional hazards model with Firth's correction showed a significant relation between low PSMA expression (0–10%) and worse 10-years RFS (HR 3.0, 95% CI 1.1–8.5, p=0.04). A >30% solid growth pattern / Perzin grade 3 (HR 3.7, 95% CI 1.3–11.2, p=0.02), tumour localization in the nasal cavity, nasopharynx or maxillary sinus (HR 41.7, 95% CI 6.2–236.8, p<0.01), and no postoperative radiotherapy (HR 5.1, 95% CI 1.2–17.5, p=0.02) were also significant prognosticators for locoregional recurrence within 10 years. Harrell's C-statistic of the predictive Cox proportional hazards model was 0.81, and without PSMA expression 0.79. PSMA expression was no significant contributor for the prediction of OS, DSS and MFS (multivariate data not shown).

Supplementary Figure 1: Differences in PSMA expression between primary, recurrent and metastatic AdCC in 18 patients, in order of PSMA expression of the primary tumour.

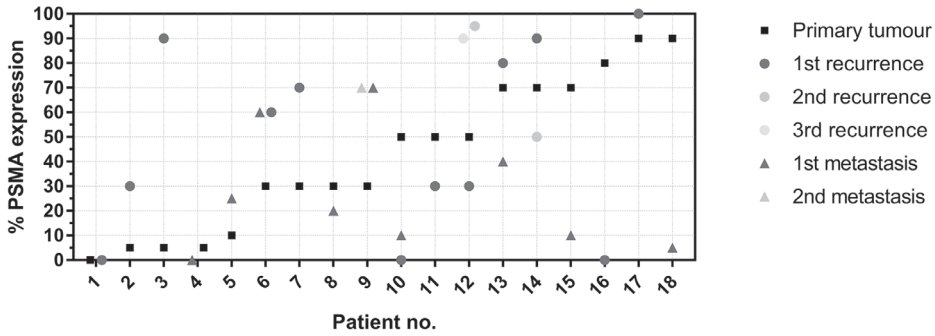

DISCUSSION

This is the first large cohort study describing PSMA expression in primary, recurrent and distant metastatic AdCC of the head and neck. Positive expression was seen in 94% of the primary tumours, 80% of recurrent tumours and 90% of the distant metastases, with PSMA expressed in 31, 60 and 23% of the tumour cells respectively. Primary tumour expression could not indicate disease progression and could not estimate expression levels in a recurrence or metastasis, although a tendency of respectively increase and decrease was observed. PSMA expression was not correlated to pathological stage and grade.

This is in contrast to PC in which high PSMA expression is correlated with prostate-specific antigen (PSA) recurrence and other prognostic factors which negatively affect survival such as tumour grade, pathological stage and castration resistance.[4,24] Multiple studies have shown that PSMA activates AKT and MAPK pathways promoting proliferation and survival of cancer cells, which may lead to an aggressive biological and clinical behaviour.[25,26] However, the currently presented inverse correlation of low primary tumour PSMA expression ≤10% as independent predictor of shortened RFS (HR 3.0; 95% CI 1.1–8.5; p=0.04) has also been described in other cancer types and might partly be explained by epigenetic silencing of the PSMA gene upon tumour progression.[27]

Analogous to PC, AdCC demonstrates expression of PSMA in the epithelial tumour cells, while expression in different other tumours mainly concentrates in endothelial cells of tumour-associated neovasculature.[3,6,28]

Of all primary PCs, 95% show heterogeneous PSMA expression with on average 53 ± 32% (mean ± SD) positive tumour cells. Mean expression in regional lymph nodes and distant metastasis is more extensive (72 ± 36% and 92 ± 10% respectively). Normal prostate tissue shows high PSMA expression in 100% of the samples (77 ± 32% positive cells), but with significantly less staining intensity than tumour tissue.[3,4]

In contrast, staining intensity in AdCC is relatively constant. Although it is known that major and minor salivary glands depict high tracer uptake on PSMA PET/CT, a comparison between expression intensity in normal salivary gland tissue and AdCC tumour tissue could not be made due to the lack of data on PSMA expression in non-pathologic salivary glands.[29] Comparing published PC data and our AdCC data, the present study concludes that similar to PC, 94% of primary AdCC expresses PSMA, but AdCC expression is more homogenous in a lower percentage of positive tumour cells.

Some points need to be addressed. Multiple Spearman's rho correlation analyses and KW non-parametric tests were carried out to analyze possible differences between a large amount of clinical parameters and tumour characteristics. False-positive findings

might have been introduced, as adjustments to correct for multiple comparisons are not desirable in explorative studies and were therefore not applied. The results of these analyses should therefore be interpreted carefully.[30]

By comparing the dichotomized groups of PSMA expression, it is noticed that a relatively large number of tumours in the low ≤10% PSMA expression group are located in the nasal cavity, nasopharynx or maxillary sinus, sites that are known to have a worse prognosis when compared to tumours originating from other subsites.[11] Notwithstanding the small sample sizes in these study subgroups, specifically the aforementioned tumour sites are, besides poor RFS, concordantly associated with poor DSS and OS (data not shown). Tumour stage T4b and bone invasion were also overrepresented in the low PSMA expression (≤10%) group. Although these parameters themselves are no independent predictors of RFS, tumour stage is strongly correlated with DSS and OS. Furthermore, tumour stage and bone invasion are mutually highly correlated (Pearson's chi-square test $p<0.01$) as all except one T4b tumour showed bone invasion. Moreover, bone invasion is significantly associated with tumour localization in the nasal cavity, nasopharynx or maxillary sinus. Tumours at these locations recur more often. These collinearities could be explained by delayed presentation of tumours from this subsite (that often involves the skull base), but may have confounded the results.

Another factor of debate is the limited discriminative strength of the 10% cut-off point. The above mentioned considerations are supported by the minimal increase of Harrell's C-statistic of the multivariate Cox proportional hazards model by 0.02 and therefore the additive value of PSMA to the prediction of RFS remains questionable.

A deep locoregional recurrence or growing distant metastases, for which conventional treatment options are no longer applicable due to functional irresectability or exceeded radiation limits, is a relevant problem in the management of AdCC. The limited experience with palliative chemotherapeutic agents and new initiatives with different targeted agents in this setting was recently reviewed.[31] The present results of high PSMA expression in primary, recurrent and metastatic tumour cells with limited spatial and temporal variability, as well as the uptake of PSMA-ligand in recurrent and distant metastatic AdCC on PET/CT, could suggest a potential role for palliative targeted treatment with Lutetium-177-PSMA.[10,32] First large trials of this radionuclide treatment of metastatic castration-resistant PC show high response rates with low toxicity, improved quality of life and even prolonged OS.[20,33] Regarding AdCC, the high amount of associated grade 1 xerostomia (87%) must be taken into account, as these patients usually have already been exposed to radiotherapy to the head and neck before.[20]

CONCLUSION

This study shows unambiguous PSMA expression in a large cohort of primary, recurrent and metastatic AdCC of the head and neck. Expression was seen in 94% of the primary tumours, which is analogous to PC except for the median lower number of positive tumour cells. In general, there was no relation between upregulated PSMA expression and pathological stage, tumour grade (growth pattern), the occurrence of locoregional recurrence or metastasis, and survival. Low primary tumour expression ≤10% is significantly associated with worsened RFS although its predictive value is limited. Of the recurrent and distant samples, respectively 80% and 90% were PSMA-positive, but staining could not be estimated based on primary tumour expression. This study provides encouraging supporting results that when other palliative systemic treatment options fail, PSMA-targeted imaging followed by experimental Lutetium-177-PSMA radionuclide therapy in AdCC, might be an alternative.

REFERENCES

1. Horoszewicz JS, Kawinsky E MG. Monoclonal antibodies to a new antigenic marker in epithelial prostatic cells and serum of prostatic cancer patients. Anticancer Res 1987;7:927–35.
2. Israeli RS, Powell CT, Corr JG, Fair WR, Heston WD. Expression of the prostate-specific membrane antigen. Cancer Res 1994;54:1807–11.
3. Wright GL, Haley C, Beckett M Lou, Schellhammer PF. Expression of prostate-specific membrane antigen in normal, benign, and malignant prostate tissues. Urol Oncol Semin Orig Investig 1995;1:18–28.
4. Ross JS, Sheehan CE, Fisher H a G, et al. Correlation of primary tumor prostate-specific membrane antigen expression with disease recurrence in prostate cancer. Clin Cancer Res 2003;9:6357–62.
5. Afshar-Oromieh A, Hetzheim H, Kratochwil C, et al. The novel theranostic PSMA-ligand PSMA-617 in the diagnosis of prostate cancer by PET/CT: biodistribution in humans, radiation dosimetry and first evaluation of tumor lesions. J Nucl Med 2015;56:1697–705.
6. Backhaus P, Noto B, Avramovic N, et al. Targeting PSMA by radioligands in non-prostate disease—current status and future perspectives. Eur J Nucl Med Mol Imaging 2018:1–18.
7. Wolf P, Freudenberg N, Bühler P, et al. Three conformational antibodies specific for different PSMA epitopes are promising diagnostic and therapeutic tools for prostate cancer. Prostate 2010;70:562–9.
8. Chang SS, Reuter VE, Heston WDW, Bander NH, Grauer LS, Gaudin PB. Five Different Anti-Prostate-specific Membrane Antigen (PSMA) Antibodies Confirm PSMA Expression in Tumor-associated Neovasculature. Cancer Res 1999;59:3192–8.
9. Silver DA, Pellicer I, Fair WR, Heston WD, Cordon-Cardo C. Prostate-specific membrane antigen expression in normal and malignant human tissues. Am Assoc Cancer Res 1997;3:81–5.
10. Klein Nulent TJW, van Es RJJ, Krijger GC, de Bree R, Willems SM, de Keizer B. Prostate-specific membrane antigen PET imaging and immunohistochemistry in adenoid cystic carcinoma-a preliminary analysis. Eur J Nucl Med Mol Imaging.2017;44:1614–21
11. Spiro RH, Huvos AG, Strong EW. Adenoid cystic carcinoma of salivary origin. A clinicopathologic study of 242 cases. Am J Surg. 1974;128:512–20.
12. Netherlands Comprehensive Cancer Organisation, The Netherlands Cancer Registry. Incidence of invasive salivary gland cancer per year. 2015 [cited 2016 Apr 1]. Available from: http://www.cijfersoverkanker.nl.
13. de Ridder M, Balm AJM, Smeele LE, Wouters MWJM, van Dijk BAC. An epidemiological evaluation of salivary gland cancer in the Netherlands (1989-2010). Cancer Epidemiol 2015;39:14-20.
14. Bjørndal K, Krogdahl A, Therkildsen MH, et al. Salivary gland carcinoma in Denmark 1990-2005: A national study of incidence, site and histology. Results of the Danish Head and Neck Cancer Group (DAHANCA). Oral Oncol 2011;47:677–82.
15. Jang S, Patel PN, Kimple RJ, McCulloch TM. Clinical Outcomes and Prognostic Factors of Adenoid Cystic Carcinoma of the Head and Neck. Anticancer Res 2017;37:3045–52.
16. Coca-Pelaz A, Rodrigo JP, Bradley PJ, et al. Adenoid cystic carcinoma of the head and neck - An update. Oral Oncol 2015;51:652–61.
17. Hellquist H, Skalova A. Adenoid Cystic Carcinoma. Histopathol. Salivary Gland., Springer Berlin Heidelberg; 2014, p. 221–60.

18. van Weert S, Reinhard R, Bloemena E, et al. Differences in patterns of survival in metastatic adenoid cystic carcinoma of the head and neck. Head Neck 2017;39:456–63.
19. Ciccolallo L, Licitra L, Cantú G, Gatta G. Survival from salivary glands adenoid cystic carcinoma in European populations. Oral Oncol 2009;45:669–74.
20. Hofman MS, Violet J, Hicks RJ, et al. [177Lu]-PSMA-617 radionuclide treatment in patients with metastatic castration-resistant prostate cancer (LuPSMA trial): a single-centre, single-arm, phase 2 study. Lancet Oncol 2018;19:825-33.
21. Perzin KH, Gullane P, Clairmont AC. Adenoid cystic carcinomas arising in salivary glands: a correlation of histologic features and clinical course. Cancer 1978;42:265–82.
22. Heinze G, Dunkler D. Avoiding infinite estimates of time-dependent effects in small-sample survival studies. Stat Med 2008;27:6455–69.
23. Harrell FEH, Lee KL, Mark DB. Multivariable prognostic models: issues in developing models, evaluating assumptions and adequacy, and measurin and reducing errors. Stat Med 1996;15:361–87.
24. Wright GL, Mayer Grob B, Haley C, et al. Upregulation of prostate-specific membrane antigen after androgen-deprivation therapy. Urology 1996;48:326–34.
25. Perico ME, Grasso S, Brunelli M, et al. Prostate-specific membrane antigen (PSMA) assembles a macromolecular complex regulating growth and survival of prostate cancer cells "in vitro" and correlating with progression "in vivo." Oncotarget 2016;7:74189–202.
26. Kaittanis C, Andreou C, Hieronymus H, et al. Prostate-specific membrane antigen cleavage of vitamin B9 stimulates oncogenic signaling through metabotropic glutamate receptors. J Exp Med 2018;215:159–75.
27. Mhawech-Fauceglia P, Smiraglia DJ, Bshara W, et al. Prostate-specific membrane antigen expression is a potential prognostic marker in endometrial adenocarcinoma. Cancer Epidemiol Biomarkers Prev 2008;17:571–7.
28. Salas Fragomeni RA, Amir T, Sheikhbahaei S, et al. Imaging of Non-Prostate Cancers Using PSMA-Targeted Radiotracers: Rationale, Current State of the Field, and a Call to Arms. J Nucl Med 2018;59:871-7.
29. Klein Nulent TJW, Valstar MH, de Keizer B, et al. Physiologic distribution of PSMA-ligand in salivary glands and seromucous glands of the head and neck on PET/CT. Oral Surg Oral Med Oral Pathol Oral Radiol 2018;125:478-86.
30. Rothman KJ. No adjustments are needed for multiple comparisons. Epidemiology 1990;1:43–6.
31. Alfieri S, Granata R, Bergamini C, et al. Systemic therapy in metastatic salivary gland carcinomas: A pathology-driven paradigm? Oral Oncol 2017;66:58–63.
32. Has Simsek D, Kuyumcu S, Agaoglu FY, Unal SN. Radionuclide Therapy With 177Lu-PSMA in a Case of Metastatic Adenoid Cystic Carcinoma of the Parotid. Clin Nucl Med 2019;44:764–6.
33. Rahbar K, Boegemann M, Yordanova A, et al. PSMA targeted radioligandtherapy in metastatic castration resistant prostate cancer after chemotherapy, abiraterone and/or enzalutamide. A retrospective analysis of overall survival. Eur J Nucl Med Mol Imaging 2018;45:12–9.

PART B

Targeted diagnostics

Physiologic distribution of PSMA-ligand in salivary glands and seromucous glands of the head and neck on PET/CT

Thomas J.W. Klein Nulent*
Matthijs H. Valstar*
Bart de Keizer
Stefan M. Willems
Laura A. Smit
Abrahim Al-Mamgani
Ludwig E. Smeele
Robert J.J. van Es
Remco de Bree
Wouter V. Vogel

*Authors contributed equally to the manuscript

Chapter as published in:
Oral Surgery, Oral Medicine, Oral Pathology and Oral Radiology 2018; 125(5): 478–486

doi: 10.1016/j.oooo.2018.01.011

ABSTRACT

Objectives

Prostate-specific membrane antigen (PSMA) positron emission tomography/computed tomography (PET/CT) is used for detection and (re)staging of prostate cancer. However, healthy salivary, seromucous, and lacrimal glands also have high PSMA-ligand uptake. This study aimed to describe physiologic PSMA-ligand uptake distribution characteristics in the head and neck to aid in PSMA PET/CT interpretation and to identify possible new clinical applications for PSMA-ligand imaging.

Study design

Thirty consecutive patients who underwent PSMA PET/CT for prostate cancer were evaluated. Tracer maximum standardized uptake values (SUV_{max}) in the salivary, seromucous, and lacrimal glands were determined visually and quantitatively. Overall and intraindividual variations were reported.

Results

All gland locations had increased tracer uptake. The mean SUV_{max} ± standard deviation varied: parotid 12.3 ± 3.9; submandibular 11.7 ± 3.5; sublingual 4.5 ± 1.9; soft palate 2.4 ± 0.5; pharyngeal wall 4.3 ± 1.3; nasal mucosa 3.4 ± 0.9; supraglottic larynx 2.7 ± 0.7; and lacrimal 6.2 ± 2.2. The parotid had the largest overall variation in SUV_{max} (5.2–22.9), and the sublingual glands had the largest mean intraindividual difference (18.1%).

Conclusion

Major and minor salivary and seromucous glands consistently have high PSMA-ligand uptake. Minor gland locations can be selectively visualized by this technique for the first time. This provides potential new applications such as quantification of present salivary gland tissues and individualization of radiotherapy for head and neck cancer or Lutetium-177-PSMA radionuclide treatment.

INTRODUCTION

Functional imaging of tissues expressing prostate-specific membrane antigen (PSMA) with radiolabelled ligand Gallium-68 [^{68}Ga]-HBED-CC-Glu-NH-CONH-Lys(Ahx) and positron emission tomography combined with computed tomography (PET/CT) is primarily used for the detection and (re)staging of prostate cancer.[1] However, binding of PSMA-ligands is not limited to prostate cancer cells. Clinical experience with PSMA PET/CT for prostate cancer has revealed consistent and significant uptake in other tissues, most notably the major salivary and lacrimal glands.[1] Because tracer uptake is based on expression of the PSMA epitope in glandular cells, it can be hypothesized that uptake of PSMA-ligand is associated with the gland volume and thus functional capacity of the gland. Two arguments support this hypothesis. First, xerostomia is a well-known side effect of Lutetium-177 (^{177}Lu)-PSMA treatment and could be explained by cell loss as a consequence of toxicity. Second, a difference can be noted in ^{68}Ga-PSMA uptake between normal and irradiated submandibular glands, with the latter having decreased glandular function after radiotherapy (Figure 1).[2,3] Current clinical tomographic imaging modalities such as CT, magnetic resonance imaging (MRI), and ^{18}F-fluorodeoxyglucose (FDG) PET/CT can adequately visualize the parotid and submandibular salivary glands, and clinicians are generally well aware of their normal location and appearance.[4]

The sublingual glands are more difficult to detect on CT or FDG PET/CT, and they require specific magnetic resonance sequences for good visualization.[5] Imaging of the minor (mucosal) salivary glands with current techniques has been a challenge because until now adequate visualization of these small (1–5 mm) glands was impossible. Imaging experts may not even be aware of their existence. In addition, the lack of tools to visualize minor salivary and seromucous glands and the inability to estimate gland viability limits the options for personalized treatment aiming to preserve the function of these glands, which play a vital role in lubrication of the oral cavity.[6,7] With the introduction of PSMA PET/CT for prostate cancer staging and follow-up, clinicians are confronted with unfamiliar uptake patterns throughout the head and neck that may lead to misinterpretation of tumour and normal tissues (Figure 1). Adequate knowledge of the normal anatomy and function of the salivary glands is relevant to further improve interpretation of the images. Assessment of salivary gland presence and function by PSMA PET/CT after treatment requires knowledge of quantitative physiologic uptake patterns, which currently are not well understood.

This study aimed to describe the physiologic PSMA-ligand uptake distribution characteristics by evaluating tracer maximum standardized uptake values (SUV_{max})

in normal salivary glands, seromucous glands of the upper aerodigestive tract, and lacrimal glands on PSMA PET/CT. In addition, this study aimed to identify potential clinical applications of PSMA PET/CT.

Figure 1. PSMA PET/CT of a patient with a history of cancer of the left parotid gland treated with surgery and radiotherapy, and prostate cancer treated with radiotherapy with current biochemical recurrence.

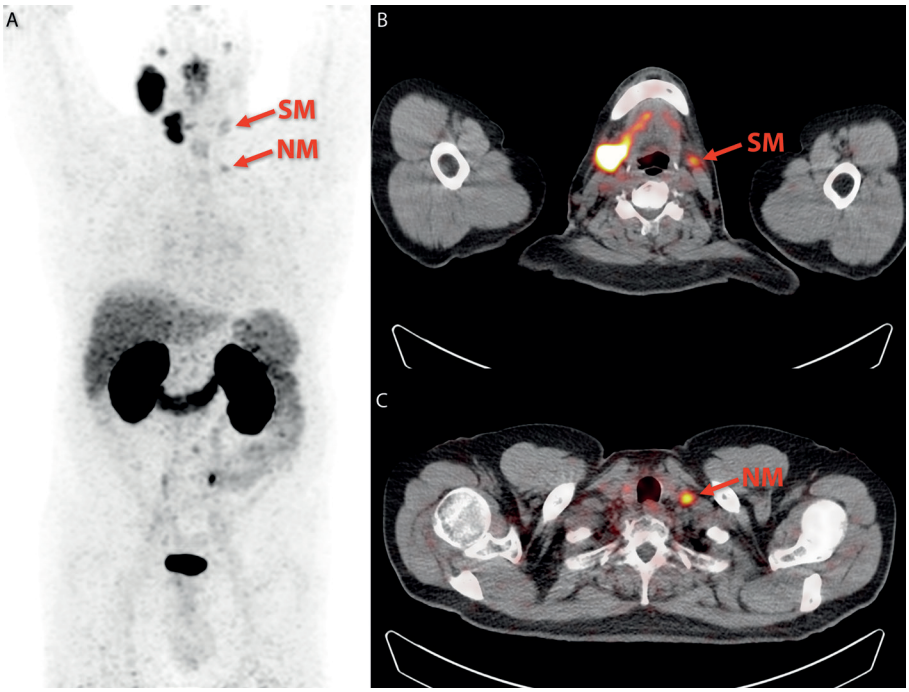

Shown are an anterior projection of the body (**A**) and transverse slices at the level of the neck (**B**) and upper thoracic outlet (**C**). The cytologically proven nodal metastasis from prostate cancer in the lower neck (NM) has equivalent uptake as the irradiated submandibular gland (SM) and several normal tissues in the neck (e.g., the glands in the supraglottic larynx). This may lead to confusion and misinterpretation when normal patterns are not adequately recognized.

MATERIALS AND METHODS

The distribution of healthy salivary and seromucous gland tissues in the head and neck area was retrospectively analyzed in 30 consecutive patients who underwent total body PSMA PET/CT for staging of prostate cancer in March and April 2016. Exclusion criteria were previous salivary gland disease, aberrant tracer uptake suspected of neoplasia, and previous surgery and/or radiotherapy in the head and neck region.

PSMA PET/CT

Specific patient preparation was not required before PET/CT imaging. Images were acquired from the skull vertex to the thighs using a TruePoint Biograph mCT40 scanner (Siemens, Erlangen, Germany), approximately 60 minutes after intravenous injection of 2 MBq/kg ^{68}Ga-HBED-CC-Glu-NH-CO-NH-Lys(Ahx). A low-dose CT scan was performed using CARE Dose 4D and CARE kV (Siemens, Erlangen, Germany), with the following reference parameters: 40 mAs and 120 kV. Subsequently, PET was acquired according to the European Association of Nuclear Medicine recommendations with the following parameters: PET with time-of-flight and point spread function reconstruction (Siemens TrueX, Erlangen, Germany), 4 iterations, 21 subsets, with a filter of 7.5 mm full width at half maximum.[8]

PSMA-ligand uptake

Tracer uptake in the head and neck was determined visually and quantitatively by a dedicated board-certified head and neck nuclear medicine physician (B.d.K.) experienced in PSMA PET/CT, in consensus in a joint session with an oral and maxillofacial surgeon (T.K.N.). Visibility was defined as visually recognizable by increased tracer uptake relative to surrounding mucosa and other normal tissues. Quantitative evaluation was performed by calculating the SUV_{max} using a freehand isocontour volume of interest and the lean body mass formula, as defined in the European Association of Nuclear Medicine guidelines.[8] In the event of disagreement on gland location margins, a forced consensus was reached. Uptake in the parotid, submandibular, sublingual, pharyngeal, and lacrimal glands was measured bilaterally.

Data analysis

Normal distribution of the SUV_{max} was evaluated per gland location using the Shapiro-Wilk test. The mean SUV_{max} ± standard deviation and range were calculated according to each gland location. Overall variations in SUV_{max} of the paired glands were reported, and intraindividual differences were visualized in a boxplot.

Statistics were performed using IBM SPSS Statistics for Windows, version 21.0 (IBM Corp., Armonk, NY, USA). The boxplot was drawn using GraphPad Prism for Windows, version 6.02 (GraphPad Software, La Jolla, CA, USA). For this study, individual consent was not required. This was approved by the institutional Medical Research Ethics Committee, protocol number 16–790, and is in accordance with the 1964 Helsinki Declaration and its later amendments or comparable ethical standards.

RESULTS

PSMA PET/CT

The 30 male patients had an average age of 68 years (range 54–82 years). The mean administered activity was 173 ± 29 MBq (range 131–273 MBq). The mean time interval between tracer administration and imaging was 66 minutes (interquartile range 58–74 minutes).

PSMA-ligand uptake

All scans clearly depicted anatomic areas of salivary, seromucous, and lacrimal gland concentrations by visualizing high and homogenous uptake of PSMA-ligand (Figure 2). These areas included the major salivary glands and submucosal minor salivary and seromucous glands in the soft palate, pharynx, nasal mucosa, supraglottic larynx, and lacrimal glands. Pharyngeal tracer uptake was concentrated around a bilateral area in the dorsal wall of the nasopharynx, measurements were presented as "pharyngeal wall". See Figures 2 and 3 for an example with anatomic atlas. The uptake of PSMA-ligand in these glands is summarized in Table 1. The highest uptake was seen in the parotid and submandibular glands, with mean SUV_{max} 12.3 ± 3.9 (range 5.2–22.9) and 11.7 ± 3.5 (6.0–22.2), respectively. For reference, the mean maximal uptake values in the liver and kidneys were 3.7 ± 0.8 (2.4–5.0) and 28.8 ± 7.6 (16.9–44.5), respectively. The intraindividual differences in SUV_{max} of the paired glands varied by location. Details are listed in Table 2 and visualized in Figure 4.

Figure 2. Anterior projection overview of combined PSMA PET/CT (left) and PSMA PET (right), showing tracer uptake in healthy salivary, seromucous, and lacrimal glands in a patient with prostate cancer and no apparent metastatic disease.

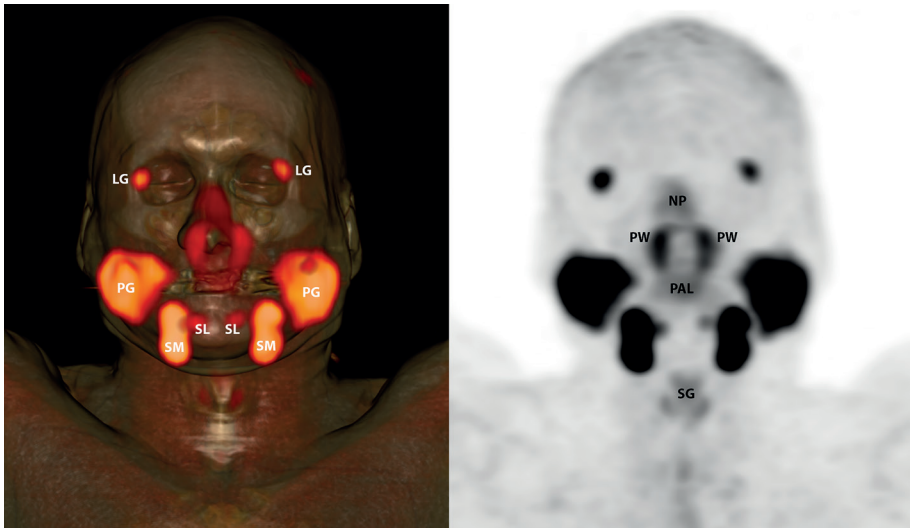

LG, lacrimal gland; NP, nasal and nasopharyngeal mucosa; PW, pharyngeal wall; PAL, soft palate; PG, parotid gland; SM, submandibular gland; SL, sublingual gland; SG, supraglottic larynx.

Table 1. Overall SUV_{max} of healthy salivary, seromucous and lacrimal glands on PSMA PET/CT in 30 patients

	N	Mean	SD	Range
Parotid	60	12.3	3.9	5.2 – 22.9
Submandibular	60	11.7	3.5	6.0 – 22.2
Sublingual	60	4.5	1.9	1.2 – 8.5
Soft palate	30	2.4	0.5	1.4 – 3.6
Pharyngeal wall	60	4.3	1.3	2.5 – 7.7
Nasal mucosa	30	3.4	0.9	2.2 – 5.5
Supraglottic larynx	30	2.7	0.7	1.7 – 3.8
Lacrimal glands	60	6.2	2.2	2.5 – 13.6

Figure 3. Low-dose CT (left), PET/CT (middle), and PET (right) images of the head and neck, showing Gallium-68 (^{68}Ga)-HBED-CC-Glu-NH-CO-NH-Lys(Ahx) uptake in healthy salivary, seromucous, and lacrimal glands in a patient with prostate cancer and no apparent metastatic disease.

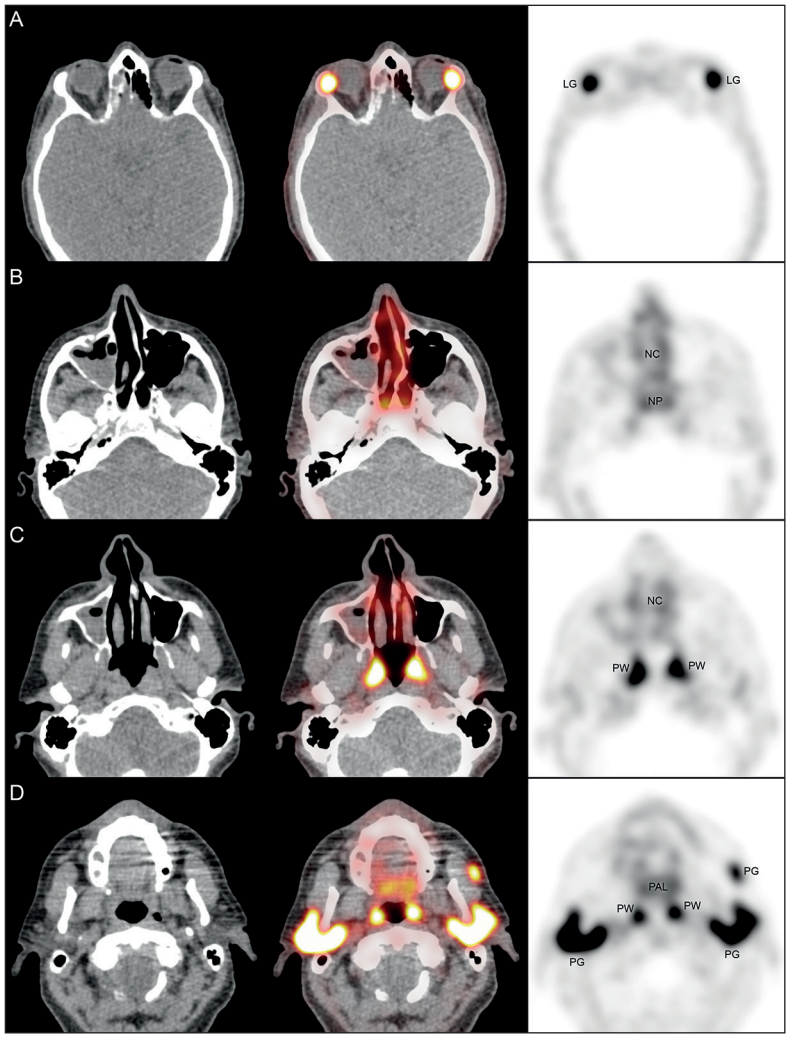

LG, lacrimal gland; NC, nasal cavity mucosa; NP, nasopharyngeal mucosa; PW, pharyngeal wall; PAL, soft palate; PG, parotid gland; SM, submandibular gland; SL, sublingual gland; SG, supraglottic larynx.

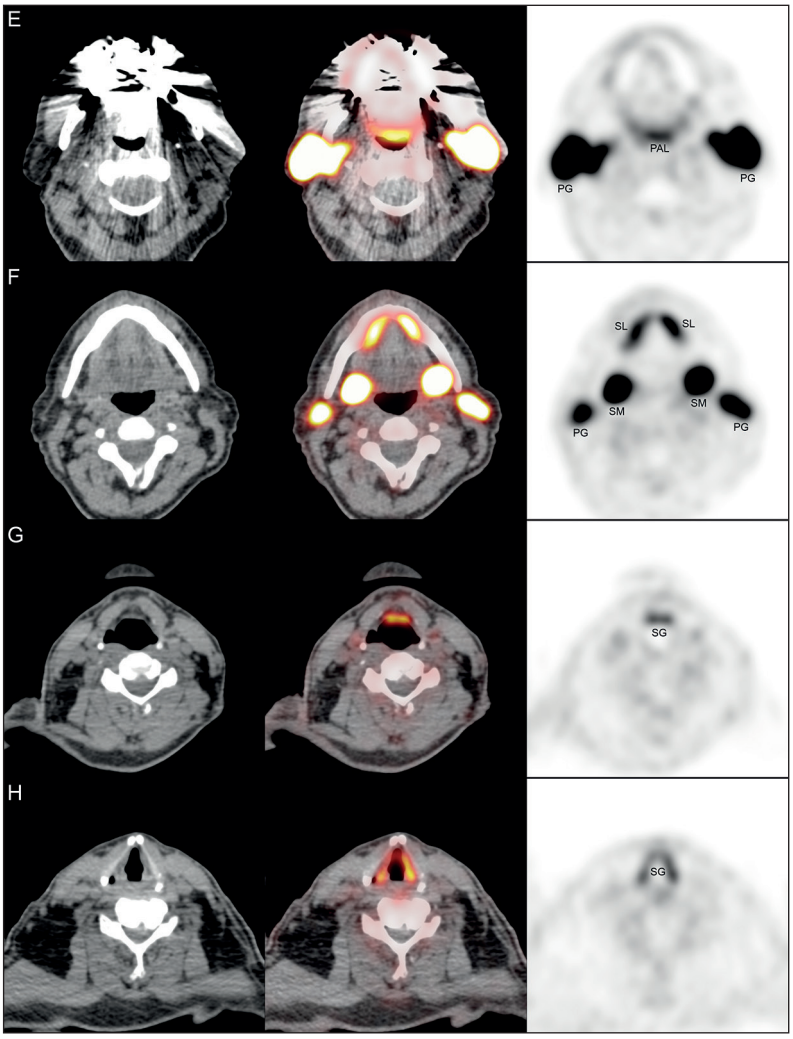
E
PAL
PG
PG
F
SL
SL
SM
SM
PG
PG
G
SG
H
SG

Table 2. Intraindividual differences in SUV_{max} of paired salivary, seromucous and lacrimal glands on PSMA PET/CT in 30 patients

	Mean difference (% difference)	SD	Maximum difference (% of the mean)
Parotid	9.9%	8.8	37.0%
Submandibular	9.0%	6.8	27.6%
Sublingual	18.1%	13.7	41.7%
Pharyngeal wall	9.8%	6.7	22.5%
Lacrimal glands	13.7%	11.3	48.2%

Figure 4. Intraindividual differences in SUV_{max} of paired salivary, seromucous, and lacrimal glands on PSMA PET/CT in 30 patients, showing a mean left/right difference of 9.0% to 18.1%.

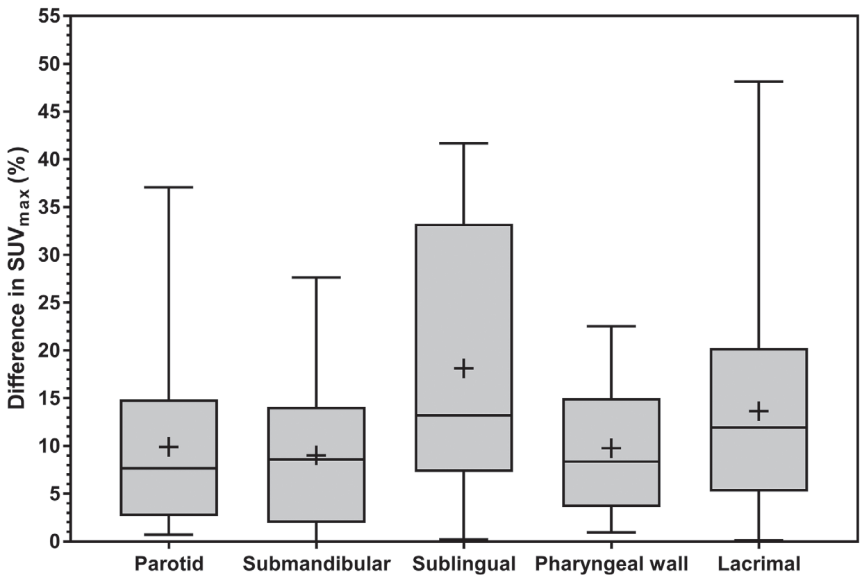

mean (+), median, interquartile range, and range

DISCUSSION

The results of this study provide a comprehensive qualitative and quantitative overview of tracer accumulation on PSMA PET/CT in salivary, seromucous, and lacrimal gland tissues in the head and neck. The presented distribution patterns of the major salivary glands are comparable to those (to a lesser extent) reported in studies on different topics using the same tracer.[9,10] In addition, our study illustrates the ability of PSMA PET/CT to visualize minor gland locations, for example, in the soft palate, pharyngeal wall, nasal mucosa, and supraglottic larynx. This has not been possible with other imaging modalities previously.

Although Demirci et al.[10] described comparable nasopharyngeal tracer concentration around the fossa of Rosenmüller, in our series this area seemed less well defined and spread over a larger area. Awareness of the physiologic tracer distribution in the upper aerodigestive tract mucosal and salivary gland tissues can contribute to a correct diagnostic interpretation of PSMA PET/CT.

Imaging of salivary glands

The saliva-producing acinar cells are distributed over 3 paired major and approximately 600 to 1,000 minor salivary glands, which are organized in small clusters of mainly mucous cells that are located in the mucosa of the palate, lips, buccal mucosa, tongue, and floor of the mouth. In addition, there are many seromucous glands in the oro-, hypo- and nasopharynx; nasal cavities; larynx; trachea; and oesophagus that contain mucous and/or serous cells.[7,11] The nasopharynx, for example, contains approximately 1,100 to 1,200 seromucous glands.[12] Anatomic imaging such as CT and MRI generally adequately depicts the parotid and submandibular glands. Therefore, their location, size, and shape are considered common knowledge.[4] The sublingual glands are more difficult to visualize with standard imaging techniques. Until recently, imaging of minor salivary and seromucous glands, located in the oral mucosa, lips, tonsils, nasal cavity, nasal sinuses, larynx, trachea, and oesophagus, was impossible because of their limited size and poor signal contrast with surrounding tissues; their detection was only possible in the case of tumour growth.[13] Today, PSMA PET/CT brings a new technique to clearly depict normal sublingual and minor submucosal gland areas and to quantify the uptake of the PSMA-ligand as a marker of the presence of glandular cells.

The biomarker PSMA

PSMA was first described in 1987.[14] In 1993 it was successfully cloned and characterized.[15] PSMA is now known as a type II transmembrane glycoprotein of the prostate secretory

acinar epithelium. Its expression has been reported in normal as well as benign and malignant prostate tumour tissue, with upregulation in advanced prostate carcinoma and metastasis.[14-16]

Organ specificity of PSMA

The original assumption of specific binding to prostate epithelium was challenged beginning in 1995 after the identification of PSMA epitopes on cells in other organs.[14,17] Other sites with proven expression include salivary glands, nervous system glia (astrocytes and Schwann cells), kidneys (proximal tubules), small intestine (jejunal brush border), ductal epithelium of normal breasts, and skeletal muscle.[18-21] The exact function of PSMA in the prostate and kidneys is unclear, although there is suggestive evidence that it may be involved in the metabolism of folate.[22] PSMA has been identified not only in healthy tissue but also in neoplasms, including subtypes of schwannoma and bladder carcinoma.[23] Subsequently, it has been found in the neovascular capillary endothelium of a wide spectrum of solid tumours, such as epithelial tumours (carcinomas), neuroendocrine tumours, mesenchymal tumours (soft tissue sarcomas), and melanoma and glioma, which might suggest PSMA involvement in the angiogenesis of developing neoplasms.[21,24] Recently, PSMA-ligand uptake and immunohistochemical expression were described in recurrent and distant metastatic adenoid cystic carcinoma and squamous cell carcinoma of the base of the tongue.[25,26]

PSMA in imaging

In 1990 the PSMA-specific immunoconjugate CYT356, derived from the prostate-reactive monoclonal antibody 7E11-C5, was labelled with Indium-111 to visualize primary prostate tumours and their metastases using radioimmunoscintigraphy.[17] In recent years, urea-based small-molecule PSMA-inhibiting ligands were developed that could be coupled to ^{68}Ga, with the currently most commonly applied ligand being Glu-NH-CO-NHLys(Ahx) coupled to the chelator HBED-CC. This allowed functional imaging with PET. Combined with CT, the imaging modality became known as PSMA PET/CT.[27] This new diagnostic tool is increasingly being used for detection and (re)staging of prostate cancer, with high sensitivity and specificity and with high impact on the clinical management of these patients.[28]

Expression of PSMA in salivary glands

Histopathologic expression of PSMA has not been extensively described. Wolf et al.[29], using immunohistochemical staining, reported that PSMA in human salivary gland specimens is expressed on the epithelium of acinar glandular cells and not on the duct

cells. Our preliminary results indicate staining of serous and mucous acinar cells as well as small (intercalated and striated) duct cells. In the present study, minor salivary glands had lower SUV_{max} values than major glands (Table 1). Most likely, this is associated with gland volume. Additionally, it is currently unclear whether this difference in SUV values also reflects a biologic difference between the gland types, such as a lower number of specific cells per volume. Direct evidence of a relation between functional capacity and PSMA-ligand uptake is expected to be provided by future research. The limited spatial resolution of current PET/CT scanners may introduce partial volume errors. For objects smaller than the voxel size, the measured tracer concentration is less than the true tracer concentration value in tissue. This could have led to a significant underestimation of the actual tracer uptake in the minor salivary and seromucous glands.[30]

The lacrimal glands

Many considerations about the salivary and seromucous glands apply similarly to the serous lacrimal glands that show a comparably high tracer accumulation in PSMA PET/CT. The main lacrimal glands are located in the superolateral orbit; each consists of 2 lobes that are separated by an aponeurosis.[31] There is currently insufficient knowledge regarding PSMA expression patterns in lacrimal gland cells.

Clinical potential of PSMA PET/CT

The ability to specifically bind PSMA in salivary and seromucous glandular tissue may open the door to several potential applications of PSMA-ligand binding and imaging of the head and neck area using PET/CT. In oncology, PSMA PET/CT may be used for the detection of recurrent and metastatic salivary gland cancers, squamous cell carcinomas, or even benign salivary gland tumours.[25,26] To differentiate salivary gland tumours from normal glandular tissue, knowledge of the level of physiologic uptake is important.

Furthermore, in external beam radiotherapy of the head and neck, it might be possible to selectively spare previously invisible salivary gland locations, especially areas with a high concentration of minor glands. When the location and functional relevance of these glands have been revealed, the amount of radiation that passes through these tissues can be reduced by optimization of the treatment plan. This may minimize the risk of persistent xerostomia and associated reduced quality of life.[32] In addition, PSMA PET/CT may identify gland locations devoid of PSMA-ligand uptake, which may not need sparing and thus provide greater flexibility in treatment planning.

Several aspects of PSMA PET imaging require further investigation, such as tissue inhomogeneity and subsequent prediction of response to treatments. Recently,

different studies have reported tumour heterogeneity levels, determined on FDG PET/CT alone or combined with MRI, to be significantly associated with survival and responsiveness to radiotherapy. When a comparable determination of metabolic prognosticators in normal tissues would be possible with PMSA PET/CT, treatment plans could be optimized to further reduce toxicity to the salivary glands.[33,34]

When the relation of PSMA-ligand uptake and the remaining number of vital glandular cells or actual glandular function after treatment can be determined, PSMA PET/CT could also be used to locally assess salivary gland toxicity after external beam radiotherapy or radionuclide treatment. Moreover, equivalent to prostate cancer, PSMA-ligand uptake suggests the possibility of adjuvant treatment with ^{177}Lu-labelled PSMA in selected salivary gland cancer cases.[35] Finally, PSMA PET/CT may also play a future role in the diagnosis and treatment evaluation of benign salivary gland disease, such as the sicca syndromes and recurrent plunging ranula.

CONCLUSION

PSMA PET/CT consistently depicts high tracer uptake in healthy major and minor salivary glands and lacrimal and seromucous glands. Minor salivary and seromucous glands can now be selectively visualized on imaging. Potential clinical applications of PSMA-ligand visualized by PET/CT include quantification of present salivary gland tissues and individualization of head and neck cancer treatment by radiotherapy field adaptation and ^{177}Lu-PSMA radionuclide treatment of salivary gland cancers.

REFERENCES

1. Afshar-Oromieh A, Hetzheim H, Kratochwil C, et al. The novel theranostic PSMA-ligand PSMA-617 in the diagnosis of prostate cancer by PET/CT: biodistribution in humans, radiation dosimetry and first evaluation of tumor lesions. *J Nucl Med.* 2015;56(11):1697-1705.
2. Rahbar K, Ahmadzadehfar H, Kratochwil C, et al. German multicenter study investigating 177Lu-PSMA-617 radioligand therapy in advanced prostate cancer patients. J Nucl Med. 2017;85(1):85-90.
3. Gensheimer MF, Liao JJ, Garden AS, et al. Submandibular gland-sparing radiation therapy for locally advanced oropharyngeal squamous cell carcinoma: patterns of failure and xerostomia outcomes. Radiat Oncol. 2014;9(1):255.
4. Afzelius P, Nielsen M-Y, Ewertsen C, Bloch KP. Imaging of the major salivary glands. Clin Physiol Funct Imaging. 2016;36(1):1-10.
5. La'Porte SJ, Juttla JK, Lingam RK. Imaging the Floor of the Mouth and the Sublingual Space. Radiographics. 2011;31(5):1215-1230.
6. Mandel ID. The role of saliva in maintaining oral homeostasis. J Am Dent Assoc. 1989;119(2):298-304.
7. Hand AR, Pathmanathan D, Field RB. Morphological features of the minor salivary glands. Arch Oral Biol. 1999; 44(Suppl 1):S3-S10.
8. Boellaard R, Delgado-Bolton R, Oyen WJG, et al. FDG PET/CT: EANM procedure guidelines for tumour imaging: version 2.0. Eur J Nucl Med Mol Imaging. 2015;42(2):328-354.
9. Kirchner J, Schaarschmidt BM, Sawicki LM, et al. Evaluation of Practical Interpretation Hurdles in 68Ga-PSMA PET/CT in 55 Patients: Physiological Tracer Distribution and Incidental Tracer Uptake. Clin Nucl Med. 2017;42(7):e322-e327.
10. Demirci E, Sahin OE, Ocak M, Akovali B, Nematyazar J, Kabasakal L. Normal distribution pattern and physiological variants of 68Ga-PSMA-11 PET/CT imaging. Nucl Med Commun. 2016;37(11):1169-1179.
11. Bailey B, Calhoun K. Head and Neck Surgery Otolaryngology, Vol 1. 3rd ed. Philadelphia: Lippincot Williams&Wilkins.; 2001.
12. Tos M. Mucous glands in the developing human rhinopharynx. Laryngoscope. 1977;87(6):987-995.
13. Wang X, Meng L, Hou T, Zheng C, Huang S. Frequency and Distribution Pattern of Minor Salivary Gland Tumors in a Northeastern Chinese Population: A Retrospective Study of 485 Patients. J Oral Maxillofac Surg. 2015;73(1):81-91.
14. Horoszewicz JS, Kawinsky E MG. Monoclonal antibodies to a new antigenic marker in epithelial prostatic cells and serum of prostatic cancer patients. Anticancer Res. 1987;7(5B):927-935.
15. Israeli RS, Powell CT, Fair WR, Heston WD. Molecular cloning of a complementary DNA encoding a prostate-specific membrane antigen. Cancer Res. 1993;53(2):227-230.
16. Wright GL, Haley C, Beckett M Lou, Schellhammer PF. Expression of prostate-specific membrane antigen in normal, benign, and malignant prostate tissues. Urol Oncol Semin Orig Investig. 1995;1(1):18-28.
17. Lopes AD, Davis WL, Rosenstraus MJ, Uveges AJ, Gilman SC. Immunohistochemical and Pharmacokinetic Characterization of the Site-specific Immunoconjugate CYT-356 Derived from Antiprostate Monoclonal Antibody 7E11-C5. Cancer Res. 1990;50(19):6423-6429.
18. Israeli RS, Powell CT, Corr JG, Fair WR, Heston WD. Expression of the prostate-specific membrane antigen. Cancer Res. 1994;54(7):1807-1811.

19. Ristau BT, O'Keefe DS, Bacich DJ. The prostate-specific membrane antigen: Lessons and current clinical implications from 20 years of research. Urol Oncol Semin Orig Investig. 2014;32(3):272-279.
20. Troyer JK, Beckett ML, Wright GL. Detection and characterization of the prostate-specific membrane antigen (PSMA) in tissue extracts and body fluids. Int J cancer. 1995;62(5):552-558.
21. Chang SS, Reuter VE, Heston WDW, Bander NH, Grauer LS, Gaudin PB. Five Different Anti-Prostate-specific Membrane Antigen (PSMA) Antibodies Confirm PSMA Expression in Tumor-associated Neovasculature. Cancer Res. 1999;59(13):3192-3198.
22. Pinto JT, Suffoletto BP, Berzin TM, et al. Prostate-specific membrane antigen: a novel folate hydrolase in human prostatic carcinoma cells. Am Assoc Cancer Res. 1996;2(9):1445-1451.
23. Mease RC, Foss CA, Pomper MG. PET imaging in prostate cancer: focus on prostate-specific membrane antigen. Curr Top Med Chem. 2013;13(8):951-962.
24. Silver DA, Pellicer I, Fair WR, Heston WD, Cordon-Cardo C. Prostate-specific membrane antigen expression in normal and malignant human tissues. Am Assoc Cancer Res. 1997;3(1):81-85.
25. Klein Nulent TJW, van Es RJJ, Krijger GC, de Bree R, Willems SM, de Keizer B. Prostate-specific membrane antigen PET imaging and immunohistochemistry in adenoid cystic carcinoma-a preliminary analysis. Eur J Nucl Med Mol Imaging. 2017;44(10):1614–1621
26. Lawhn-Heath C, Flavell RR, Glastonbury C, Hope TA, Behr SC. Incidental Detection of Head and Neck Squamous Cell Carcinoma on 68Ga-PSMA-11 PET/CT. Clin Nucl Med. 2017;42(4):e218-e220.
27. Lütje S, Heskamp S, Cornelissen AS, et al. PSMA Ligands for Radionuclide Imaging and Therapy of Prostate Cancer: Clinical Status. Theranostics. 2015;5(12):1388-1401.
28. Maurer T, Eiber M, Schwaiger M, Gschwend JE. Current use of PSMA–PET in prostate cancer management. Nat Rev Urol. 2016;13(4):226-235.
29. Wolf P, Freudenberg N, Bühler P, et al. Three conformational antibodies specific for different PSMA epitopes are promising diagnostic and therapeutic tools for prostate cancer. Prostate. 2010;70(5):562-569.
30. Kinahan PE, Fletcher JW. Positron emission tomography-computed tomography standardized uptake values in clinical practice and assessing response to therapy. Semin Ultrasound, CT MRI. 2010;31(6):496-505.
31. Różycki R. Diagnostic imaging of the nasolacrimal drainage system. Part I. Radiological anatomy of lacrimal pathways. Physiology of tear secretion and tear outflow. Med Sci Monit. 2014;20:628-638.
32. Almståhl A, Alstad T, Fagerberg-Mohlin B, Carlén A FC. Explorative study on quality of life in relation to salivary secretion rate in patients with head and neck cancer treated with radiotherapy. Head Neck. 2016;38(5):782-791.
33. Jang JY, Pak KJ, Yi K-I, et al. Differential Prognostic Value of Metabolic Heterogeneity of Primary Tumor and Metastatic Lymph Nodes in Patients with Pharyngeal Cancer. Anticancer Res. 2017;37(10):5899-5905.
34. Chan S-C, Cheng N-M, Hsieh C-H, et al. Multiparametric imaging using (18)F-FDG PET/CT heterogeneity parameters and functional MRI techniques: prognostic significance in patients with primary advanced oropharyngeal or hypopharyngeal squamous cell carcinoma treated with chemoradiotherapy. Oncotarget. 2017;8(37):62606-62621.
35. Weineisen M, Schottelius M, Simecek J, et al. 68Ga- and 177Lu-Labeled PSMA I&T: Optimization of a PSMA-Targeted Theranostic Concept and First Proof-of-Concept Human Studies. J Nucl Med. 2015;56(8):1169-1176.

Prostate-specific membrane antigen PET imaging and immuno-histochemistry in adenoid cystic carcinoma – a preliminary analysis

Thomas J.W. Klein Nulent
Robert J.J. van Es
Gerard C. Krijger
Remco de Bree
Stefan M. Willems
Bart de Keizer

Chapter as published in:
European Journal of Nuclear Medicine and Molecular Imaging 2017; 44(10): 1614–1621

doi: 10.1007/s00259-017-3737-x

ABSTRACT

Background

Adenoid cystic carcinoma (AdCC) of the head and neck is an uncommon malignant epithelial tumour of the secretory glands. Many patients develop slowly growing local recurrence and/or distant metastasis, for which treatment options are limited. A retrospective analysis of nine AdCC patients was conducted to analyze the visualization of AdCC on PSMA PET/CT and to investigate the expression of PSMA on primary, recurrent and metastatic AdCC tumour tissue using immunohistochemistry.

Results

Local recurrence occurred in six patients and eight developed distant metastasis. All PET/CTs depicted PSMA-ligand uptake. Four PSMA PET/CTs showed suspected residual disease, eight scans depicted uptake in areas suspected of distant metastasis. Median maximum standardized uptake value (SUV_{max}) in local recurrent and distant metastatic AdCC was 2.52 (IQR 2.41–5.95) and 4.01 (IQR 2.66–8.71), respectively. All primary tumours showed PSMA expression on immunohistochemistry (5–90% expression), as well as all available specimens of local recurrence and distant metastases.

Conclusion

PSMA PET/CT is able to detect and visualize local recurrent and distant metastatic AdCC. PSMA-specific targeting is supported by PSMA expression on immunohistochemistry.

BACKGROUND

Adenoid cystic carcinoma (AdCC) is an uncommon malignant epithelial tumour of the secretory glands in the head and neck region, accounting for approximately 20–35% of all salivary gland malignancies.[1,2] Its annual incidence in Europe is approximately 2–3/1,000,000.[2,3] AdCC arises in the major salivary glands and more often in the minor salivary glands of the lip, oral cavity, oropharynx, nasopharynx, nasal cavity, paranasal sinus, larynx and tracheobronchial tree. Occasionally it is seen in the lacrimal and ceruminous glands.[1,4,5] AdCC is characterized by slow local progression, extensive perineural spread and a tendency for delayed onset of distant metastasis. Current guidelines consider ^{18}F–fluorodeoxyglucose PET/CT (FDG PET/CT) at initial presentation to be of additional value to assess disseminated disease of AdCC and therefore to be of influence on treatment planning in these patients.[6] However, FDG uptake in AdCC is lower than in squamous cell carcinoma (SCC) and not all AdCCs show detectable FDG uptake.[7] Surgery is the primary treatment option, frequently followed by adjuvant radiation therapy to improve local and regional control.[1] Almost half of all patients develop slowly growing distant metastasis within the first five years after diagnosis, mostly to the lungs and skeleton.[5,8] As a result, long-term mortality is usually caused by distant metastasis or deep local recurrence, of which salvage (re)resection is often impossible.[1] In large European cohort studies, overall five and ten year disease specific survival rates are 68–75% and 52–65%, respectively.[8,9] Survival is significantly decreased after the diagnosis of distant metastasis, with one and five year survival rates of 54–68% and 7–32%, respectively.[8,10]

The prostate-specific membrane antigen (PSMA), a type II transmembrane glycoprotein of the prostate secretory acinar epithelium, is upregulated in prostate carcinoma and its metastasis.[11,13] Functional imaging of cells expressing PSMA using radiolabelled ligands, e.g. ^{68}Gallium-PSMA-HBED-CC (also called Gallium-PSMA-11) and positron emission tomography combined with computed tomography (commonly referred to as PSMA PET/CT), is primarily used for the detection and (re)staging of prostate cancer.[14] However, prostate specificity of PSMA has been disproved. Clinical experience with PSMA PET/CT for prostate cancer has revealed consistent and significant physiological uptake in normal tissues, including the salivary and lacrimal glands, liver and kidneys.[14] Furthermore, PSMA PET/CT depicts tracer uptake in numerous benign neoplasms and malignancies. Benign lesions include Schwannoma, sarcoidosis, Paget's disease, desmoid tumours and adenoma of thyroid, pancreas and adrenal gland.[15,22] Non-prostatic malignancies include sarcoma, follicular lymphoma, brain tumours and carcinoma of breast, lung, kidney, thyroid and liver.[23,30] PSMA expression has been

frequently investigated by immunohistochemistry and was found to be associated with endothelial cells or tumour neovasculature in malignant disease.[31,32]
PSMA-ligand uptake in metastatic AdCC on PSMA PET/CT has been described previously in two case reports.[33,34] As PSMA targeted tumour-specific treatment will be widely available soon, it might also be suitable in selected cases of AdCC. Data on the presence of PSMA on AdCC are lacking, therefore the aim of this study was to analyze the visualization of local recurrent or distant metastatic AdCC on PSMA PET/CT and to investigate the expression of PSMA on AdCC tumour tissues, both primary and metastatic.

METHODS

Patient selection

All patients that were diagnosed with AdCC in our institute were retrospectively reviewed. All patients that underwent full-body PSMA PET/CT for the evaluation of AdCC of the head and neck were included. The following clinical parameters were retrieved from the medical files: gender, age, year of diagnosis, tumour location and diameter, presence of local recurrence or distant metastasis.
All performed PSMA PET/CT scans were collected and reviewed by a dedicated board-certified head and neck nuclear medicine physician (B.d.K.) experienced in PSMA PET/CT, in consensus with a head and neck surgeon (R.v.E.). On each scan all areas of focal tracer uptake were assessed. This included both the region of the (former) primary tumour, as well as regional or distant metastasis. Maximum standardized uptake values (SUV_{max}) were measured using a freehand isocontour volume of interest in these areas. For reference, SUV_{max} was also measured in normal functioning parotid gland, kidneys and liver. Also, all FDG PET/CTs performed within three months before or after PSMA PET/CT were re-examined for direct comparison.
Representative formaldehyde-fixed, paraffin-embedded tissue blocks of the primary tumours and, when applicable, biopsies or resection specimens of recurrences and/or distant metastases, were retrieved from the pathology archives. Tumour specimens were re-examined by a dedicated head and neck pathologist (S.W.) for the following parameters: type and diameter of the tumour, histopathological grade according to the differentiation of Perzin et al.[35], surgical resection margins and the presence of perineural growth, vaso-invasive growth and bone invasion.

PET/CT image acquisition

^{68}Gallium-HBED-CC was prepared using a GMP-grade ^{68}Ge-^{68}Ga-generator (Gallia-Pharm) in combination with an automated system (Modular-Lab Easy), cassettes and buffers as instructed by Eckert & Ziegler Eurotope (Berlin, Germany). 30 µg PSMA-HBED-CC (ABX, Radeberg, Germany) was used per preparation.

Labelling quality control was performed by both instant thin layer chromatography and high performance liquid chromatography (Thermo Scientific Dionex UltiMate 3000), in combination with gamma detection. Images were acquired from skull vertex to the thighs using a TruePoint Biograph mCT40 scanner (Siemens, Erlangen, Germany), approximately 60 min after intravenous injection of 2 MBq/kg ^{68}Ga-HBED-CC-Glu-NH-CO-NHLys(Ahx) or 2 MBq/kg FDG in case of FDG-PET/CT imaging. A low dose CT scan was performed using Care Dose 4D and Care kV, reference parameters: 40 mAs, 120 kV. Subsequently, PET was acquired according to the European Association of Nuclear Medicine (EANM) recommendations with the following parameters: PET with time-of-flight and point spread function (TrueX) reconstruction, 4 iterations, 21 subsets, with a filter of 7.5 mm full width at half maximum.[36]

Immunohistochemistry

Representative paraffin sections 4 µm thick were analyzed immunohistochemically using fully automated protocols on the Benchmark XT (Ventana Medical Systems, Tucson, AZ, USA). For the primary antibody, we used a mouse antihuman PSMA monoclonal antibody (3E6; DAKO, Carpinteria, CA) of the IgG1 isotype directed against the internal domain of the PSMA antigen (DAKO, cat. no. M3620, Carpinteria, CA, dilution 1/80). The tissue sections were deparaffinized with xylene and ethanol followed by heat induced epitope retrieval in Ventana Cell Conditioning 1 for 24 min and, subsequently, primary antibody incubation for 60 min. Antigen-antibody reactions were visualized using Ventana OptiView™ Amplification kit, followed by Ventana OptiView™ Universal DAB Detection Kit (Optiview HQ Linker 8 min, Optiview HRP Multimer 8 min, Optiview Amplifier H2O2/ Amplifier 4 min, Optiview Amplifier Multimer 4 min). Finally, the slides were counterstained with haematoxylin, dehydrated and mounted. PSMA immunohistochemically stained slides were scored for percentage of positive tumour cells.

Statistics

Statistics were performed using IBM SPSS Statistics for Windows, version 21.0 (Armonk, NY: IBM Corp., 2012). Patient characteristics and outcome measurements are provided as means ± standard deviation and range, or median with interquartile range (IQR) when these data were not distributed normally.

RESULTS

Since 1990, fifty-six patients were diagnosed with AdCC at our institute, of which thirteen patients are in active follow-up because of local recurrent or distant metastatic disease. Since October 2015, nine of these patients had been referred for restaging by PSMA PET/CT either because of suspected local recurrence or distant metastasis. These patients, four men and five women, had an average age at diagnosis of 51 ± 15 years (range 31–76 years). Local recurrence occurred in six out of nine patients, with a median time span of 2.8 years after first diagnosis (IQR 2.1–7.6 years). Eight patients eventually developed distant metastasis, on average 5.8 ± 4.1 years after first diagnosis (range 0–12.5 years). Clinical and histopathological tumour characteristics are summarized in Table 1.

PSMA PET/CT

The mean administered tracer activity was 150 ± 31 MBq (range 107–207 MBq). The time interval between tracer administration and imaging was on average 71 ± 15 min (range 51–91 min). All nine PET/CTs clearly depicted PSMA-ligand uptake in areas of the former primary tumour or localizations of distant metastasis (Table 2). Four PSMA PET/CTs showed tracer accumulation suspected of residual or recurrent AdCC, eight PSMA PET/CTs depicted uptake in areas suspected of distant metastasis. Three scans showed tracer uptake in four new lesions suspected of metastasis; progression of formerly diagnosed metastases was seen in four patients. In one patient, a simultaneous primary prostate carcinoma was detected. When positive, median SUV_{max} in local recurrent AdCC was 2.52 (IQR 2.41–5.95) and median SUV_{max} in distant metastatic AdCC was 4.01 (IQR 2.66–8.71). For reference, median $SUVs_{max}$ in normal parotid, liver and kidneys were 10.9 (IQR 9.01–15.55), 3.83 (IQR 2.99–4.88) and 23.76 (IQR 15.00–35.00), respectively. Three patients underwent concurrent FDG PET/CT within three months from PSMA PET/CT, and data were available for direct comparison. In two patients, PSMA SUV_{max} was comparable to FDG SUV_{max} and in one patient only PSMA PET/CT depicted increased tracer uptake in an area suspected of recurrent AdCC (Table 2). Figure 1 shows projection examples of PSMA-ligand uptake in local recurrent and distant metastatic AdCC.

PSMA expression by immunohistochemistry

Revision of the nine tumour specimens revealed positive resection margins in all cases of primary resection, for which all these patients received postoperative radiotherapy. Eight tumours demonstrated perineural growth. All primary tumours, as well as all

Table 1. Patient characteristics

No.	Gender	Age at diagnosis (yr)	Year of diagnosis	Tumour site	Diameter (cm)	Perzin[35] grade	Growth pattern
1	M	36	2003	nasal cavity	1.8	2	BI
2	M	31	2003	palate	3.8	2	PN/BI
3	F	54	2005	palate	1.6	2	PN
4	F	58	2007	palate	7.0	1	PN/VI/BI
5	F	61	2008	parotid	3.5	2	PN/VI
6	F	59	2008	parotid	3.5	1	PN
7	F	40	2009	parotid	2.0	3	PN/VI
8	M	41	2013	parotid	0.7	2	PN
9	M	76	2015	nasal cavity	3.3	3	PN/BI

PN: perineural invasion; VI: vaso-invasive growth; BI: bone invasion

available tumour specimens of local recurrence and distant metastases were positive on PSMA immunohistochemistry. Expression was seen in a granular fashion, mainly cytoplasmic or concentrated at the luminal side of the cell membrane and varied widely between 5 to 90%. Of the primary tumour specimens, a median of 30% of the tumour cells (IQR 15–70%) demonstrated PSMA expression. Examples of different staining patterns are shown in Figure 2, results per patient are summarized in Table 2.

Implications for treatment

In four patients, the newly obtained results by PSMA PET/CT led to alteration of treatment. Patient no. 3 is currently undergoing palliative targeted radionuclide therapy with Lutetium-177-PSMA-617, because of progressive dyspnoea due to pulmonary metastases. Patients no. 7 and 9 were referred for adjuvant irradiation therapy and patient no. 8 was referred to another hospital for experimental chemotherapy. The other five patients received best supportive care only.

Table 2. PSMA PET/CT, FDG PET/CT and immunohistochemical characteristics

No.	Primary tumour		Local recurrence				Distant metastasis			
	site	IHC (%)	site	PSMA SUV_{max}	FDG SUV_{max}	IHC (%)	site	PSMA SUV_{max}	FDG SUV_{max}	IHC (%)
1	2003 nasal cavity	70%	2006 nasopharynx / retrobulbar 2014 nasopharynx 2016 nasopharynx / masticator space	* * 7.06		90% 50% n/a	2016 leptomeningeal	8.71		
2	2003 palate	30%	-				2011 lungs 2016 peritoneal 2016 liver 2016 iliac crest	0 0 0 2.04	0 0 2.39 2.34	70% 70%
3	2005 palate	5%	2007 palate	*		30%	2007 lungs **2016 liver**	2.66 4.01		
4	2007 palate	5%	2015 maxilla / retrobulbar	*			2015 intracranial **2016 vertebra**	12.81 3.47		
5	2008 parotid	70%	2015 scalp	2.42		10%	2015 leptomeningeal	2.42		
6	2008 parotid	25%	-				2010 lungs	3.64		
7	2009 parotid	50%	2011 ext. auditory canal 2015 ext. auditory canal	* 2.41	4.00	30% 90%	2013 lungs	4.68	3.60	
8	2013 parotid	30%	**2016 parotid**	2.62	1.90**		-			
9	2015 nasal cavity	90%	-				**2015 iliac crest** **2015 lungs**	12.97 6.66		5%

Entries in bold are newly discovered on PSMA PET/CT
n/a: biopsy specimen contained no tumour tissue;
* no PET imaging at time of diagnosis of recurrence; ** physiological uptake

DISCUSSION

This is the first study on a series of patients in which the presence of PSMA in AdCC of the head and neck is demonstrated. PSMA PET/CT was able to visualize local recurrent and/or distant metastatic AdCC in all cases. Furthermore, all primary resection specimens showed PSMA expression on immunohistochemistry, as well as all available tumour tissues of local recurrence and distant metastases.

Figure 1. Overview of PSMA PET (**a** and **c**) and axial PSMA PET/CT slides (**b** and **d**) of PSMA-ligand uptake in AdCC.

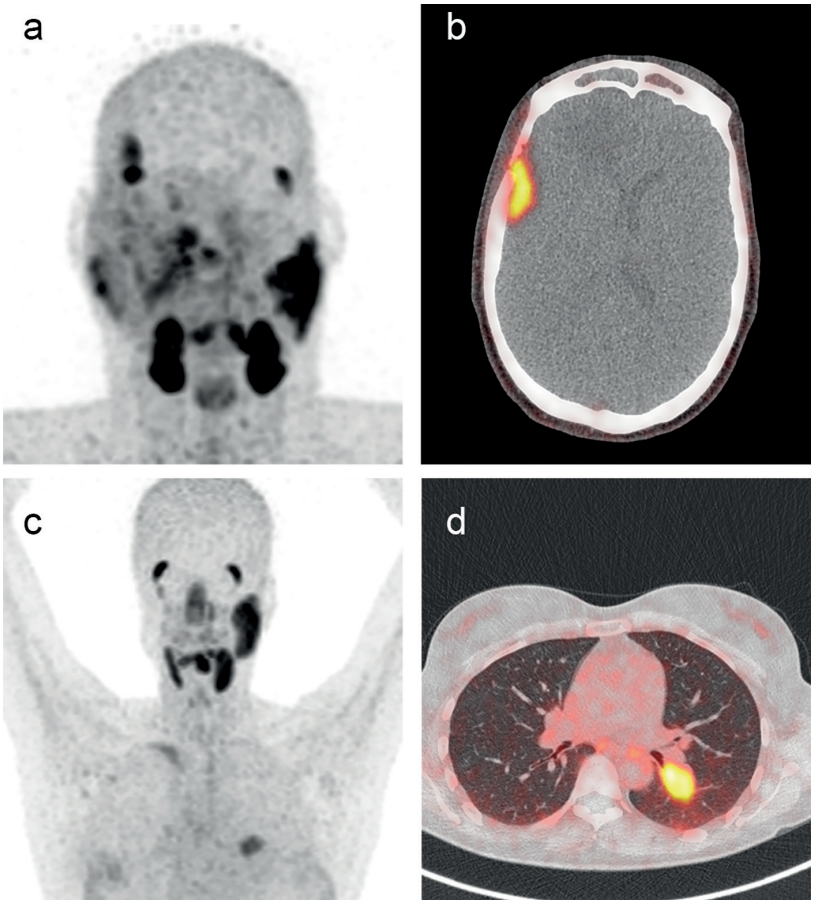

Patient no. 1 (**a** and **b**): nasopharyngeal recurrence and leptomeningeal metastasis;
Patient no. 7 (**c** and **d**): local recurrence in the right maxillofacial region and pulmonary metastasis.

PSMA expression

Although little is known about the presence and function of PSMA in salivary gland tissue, the presence of PSMA mRNA in salivary gland extracts had already been detected in 1994 using Western blot analysis.[37,38] Later, PSMA expression was described in human salivary gland specimen by demonstrating cytoplasmatic immunohistochemical staining of the epithelium of acinar glandular cells.[39] In accordance with two recent case reports on PSMA in AdCC, the present results of functional imaging and immunohistochemistry of primary, local recurrent and distant metastatic AdCC also clearly demonstrate PSMA expression in these tumours.[33,34] Different protein expression between the primary tumour and residual or local recurrent disease is probably due to upregulation or downregulation of PSMA. However, this tumour heterogeneity seems relatively limited, as all matched cases show concordant positive expression between primary and recurrent cases.

PSMA PET/CT vs FDG PET/CT

Today, FDG PET/CT plays a major role in detection and staging of patients with head and neck cancer, with most studies focusing on SCC.[40] However, it is known that AdCC has different biological characteristics and its FDG-uptake is lower as compared to SCC.[7] A recent study comparing FDG PET/CT and conventional contrast-enhanced CT in patients with AdCC showed similar sensitivity for primary lesion detection. However, in two of the 40 patients the primary tumour showed no FDG uptake at all. FDG PET/CT was superior in identification of lymph node and distant metastasis when compared to conventional CT.[7]

In the present study, three patients received concurrent FDG PET/CT and PSMA PET/CT (Table 2). Patient no. 2 had histopathologically confirmed pulmonary and peritoneal metastases and was suspected of liver metastasis, of which none depicted PSMA-ligand uptake on PSMA PET/CT. Pulmonary nodules and peritoneal metastases showed no FDG uptake either. Although the liver lesion was previously suspected of metastasis on magnetic resonance imaging (MRI), it showed only slightly increased and diffuse FDG uptake just above normal liver parenchyma on FDG PET/CT. FDG and PSMA-ligand uptake in iliac crest metastasis was comparable on both scans.

The area of local recurrence and pulmonary metastases of patient no. 7 showed similar pathological accumulation of both tracers. In patient no. 8, the local recurrence of parotideal AdCC showed only physiological background FDG uptake on FDG PET/CT in the area of the former tumour, in contrast to increased PSMA-ligand uptake suggesting recurrent disease.

Anticipating the presence of high PSMA-ligand uptake in normal salivary gland tissue and the SUV of presently described locally recurrent AdCC, PSMA PET/CT is probably not useful in detecting primary AdCC of major salivary glands. At initial presentation of AdCC, the value of PSMA PET/CT therefore appears comparable to FDG PET/CT, with a main focus on the visualization of nodal or distant metastasis. During follow-up, this study indicates PSMA PET/CT to be able to visualize disease progression, recurrence and distant metastases. PSMA PET/CT is considered to be as reliable as FDG PET/CT, when background tracer accumulation is taken into account.

PSMA histopathology vs imaging

In three patients (no. 1, 2 and 4), results of both imaging and immunohistochemistry did not match completely (Table 2). In patient no. 2, both primary and metastatic tissues stained positive on PSMA immunohistochemistry. However, there was no uptake of PSMA-ligand in any of the pulmonary, liver or peritoneal metastases on PET/CT. In comparison, there was also no FDG uptake in the pulmonary and peritoneal metastases, and only slight uptake of FDG in the liver metastasis. The absence of metastatic tracer uptake on PSMA PET/CT is due to surgical resection of the pulmonary metastases by a lobectomy in 2011, which made these available for immunohistochemistry. The remaining suspicious pulmonary nodules, which were not cytologically proven malignant, were only 5 mm or less in diameter. If indeed these nodules were metastases, insufficient tracer uptake in small tumour volumes may be an explanation, analogous to FDG PET/CT.[41] The invisibility of immunohistochemically positive liver and peritoneal metastases on PSMA PET/CT may be explained by the physiological distribution of PSMA in these tissues. We assume the PSMA-ligand uptake in these liver and peritoneal metastases to be equal to or less than background uptake of PSMA.[14]

In patient no. 1, an early 2016 MRI was suspicious of nasopharyngeal recurrence and leptomeningeal metastasis, which was supported by high tracer uptake on PSMA PET/CT one month later (SUV_{max} 7.06 and 8.71 respectively). Unfortunately, a biopsy specimen of this area contained no tumour tissue and histopathological samples of the leptomeningeal lesions were not obtained. The primary tumour of patient no. 4 was weakly positive on PSMA immunohistochemistry. The early 2015 local recurrence, diagnosed on previous MRI, depicted no tracer uptake on 2016 PSMA PET/CT, probably because it was previously treated by stereotactic radiotherapy. Based on this PSMA PET/CT, it is therefore not entirely clear whether the reported local abnormalities indicate recurrent disease or should be classified as post-irradiation effects. In addition, there was intracranial and vertebral PSMA-ligand uptake, highly suspicious of distant

metastases. Histopathological confirmation of these lesions was not sought due to their location.

Figure 2. Immunohistochemical PSMA expression in AdCC. *Magnification: (**a b c**) 400x; (**d**) 700x.*

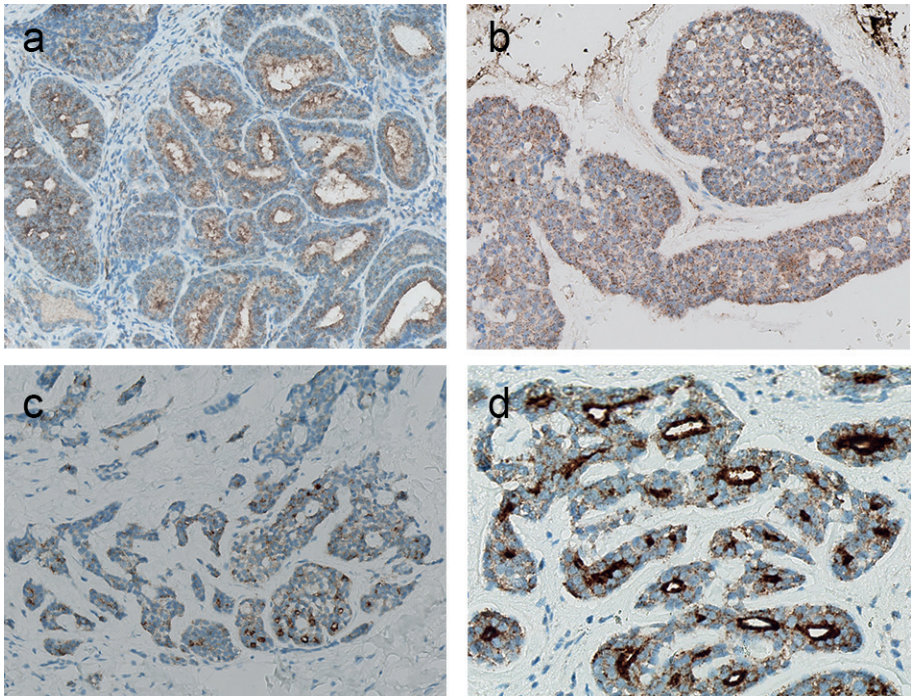

(**a**) nasal cavity primary AdCC, 70%; (**b**) nasopharyngeal recurrence, 90%; (**c**) peritoneal metastasis, 70%; and (**d**) luminal staining of primary parotideal AdCC, 70%.

New treatment option

As shown in this series, recurrent and metastatic disease is a relevant issue in AdCC patients. As a result, survival rates have not improved over the past decades, as no progress has been made in developing new treatment modalities. Disease specific survival is mainly affected by stage, margin status and histopathological grade, i.e., a solid growth pattern, and subsequent to these the occurrence of distant metastasis. Postoperative radiotherapy does improve locoregional control, but does not affect survival.[8,10,42] In advanced metastatic castration-resistant prostate carcinoma, patients are now receiving a radionuclide tumour-specific treatment directed against PSMA-overexpressing prostate cancer cells. With this therapy, a PSMA-ligand is labelled with

the β-emitter Lutetium-177 which causes internal radiation.[43] The results are encouraging with a ≥50% decrease of plasma prostate-specific antigen (PSA) in 45% of patients after one cycle of ^{177}Lu-PSMA-617, as well as a decrease of SUV_{max} on PET/CT.[43,44] Treatment with this radionuclide was deemed to be safe and well tolerated in a large multicentre retrospective study. Bone-marrow depression, renal failure and xerostomia are reported side-effects.[44] In comparison with PSMA PET/CT imaging of prostate cancer, using the same radiotracer, prostate cancer tumour lesions have an average SUV_{max} of 13.3 ± 14.6 (range 0.7–122.5).[45] Uptake of PSMA-tracer in AdCC, given our results, is considered moderate. Therefore, we are currently evaluating whether this ^{177}Lu-PSMA-617-therapy, using the same therapy regimen and activity which has already shown to be associated with limited adverse effects in prostate cancer, will be as effective in patients suffering from irresectable recurrent and/or metastatic AdCC. In most malignancies, other than prostate cancer, PSMA is localized in the neovasculature.[23,27,31,32,46] Because the localization of PSMA in AdCC is mainly cytoplasmic or concentrated at the luminal side of the cell membrane, therapy with alpha-emitting ^{225}Ac-PSMA-617 might also be a viable therapeutic option.[47]

This study has some limitations. As this was a retrospective analysis, in five recurrent lesions of four patients PSMA PET/CT was not available at the time of diagnosis. However, only two recurrent cases had no PSMA PET imaging at all, and moreover all PSMA PET/CTs showed concordant positive tracer uptake. More importantly, only two patients suspected of recurrence underwent concurrent FDG PET/CT, of which one was suggested to have disease recurrence and one was underestimated as physiological uptake. In detection of distant sites, eight patients with eleven sites were detected by PSMA PET/CT, of which two could be compared to FDG PET/CT and showed similar tracer accumulation. The results of this study should be interpreted as a preliminary descriptive analysis of PSMA in these tumours. The additive value of PSMA PET/CT over FDG PET/CT needs to be further investigated.

CONCLUSION

PSMA PET/CT is able to detect and visualize local recurrent and distant metastatic AdCC. Additionally, PSMA-specific targeting is supported by high PSMA expression on immunohistochemistry. When compared to FDG PET/CT, we found concordant tracer uptake without underdiagnosing clinically relevant disease progression of both local recurrence and distant metastasis.

REFERENCES

1. Coca-Pelaz A, Rodrigo JP, Bradley PJ, Vander Poorten V, Triantafyllou A, Hunt JL, et al. Adenoid cystic carcinoma of the head and neck - An update. Oral Onco. 2015;51(7):652–61.
2. Bjørndal K, Krogdahl A, Therkildsen MH, Overgaard J, Johansen J, Kristensen CA, et al. Salivary gland carcinoma in Denmark 1990-2005: A national study of incidence, site and histology. Results of the Danish Head and Neck Cancer Group (DAHANCA). Oral Oncol. 2011;47(7):677–82.
3. Netherlands Comprehensive Cancer Organisation, The Netherlands Cancer Registry. Incidence of invasive salivary gland cancer per year. 2015 [cited 2016 Apr 1]. Available from: http://www.cijfersoverkanker.nl
4. Hellquist H, Skalova A. Adenoid Cystic Carcinoma. In: Histopathology of the Salivary Glands. Springer Berlin Heidelberg; 2014. p. 221–60.
5. Spiro RH, Huvos AG, Strong EW. Adenoid cystic carcinoma of salivary origin. A clinicopathologic study of 242 cases. Am J Surg. 1974;128(4):512–20.
6. Freling N, Crippa F, Maroldi R. Staging and follow-up of high-grade malignant salivary gland tumours: The role of traditional versus functional imaging approaches - A review. Oral Oncol. 2016;60:157–66.
7. Jung JH, Lee SW, Son SH, Kim CY, Lee CH, Jeong JH, et al. Clinical impact of (18) F-FDG positron emission tomography/CT on adenoid cystic carcinoma of the head and neck. Head Neck. 2017;39(3):447–55.
8. Van Weert S, Reinhard R, Bloemena E, Buter J, Witte BI, Vergeer MR, et al. Differences in patterns of survival in metastatic adenoid cystic carcinoma of the head and neck. Head Neck. 2017;39(3):456–63.
9. Ciccolallo L, Licitra L, Cantú G, Gatta G. Survival from salivary glands adenoid cystic carcinoma in European populations. Oral Oncol. 2009;45(8):669–74.
10. Terhaard CHJ, Lubsen H, Van Der Tweel I, Hilgers FJM, Eijkenboom WMH, Marres HAM, et al. Salivary gland carcinoma: Independent prognostic factors for locoregional control, distant metastases, and overall survival: Results of the Dutch Head and Neck Oncology Cooperative Group. Head Neck. 2004;26(8):681–92.
11. Horoszewicz JS, Kawinsky E MG. Monoclonal antibodies to a new antigenic marker in epithelial prostatic cells and serum of prostatic cancer patients. Anticancer Res. 1987;7(5B):927–35.
12. Israeli RS, Powell CT, Fair WR, Heston WD. Molecular cloning of a complementary DNA encoding a prostate-specific membrane antigen. Cancer Res. 1993 Jan;53(2):227–30.
13. Wright GL, Haley C, Beckett M Lou, Schellhammer PF. Expression of prostate-specific membrane antigen in normal, benign, and malignant prostate tissues. Urol Oncol Semin Orig Investig. 1995;1(1):18–28.
14. Afshar-Oromieh A, Hetzheim H, Kratochwil C, Benesova M, Eder M, Neels OC, et al. The novel theranostic PSMA-ligand PSMA-617 in the diagnosis of prostate cancer by PET/CT: biodistribution in humans, radiation dosimetry and first evaluation of tumor lesions. J Nucl Med. 2015;56(11):1697–705.
15. Rischpler C, Maurer T, Schwaiger M, Eiber M. Intense PSMA-expression using 68Ga-PSMA PET/CT in a paravertebral schwannoma mimicking prostate cancer metastasis. Eur J Nucl Med Mol Imaging. 2016;43(1):193–4.
16. Ardies PJ, Gykiere P, Goethals L, De Mey J, De Geeter F, Everaert H. PSMA Uptake in Mediastinal Sarcoidosis. Clin Nucl Med. 2017;42(4):303–5.

17. Jochumsen MR, Vendelbo MH, Høyer S, Bouchelouche K. Subcutaneous Lobular Capillary Hemangioma on 68Ga-PSMA PET/CT. Clin Nucl Med. 2017;42(4):e214–5.
18. Artigas C, Alexiou J, Garcia C, Wimana Z, Otte F-X, Gil T, et al. Paget bone disease demonstrated on 68Ga-PSMA ligand PET/CT. Eur J Nucl Med Mol Imaging. 2016;43(1):195–6.
19. Kanthan GL, Hsiao E, Kneebone A, Eade T, Schembri GP. Desmoid Tumor Showing Intense Uptake on 68Ga PSMA-HBED-CC PET/CT. Clin Nucl Med. 2016;41(6):508–9.
20. Kanthan GL, Drummond J, Schembri GP, Izard MA, Hsiao E. Follicular Thyroid Adenoma Showing Avid Uptake on 68Ga PSMA-HBED-CC PET/CT. Clin Nucl Med. 2016;41(4):331–2.
21. Chan M, Schembri GP, Hsiao E. Serous Cystadenoma of the Pancreas Showing Uptake on 68Ga PSMA PET/CT. Clin Nucl Med. 2017;42(1):56–7.
22. Law WP, Fiumara F, Fong W, Miles KA. Gallium-68 PSMA uptake in adrenal adenoma. J Med Imaging Radiat Oncol. 2016;60(4):514–7.
23. Heitkötter B, Trautmann M, Grünewald I, Bögemann M, Rahbar K, Gevensleben H, et al. Expression of PSMA in tumor neovasculature of high grade sarcomas including synovial sarcoma, rhabdomyosarcoma, undifferentiated sarcoma and MPNST. Oncotarget. 2017;8(3):4268–76.
24. Kanthan GL, Coyle L, Kneebone A, Schembri GP, Hsiao E. Follicular Lymphoma Showing Avid Uptake on 68Ga PSMA-HBED-CC PET/CT. Clin Nucl Med. 2016;41(6):500–1.
25. Sasikumar A, Joy A, Pillai MRA, Nanabala R, Anees K M, Jayaprakash PG, et al. Diagnostic Value of 68Ga PSMA-11 PET/CT Imaging of Brain Tumors—Preliminary Analysis. Clin Nucl Med. 2017;42(1):e41–8.
26. Sathekge M, Lengana T, Modiselle M, Vorster M, Zeevaart J, Maes A, et al. 68Ga-PSMA-HBED-CC PET imaging in breast carcinoma patients. Eur J Nucl Med Mol Imaging. 2017;44(4):689–94.
27. Wang H, Wang S, Song W, Pan Y, Yu H, Si T, et al. Expression of prostate-specific membrane antigen in lung cancer cells and tumor neovasculature endothelial cells and its clinical significance. PLoS One. 2015;10(5):e0125924.
28. Demirci E, Ocak M, Kabasakal L, Decristoforo C, Talat Z, Halaç M, et al. 68Ga-PSMA PET/CT imaging of metastatic clear cell renal cell carcinoma. Eur J Nucl Med Mol Imaging. 2014;41(7):1461–2.
29. Verburg FA, Krohn T, Heinzel A, Mottaghy FM, Behrendt FF. First evidence of PSMA expression in differentiated thyroid cancer using [68Ga]PSMA-HBED-CC PET/CT. Eur J Nucl Med Mol Imaging. 2015;42(10):1622–3.
30. Sasikumar A, Joy A, Nanabala R, Pillai MRA, Thomas B, Vikraman KR. (68)Ga-PSMA PET/CT imaging in primary hepatocellular carcinoma. Eur J Nucl Med Mol Imaging. 2016;43(4):795–6.
31. Chang SS, Reuter VE, Heston WDW, Bander NH, Grauer LS, Gaudin PB. Five Different Anti-Prostate-specific Membrane Antigen (PSMA) Antibodies Confirm PSMA Expression in Tumor-associated Neovasculature. Cancer Res. 1999;59(13):3192–8.
32. Silver DA, Pellicer I, Fair WR, Heston WD, Cordon-Cardo C. Prostate-specific membrane antigen expression in normal and malignant human tissues. Am Assoc Cancer Res. 1997;3(1):81–5.
33. De Keizer B, Krijger GC, Ververs FT, van Es RJJ, de Bree R, Willems S. 68Ga-PSMA PET-CT Imaging of Metastatic Adenoid Cystic Carcinoma. Nucl Med Mol Imaging. 2017;51(4):360-1.
34. Lütje S, Sauerwein W, Lauenstein T, Bockisch A, Poeppel TD. In Vivo Visualization of Prostate-Specific Membrane Antigen in Adenoid Cystic Carcinoma of the Salivary Gland. Clin Nucl Med. 2016;41(6):476–7.

35. Perzin KH, Gullane P, Clairmont AC. Adenoid cystic carcinomas arising in salivary glands: a correlation of histologic features and clinical course. Cancer. 1978;42(1):265–82.
36. Boellaard R, Delgado-Bolton R, Oyen WJG, Giammarile F, Tatsch K, Eschner W, et al. FDG PET/CT: EANM procedure guidelines for tumour imaging: version 2.0. Eur J Nucl Med Mol Imaging. 2015;42(2):328–54.
37. Israeli RS, Powell CT, Corr JG, Fair WR, Heston WD. Expression of the prostate-specific membrane antigen. Cancer Res. 1994;54(7):1807–11.
38. Troyer JK, Beckett ML, Wright GL. Detection and characterization of the prostate-specific membrane antigen (PSMA) in tissue extracts and body fluids. Int J cancer. 1995 Sep;62(5):552–8.
39. Wolf P, Freudenberg N, Bühler P, Alt K, Schultze-Seemann W, Wetterauer U, et al. Three conformational antibodies specific for different PSMA epitopes are promising diagnostic and therapeutic tools for prostate cancer. Prostate. 2010;70(5):562–9.
40. Lonneux M, Hamoir M, Reychler H, Maingon P, Duvillard C, Calais G, et al. Positron emission tomography with [18F]fluorodeoxyglucose improves staging and patient management in patients with head and neck squamous cell carcinoma: a multicenter prospective study. J Clin Oncol. 2010;28(7):1190–5.
41. Kinahan PE, Fletcher JW. Positron emission tomography-computed tomography standardized uptake values in clinical practice and assessing response to therapy. Semin Ultrasound, CT MRI. 2010;31(6):496–505.
42. Bjørndal K, Krogdahl A, Therkildsen MH, Charabi B, Kristensen CA, Andersen E, et al. Salivary adenoid cystic carcinoma in Denmark 1990-2005: Outcome and independent prognostic factors including the benefit of radiotherapy. Results of the Danish Head and Neck Cancer Group (DAHANCA). Oral Oncol. 2015;51(12):1138–42.
43. Fendler WP, Reinhardt S, Ilhan H, Delker A, Böning G, Gildehaus FJ, et al. Preliminary experience with dosimetry, response and patient reported outcome after 177Lu-PSMA-617 therapy for metastatic castration-resistant prostate cancer. Oncotarget. 2017;8(2):3581–90.
44. Rahbar K, Ahmadzadehfar H, Kratochwil C, Haberkorn U, Schäfers M, Essler M, et al. German multicenter study investigating 177Lu-PSMA-617 radioligand therapy in advanced prostate cancer patients. J Nucl Med. 2016;85(1):85–90.
45. Afshar-Oromieh A, Avtzi E, Giesel FL, Holland-Letz T, Linhart HG, Eder M, et al. The diagnostic value of PET/CT imaging with the 68Ga-labelled PSMA ligand HBED-CC in the diagnosis of recurrent prostate cancer. Eur J Nucl Med Mol Imaging. 2015;42(2):197–209.
46. Wernicke AG, Kim S, Liu H, Bander NH, Pirog EC. Prostate-specific Membrane Antigen (PSMA) Expression in the Neovasculature of Gynecologic Malignancies: Implications for PSMA-targeted Therapy. Appl Immunohistochem Mol Morphol. 2017;25(4):271-6.
47. Kratochwil C, Bruchertseifer F, Rathke H, Bronzel M, Apostolidis C, Weichert W, et al. Targeted Alpha Therapy of mCRPC with (225)Actinium-PSMA-617: Dosimetry estimate and empirical dose finding. J Nucl Med. 2017;58(10):1624-31

6

PART C

Targeted therapy

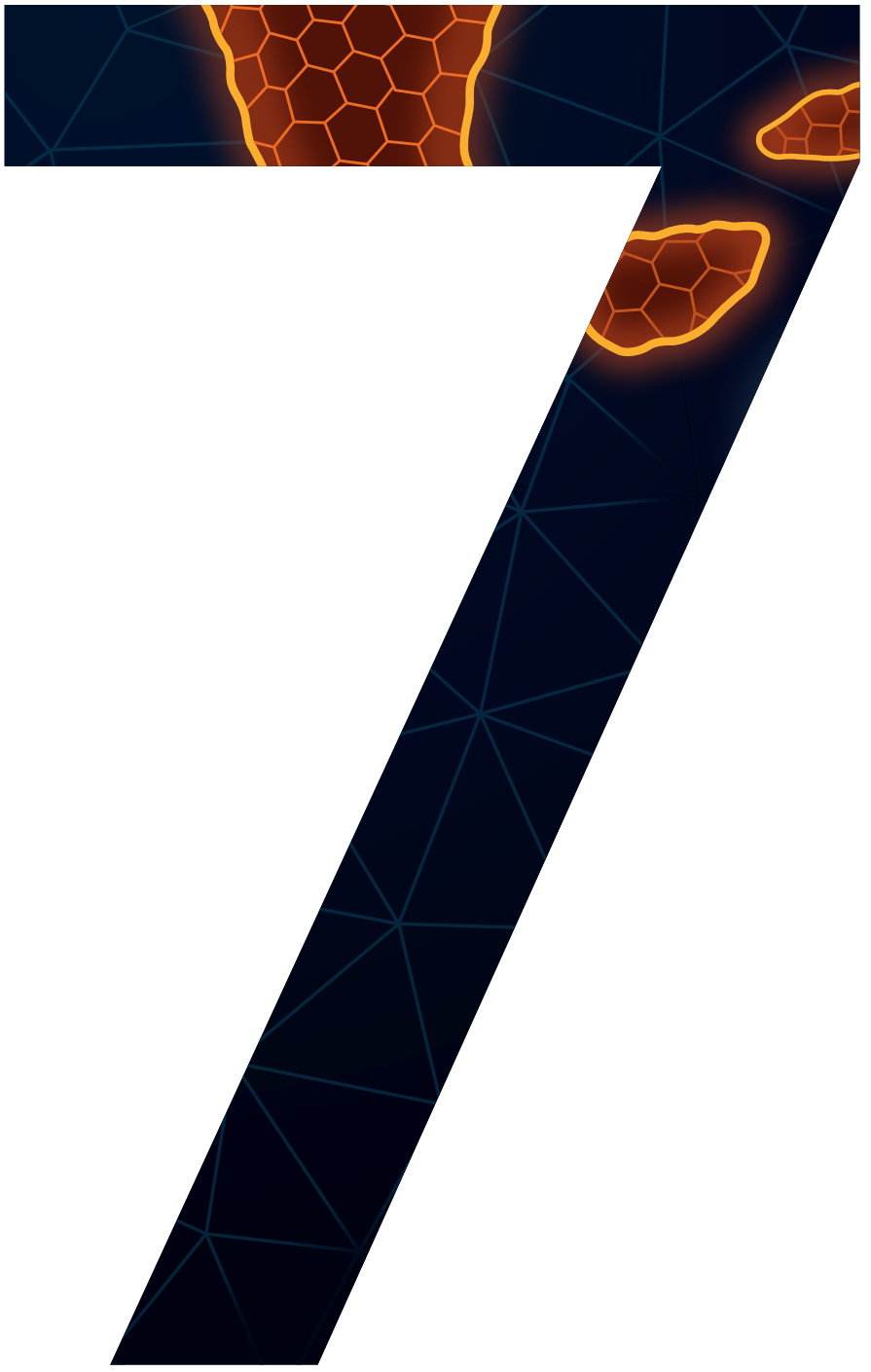

First experiences with ^{177}Lu-PSMA-617 therapy for recurrent or metastatic salivary gland cancer

Thomas J.W. Klein Nulent
Robert J.J. van Es
Stefan M. Willems
Arthur J.A.T. Braat
Lot A. Devriese
Remco de Bree
Bart de Keizer

Chapter as published in:
EJNMMI Research 2021; 11(1): 126

doi: 10.1186/s13550-021-00866-8

ABSTRACT

Background:

Advanced salivary gland cancers become difficult to treat when they are technically irresectable and radiotherapy limits are exceeded. There is also an unmet need to improve palliative systemic therapy. Salivary glands depict the prostate-specific membrane antigen (PSMA) on ^{68}Ga-PSMA PET/CT, a transmembrane protein that is targeted for diagnosis and treatment of advanced prostate cancer. Some salivary gland carcinomas also express PSMA.

Methods

This study aimed to retrospectively evaluate the effectiveness of ^{177}Lu-PSMA-617 therapy for recurrent or metastatic salivary gland cancers, as a last resort treatment. Patients with serious tumour-related discomfort for whom no regular option was available were selected and critically re-assessed by the tumour board. Radionuclide therapy eligibility was confirmed when tumour targeting was greater than liver SUV_{max} on ^{68}Ga-PSMA PET/CT. The protocol aimed at four cycles of 6.0–7.4 GBq ^{177}Lu-PSMA-617 every 6–8 weeks. Clinical response was evaluated by questionnaires and radiological response by ^{68}Ga-PSMA PET/CT.

Results

Six patients were treated with ^{177}Lu-PSMA: four adenoid cystic carcinomas, one adenocarcinoma NOS and one acinic cell carcinoma. In two patients, radiological response was observed, showing either stable disease or a partial response, and four patients reported immediate relief of tumour-related symptoms. Most reported side effects were grade 1–2 fatigue, nausea, bone pain and xerostomia. Four patients prematurely discontinued therapy: three due to disease progression and one due to demotivating (grade 1) side-effects.

Conclusion

Palliative ^{177}Lu-PSMA therapy for salivary gland cancer may lead to rapid relief of tumour-associated discomfort and may even induce disease stabilization. It is safe, relatively well tolerated and can be considered when regular treatment options fail.

INTRODUCTION

Salivary gland cancer is a rare malignant head and neck tumour. They account for 3–10% of all head and neck malignancies and exhibit a diverse clinical and biological behaviour. Adenoid cystic carcinoma (AdCC) is one of the most common malignant salivary gland tumours, comprising 20–35% of all cases.[1,2] After initial treatment with surgery and often radiotherapy, patients with advanced disease are frequently confronted with a locoregional recurrence, as reflected by a local control rate of 58% after 10 years. Curation of progressive disease is challenging when a deep recurrence is technically irresectable and radiation limits are exceeded. Additionally, almost half of the patients develop slowly growing pulmonary or osseous distant metastases within 5 years after diagnosis that shorten life expectancy[1,3,5] Disease-specific survival (DSS) is moderate with 5- and 10-year survival rates of 68–78% and 54–65%, respectively.[5,6] The effectiveness of both systemic chemotherapy and targeted immunotherapy is limited for symptomatic recurrent or distant disease and might only be beneficial to a small group of patients.[7,8]

The prostate-specific membrane antigen (PSMA), a transmembrane glycoprotein of the prostate secretory acinar epithelium, is known from its widely adopted use in diagnostics for metastatic prostate carcinoma using ^{68}Ga-PSMA PET/CT.[9] Research revealed tracer accumulation on ^{68}Ga-PSMA PET/CT not only in normal salivary and lacrimal glands, but also in areas of adenomas and adenocarcinomas such as AdCC, and more recently also in salivary duct carcinoma (SDC). Although intracellular PSMA expression was confirmed by histopathology in AdCC and in tumour-induced vessels of SDC, it is in general not correlated to PSMA-ligand uptake on PET/CT.[9,13] Palliative targeted radionuclide therapy with Lutetium-177-labelled PSMA-617 (^{177}Lu-PSMA) is increasingly used in metastatic castration-resistant prostate cancer and well-tolerated with few side effects.[14,15] Because of the clear visualization of AdCC and possible other salivary gland cancer localizations on PSMA PET/CT, it is of interest whether palliative salivary gland cancer patients could benefit from targeted therapy with ^{177}Lu-PSMA, when other treatment options fail.[12]

METHODS

Since mid-2018, the head and neck multidisciplinary tumour board (MTB) of the University Medical Center Utrecht offers compassionate use of the PSMA-targeted radionuclide ^{177}Lu-PSMA therapy for patients with recurrent or metastatic salivary

gland malignancies, as a last resort treatment. All consecutive patients who received this therapy until January 2021 were retrospectively analyzed in this study.
Patients with increasing tumour-related discomfort, either during active follow-up or referred for a second opinion, deemed irresectable and without other standard palliative treatment options, were re-assessed at MTB and considered for ^{177}Lu-PSMA therapy. Patient's tumour PSMA-status was assessed in two ways: by analyzing the tumour tissue PSMA expression by immunohistochemistry and by assessing PSMA-ligand uptake on ^{68}Ga-PSMA PET/CT, as described previously.[12] Sufficient PSMA-ligand uptake assumed effective for ^{177}Lu-PSMA targeting, was defined as a site of recurrent or metastatic disease with tracer uptake greater than normal liver uptake. When these conditions were met, patients were considered eligible for this radionuclide therapy.

Treatment protocol

Patients were informed that the applied treatment was non-standard and involved the administration of a —for this application— non-registered radiopharmaceutical in a compassionate use programme. Treatment aimed at four cycles of intravenous administration of 6.0–7.4 GBq ^{177}Lu-PSMA-617 with an interval of 6–8 weeks. Prior to the start and during treatment, all tumour-related symptoms were accurately recorded. Moreover, laboratory red and white blood cell counts were obtained at all visits. All relevant treatment related clinical and haematological adverse events were graded using the Common Terminology Criteria for Adverse Events (CTCAE) criteria, version 5.0.
For response evaluation a ^{68}Ga-PSMA PET/CT was performed. PET/CT was acquired from skull vertex to the thighs using a TruePoint Biograph mCT40 scanner (Siemens, Erlangen, Germany). A low dose CT scan was performed using Care Dose 4D and Care kV, reference parameters: 40 mAs, 120 kV. Subsequently, PET was acquired according to the European Association of Nuclear Medicine recommendations with the following parameters: PET with time-of-flight and point spread function (TrueX) reconstruction, 4 iterations, 21 subsets, with a filter of 7.5 mm full width at half maximum.[16]
Evaluation was performed after each two cycles by ^{68}Ga-PSMA PET/CT.[12] SUV_{max} of the most accumulating lesion was measured on both the pre- and post-treatment scans using a freehand isocontour volume of interest and lean body mass corrected formula. Response was defined as complete when all tumour localizations disappeared, as partial when SUV_{max} decreased ≥30%, as stable disease when there was neither a partial response nor progressive disease; and as progressive disease when SUV_{max} or tumour volume increased ≥20% or when new lesion(s) were discovered. In case of clinical or radiological progression of disease, the radionuclide treatment was discontinued.

RESULTS

Six patients were treated with ^{177}Lu-PSMA of which four were diagnosed with AdCC, one with salivary gland adenocarcinoma, not otherwise specified and one with acinic cell carcinoma. The tumours originated in the parotid gland in three, in the minor salivary glands of the oral cavity in two and in the submandibular gland in one patient. Further details are shown in Table 1. At the time of analysis, five of these six patients had died due to the disease, median 6 months after the start of the therapy. Targeting of the ^{177}Lu-PSMA-ligand was on average moderate and the mean SUV_{max} of patient's most accumulating lesions was 8.2 (range 3.5–12.5; Figure 1).

Two patients completed the full study protocol of four cycles (no. 1 and 2). Patient no. 1 showed radiological stable disease of its lung metastases during the full treatment. The ^{68}Ga-PSMA PET/CT of patient no. 2 depicted a SUV_{max} decrease of 30% in the area of the recurrence that was classified as partial response, disease stabilization was up to 10 months after the start of the treatment —three months after the last cycle— when tumour growth was seen on ^{68}Ga-PSMA PET/CT.

Four patients reported subjective response by clear relief of tumour symptoms within the first weeks after the first cycle. The most common improvement was reduction in pain, followed by decrease in fatigue, less dyspnoea and improvement of facial expression by diminution of facial nerve palsy.

The therapy was well-tolerated in all cases except patient no. 3, who developed severe grade 3 thrombocytopenia (25.0–50.0 × 10e9/L) that led to discontinuation of the treatment, a possible adverse effect. There were no treatment-related deaths. Common side effects that were reported were fatigue, nausea, bone pain and xerostomia (graded CTCAE 1–2). Due to increase in fatigue and xerostomia, patient no. 4 was no longer motivated to continue the therapy after one cycle.

Immunohistochemical expression of PSMA showed similar expression patterns within the neoplastic cells of the different tumour subtypes and ranged from 5 to 95%. Within this small study population there was no correlation between pre-treatment SUV_{max} and tumour tissue PSMA expression. Patients no. 5 and 6 depicted the highest PSMA expression on immunohistochemistry (95% and 30%, respectively) and had a good initial clinical response. However, the intermediate ^{68}Ga-PSMA PET/CT after two cycles showed disease progression and the therapy was discontinued.

Table 1. Patient, disease and treatment characteristics

	Pt 1	Pt 2	Pt 3	Pt 4	Pt 5	Pt 6
Sex	F	M	M	F	M	F
Age at diagnosis	56	41	32	74	32	39
Year of diagnosis	2005	2013	2006	2016	2004	2017
Tumour type	AdCC	AdCC	AdCC	Adeno-carcinoma NOS	Acinic cell carcinoma	AdCC
Tumour site	Hard palate	Parotid	Cheek mucosa	Parotid	Parotid	Submandibular gland
Treatment	Local excision	Local excision + radiotherapy	Local excision + radiotherapy	Palliative radiotherapy	Local excision + radiotherapy	Local excision + radiotherapy
DISEASE						
Locoregional recurrence	-	Parapharyngeal, intracranial	-	-	-	Parapharyngeal, lymphatic
Distant metastases	Lung, liver	-	Lung, bone (vertebra)	Bone (skull, vertebra)	Lymphatic (inguinal), lung, bone (vertebra)	-
Completed "conventional" palliative treatment	None	None	Chemotherapy (CAP), radiotherapy	Radiotherapy	Chemotherapy (CAP), radiotherapy	Chemotherapy (CAP), radiotherapy
PSMA expression on IHC (%)	5	30	n/a	30	95	30
SUV_{max} VOI before treatment	3.5 lung	6.5 intracranial	10.2 pelvis	12.5 pelvis	9.7 pelvis	7.0 parapharyngeal

TREATMENT						
Diagnosis to ^{177}Lu-PSMA (years)	12	6	12	1	14	2
No. cycles	4	4	2	1	2	2
SUV_{max} VOI after treatment	n/a	4.5	n/a	n/a	17.6	9.4
Reason of discontinuation	End of protocol	End of protocol	Disease progression, adverse effects	Demotivation due to side-effects	Disease progression	Disease progression
SIDE EFFECTS						
Side effects (CTCAE grade)	Fatigue (2) Dyspnoea (2) Nausea (1)	Fatigue (1) Nausea (1) Vomiting (1) Xerostomia (1)	Fatigue (1) Bone pain (2) Thrombocytopenia (3)	Fatigue (1) Xerostomia (1)	Fatigue (1) Xerostomia (1) Bone pain (2)	Fatigue (1) Xerostomia (2)
RESPONSE						
Clinical	Less dyspnoea, less fatigue	Improved facial expression and sensibility, less fatigue	Disease progression	n/a	Significant pain relief (6 weeks)	Diminution of facial nerve palsy, pain relief
Radiological	Stable lung lesions, minimal progression of liver metastases	Stable disease, decrease SUV_{max}	Disease progression	n/a	Disease progression	Disease progression
Follow-up (months after first treatment)	Deceased (7)	Alive with disease (36)	Deceased (3)	Deceased (5)	Deceased (6)	Deceased (9)

CAP: Cyclophosphamide, Adriamycin, Cisplatin; n/a: not available

Figure 1. Patient no. 2 suffering from recurrent and metastatic AdCC of the right parotid gland.
Imaging depicts moderate PSMA-ligand uptake in the recurrent parapharyngeal and intracranial tumour localizations: before (**A**, **B** and **C**) and after (**D**) therapy.

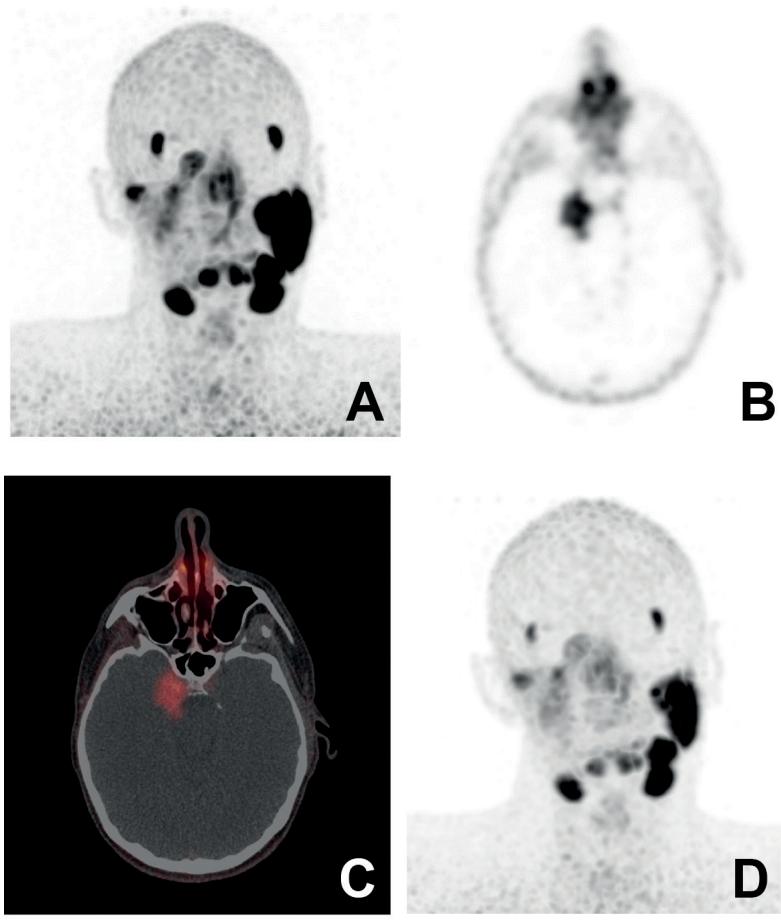

(**A**) Coronal maximum intensity projection (before therapy SUV_{max} 6.5); (**B**) axial PET; (**C**) axial PET/CT reconstruction; (**D**) coronal maximum intensity projection (after therapy SUV_{max} 4.5).

DISCUSSION

This study describes our first experiences with ^{177}Lu-PSMA as palliative radionuclide treatment for recurrent and/or metastatic salivary gland malignancies of the head and neck. When regular palliative options fail, the present case series demonstrate that patients with sufficient tumour targeting on ^{68}Ga-PSMA PET/CT can be treated with PSMA-targeted radioligand therapy using ^{177}Lu-PSMA, that may result in temporary radiological disease stabilization and relief of tumour-related discomfort. Two out of six patients showed disease stabilization for approximately 6 and 10 months respectively, four patients reported immediate reduction in symptoms, and disease progression was seen in three patients.

^{177}Lu-PSMA therapy was generally well-tolerated and most side effects mentioned in this study are CTCAE graded 1–2. One patient was not motivated to continue treatment due to cumulative (grade 1) side-effects, and one patient developed severe (grade 3) thrombocytopenia that caused discontinuation of treatment. However, this adverse effect was more likely related to progressive bone-marrow metastases, as haemoglobin and leukocyte counts were severely suppressed as well.

In prostate cancer, palliative treatment with ^{177}Lu-PSMA is known to achieve a prolonged progression-free survival and is considered safe. Hofman et al.[14] described the results of this therapy in a selected group of 30 patients with intense PSMA-ligand binding on PET/CT and almost all (97%) of these patients showed biochemical response. Three months after a maximum of four cycles, a response evaluation was executed by ^{68}Ga-PSMA PET/CT: complete or partial radiological response was observed in, respectively, 10% and 30% and disease progression was reported in 57% of the patients. A large meta-analysis incorporated these results in their pooled analyses of 175 patients and reported even higher rates: 37% partial response, 38% stable disease and 25% progressive disease.[17] The recently published randomized VISION trial concluded a median increase in progression-free survival from 3.4 to 8.7 months, and an increased overall survival from 11.3 to 15.3 months when ^{177}Lu-PSMA therapy was added to standard care.[15]

Although both the treatment protocol and the administered activity in the present study were equal to the prostate cancer treatment schedules, response rates were less favourable: one out of six patients obtained a partial response on ^{68}Ga-PSMA PET/CT, and one patient had stable disease of lung metastases.

Remarkably, these two patients were the only two that completed all intended four cycles, whereas much more prostate cancer patients completed the full study protocol. The VISION trial even reported a median of five cycles per patient.[9,14,15]

Another difference that may explain the less objective response of ^{177}Lu-PSMA in salivary gland cancers is probably the lower PSMA-ligand uptake in the salivary gland tumours compared to prostate cancer lesions: a mean SUV_{max} 8.2 (range 3.5–12.5) versus 13.3 (range 0.7–122.5).

Clinical improvements and side-effects presented by this study are comparable to those mentioned in large prostate cancer radionuclide therapy reports: validated questionnaires revealed significant decrease in pain (≥1 point on Brief Pain Inventory pain severity score) and increased quality of life (≥10 points increase in EORTC QLQ-C30 global health score) in approximately half of the patients after two cycles.[14,18] Most reported side effects in these reports were fatigue (43%), dry mouth (39%), nausea (35%), bone-marrow depression (32%) and back pain/arthralgia (23%); loss of appetite, diarrhoea or constipation, vomiting and nephrotoxicity were less common.[15,17]

First studies on radionuclide therapy for other solid tumours that express PSMA have recently been summarized.[19] When compared to glioblastoma, thyroid carcinoma, renal cell carcinoma and hepatocellular carcinoma that all express PSMA in the tumour's neovasculature and not intracellular, ligand uptake in salivary gland tumours is moderate to weak. Further research should reveal whether salivary gland cancer patients could benefit from a higher dose or shortened interval of ^{177}Lu-PSMA. Furthermore, alpha-emitting agents such as ^{225}Ac-PSMA-617 may be more successful due to their higher linear energy transmission.[20]

Until now, a few studies report on PSMA related imaging and/or therapy in salivary gland tumours. We previously described visualization of local recurrent and distant metastatic AdCC on ^{68}Ga-PSMA PET/CT, and confirmed the PSMA-specific targeting of these tumours by high intratumoural PSMA expression on immunohistochemistry.[12,21]

Only one case report has been published regarding radionuclide therapy in metastatic AdCC of the parotid. ^{68}Ga-PSMA uptake was seen in all sites of known AdCC bone metastases and subsequently ^{177}Lu-PSMA was administered after all regular treatment options failed. The post-therapy imaging showed intense tracer uptake and the patient reported immediate significant pain relief in the weeks after the therapy. Due to severe hypercalcaemia the treatment was discontinued after one cycle, an adverse effect that we did not encounter before.[22] Although a recent study focussed on PSMA-ligand uptake in SDC, there are no other reports that support the results of the present study.[13]

Clinical response that combines decrease in tumour-related discomfort with only limited toxic side effects is of importance in palliative treatment. In our opinion, the current therapy positively affects quality of life and meets the criteria of a noteworthy palliative option.[23]

CONCLUSION

When tumour targeting is sufficient, palliative PSMA-targeted radioligand therapy of advanced or metastasized salivary gland cancers with ^{177}Lu-PSMA may cause a significant relief of tumour-associated discomfort in the majority of the patients, and may induce a partial response or even stable disease in one-third of the cases. The presented protocol is safe and relatively well-tolerated. When regular treatment options fail, indicative targeted imaging using ^{68}Ga-PSMA PET/CT can be considered to assess eligibility for ^{177}Lu-PSMA therapy.

REFERENCES

1. Coca-Pelaz A, Rodrigo JP, Bradley PJ, Vander Poorten V, Triantafyllou A, Hunt JL, et al. Adenoid cystic carcinoma of the head and neck - An update. Oral Oncol 2015;51:652–61.
2. Bjørndal K, Krogdahl A, Therkildsen MH, Overgaard J, Johansen J, Kristensen CA, et al. Salivary gland carcinoma in Denmark 1990-2005: A national study of incidence, site and histology. Results of the Danish Head and Neck Cancer Group (DAHANCA). Oral Oncol 2011;47:677–82.
3. Jang S, Patel PN, Kimple RJ, McCulloch TM. Clinical Outcomes and Prognostic Factors of Adenoid Cystic Carcinoma of the Head and Neck. Anticancer Res 2017;37:3045–52.
4. Spiro RH, Huvos AG, Strong EW. Adenoid cystic carcinoma of salivary origin. A clinicopathologic study of 242 cases. Am J Surg 1974;128:512–20.
5. van Weert S, Reinhard R, Bloemena E, Buter J, Witte BI, Vergeer MR, et al. Differences in patterns of survival in metastatic adenoid cystic carcinoma of the head and neck. Head Neck 2017;39:456–63.
6. Ciccolallo L, Licitra L, Cantú G, Gatta G. Survival from salivary glands adenoid cystic carcinoma in European populations. Oral Oncol 2009;45:669–74.
7. Laurie SA, Ho AL, Fury MG, Sherman E, Pfister DG. Systemic therapy in the management of metastatic or locally recurrent adenoid cystic carcinoma of the salivary glands: a systematic review. Lancet Oncol 2011;12:815–24.
8. Alfieri S, Granata R, Bergamini C, Resteghini C, Bossi P, Licitra LF, et al. Systemic therapy in metastatic salivary gland carcinomas: A pathology-driven paradigm? Oral Oncol 2017;66:58–63.
9. Afshar-Oromieh A, Avtzi E, Giesel FL, Holland-Letz T, Linhart HG, Eder M, et al. The diagnostic value of PET/CT imaging with the 68Ga-labelled PSMA ligand HBED-CC in the diagnosis of recurrent prostate cancer. Eur J Nucl Med Mol Imaging 2015;42:197–209.
10. Klein Nulent TJW, Valstar MH, de Keizer B, Willems SM, Smit LA, Al-Mamgani A, et al. Physiologic distribution of PSMA-ligand in salivary glands and seromucous glands of the head and neck on PET/CT. Oral Surg Oral Med Oral Pathol Oral Radiol 2018;125:478–86.
11. Backhaus P, Noto B, Avramovic N, Grubert LS, Huss S, Bögemann M, et al. Targeting PSMA by radioligands in non-prostate disease—current status and future perspectives. Eur J Nucl Med Mol Imaging 2018;45:860–77.
12. Klein Nulent TJW, van Es RJJ, Krijger GC, de Bree R, Willems SM, de Keizer B. Prostate-specific membrane antigen PET imaging and immunohistochemistry in adenoid cystic carcinoma-a preliminary analysis. Eur J Nucl Med Mol Imaging 2017;44:1614–21.
13. Van Boxtel W, Lütje S, Van Engen-Van Grunsven ICH, Verhaegh GW, Schalken JA, Jonker MA, et al. 68Ga-PSMA-HBED-CC PET/CT imaging for adenoid cystic carcinoma and salivary duct carcinoma: A phase 2 imaging study. Theranostics 2020;10:2273–83.
14. Hofman MS, Violet J, Hicks RJ, Ferdinandus J, Ping Thang S, Akhurst T, et al. [177Lu]-PSMA-617 radionuclide treatment in patients with metastatic castration-resistant prostate cancer (LuPSMA trial): a single-centre, single-arm, phase 2 study. Lancet Oncol 2018;19:825–33.
15. Sartor O, de Bono J, Chi K, et al. Lutetium-177-PSMA-617 for Metastatic Castration-Resistant Prostate Cancer. N Engl J Med 2021;385:1091-103.
16. Boellaard R, Delgado-Bolton R, Oyen WJG, Giammarile F, Tatsch K, Eschner W, et al. FDG PET/CT: EANM procedure guidelines for tumour imaging: version 2.0. Eur J Nucl Med Mol Imaging 2015;42:328–54.

17. Yadav MP, Ballal S, Sahoo RK, Dwivedi SN, Bal C. Radioligand therapy with 177Lu-PSMA for metastatic castration-resistant prostate cancer: A systematic review and meta-analysis. Am J Roentgenol 2019;213:275–85.
18. Fendler WP, Reinhardt S, Ilhan H, Delker A, Böning G, Gildehaus FJ, et al. Preliminary experience with dosimetry, response and patient reported outcome after 177Lu-PSMA-617 therapy for metastatic castration-resistant prostate cancer. Oncotarget 2017;8:3581–90.
19. Uijen MJM, Derks YHW, Merkx RIJ, Schilham MGM, Roosen J, Privé BM, et al. PSMA radioligand therapy for solid tumors other than prostate cancer: background, opportunities, challenges, and first clinical reports. Eur J Nucl Med Mol Imaging 2021;48:4350-68.
20. Kratochwil C, Bruchertseifer F, Rathke H, Bronzel M, Apostolidis C, Weichert W, et al. Targeted Alpha Therapy of mCRPC with (225)Actinium-PSMA-617: Dosimetry estimate and empirical dose finding. J Nucl Med 2017;58:1624–31.
21. Klein Nulent TJW, Valstar MH, Smit LA, Smeele LE, Zuithoff NPA, de Keizer B, et al. Prostate-specific membrane antigen (PSMA) expression in adenoid cystic carcinoma of the head and neck. BMC Cancer 2020;20:519.
22. Has Simsek D, Kuyumcu S, Agaoglu FY, Unal SN. Radionuclide Therapy With 177Lu-PSMA in a Case of Metastatic Adenoid Cystic Carcinoma of the Parotid. Clin Nucl Med 2019;44:764–6.
23. WHO Fact Sheet Palliative Care, World Health Organization 2020. https://www.who.int/news-room/fact-sheets/detail/palliative-care (accessed March 19, 2021).

Summarizing discussion and future perspectives

Adenoid cystic carcinoma (AdCC) is one of the most aggressive and challenging-to-treat salivary gland malignancies, characterized by its pathological complexity and clinical unpredictability.[1] Managing AdCC requires a comprehensive approach encompassing accurate diagnosis, effective treatment, and reliable prognostication. However, each of these aspects involves significant difficulty, complicating efforts to optimize patient outcomes.[2,3]

Accurate diagnosis of AdCC is essential but remains demanding. Histopathological evaluation is the cornerstone, relying on microscopic analysis to identify its characteristic growth patterns.[4,5] However, overlapping features with other salivary gland tumours can complicate diagnosis. While molecular diagnostics provide higher specificity, their limited availability due to technical and resource constraints remains a barrier.[1,6] Furthermore, current imaging techniques, critical for assessing disease extent, often struggle to differentiate recurrent or metastatic AdCC from post-treatment changes, delaying timely therapeutic decisions.[7,8]

The challenges in diagnosing AdCC mirror its treatment complexities. Surgery remains the primary modality aiming to achieve complete tumour resection with clear margins. However, the invasive nature of AdCC often complicates this goal, and even with adjuvant radiotherapy, locoregional recurrences are common.[1,2,9] For recurrent or metastatic disease, systemic treatments have demonstrated limited efficacy without substantial survival benefit. Palliative chemotherapy, such as cisplatin, can stabilize tumours with an acceptable toxicity profile, yet response rates remain low, and no standard regimen has been established. The most effective regimen is cisplatin combined with docetaxel, offering a progression-free survival of up to 7.2 months, though this modest achievement reflects the relative resistance of AdCC to platinum-based chemotherapy.[10–12] Targeted therapies, particularly VEGF inhibitors like apatinib, hold potential for controlling disease by inhibiting pathways critical to tumour growth and angiogenesis, although their success is inconsistent. The efficacy of immunotherapy has also been limited due to the AdCC's tumour microenvironment, which restricts immune cells from infiltrating the tumour. This exclusion, combined with low PD-L1 expression, reduces the effectiveness of checkpoint inhibitors. Agents targeting PD-L1 such as pembrolizumab and avelumab have been explored, with combinations involving VEGF inhibitors demonstrating varying results. Currently, these therapies remain confined to clinical trials for advanced tumours, with limited applicability in standard care.[13,14] Revolutionizing therapeutic strategies for AdCC requires novel approaches that target biomarkers, molecular pathways, and promote immune system engagement.[1]

Prognostication in AdCC is equally intricate due to its highly variable clinical course. Aggressive subtypes, such as the solid growth pattern, are associated with poorer

outcomes, while less aggressive forms may still present with late recurrences or distant metastases.[2,9,15] This unpredictable nature emphasizes the need for robust prognostic markers to guide personalized treatment and surveillance strategies.[1,16]

By integrating molecular histopathology, state-of-the-art imaging modalities, and innovative treatments, this thesis aims to address these challenges by exploring three key biomarkers —cellular myeloblastosis gene (*c-MYB* or *MYB*); chemokine receptor type 4 (CXCR4); and prostate-specific membrane antigen (PSMA)— to enhance diagnostic precision, guide clinical decision-making, and identify actionable targets for therapy.[17–19] Ultimately, it seeks to deepen the understanding of AdCC, improving clinical outcomes and optimizing patient quality of life through more tailored and effective care for those affected by this complex malignancy.

PART A: BIOMARKERS

Diagnosing salivary gland cancers through histopathology on small biopsies and cytological specimens can be challenging. In AdCC, the cribriform growth pattern —a distinctive architecture resembling a "sieve" due to its well-defined, perforated gland-like structures— is widely recognized. In contrast, other growth patterns in AdCC are less distinct, contributing to high reclassification rates of 14% to 29% observed in surgical specimens after definitive treatment.[1,4]

To enhance the diagnostic accuracy for AdCC, **Chapter 2** of this thesis explores the value of MYB immunohistochemistry (IHC) as a practical alternative to fluorescence in situ hybridization (FISH) for predicting the *MYB::NFIB* translocation that is pathognomonic for AdCC.[17] By analyzing 110 AdCC cases, a *MYB::NFIB* fusion was identified in 44 of 79 tumours (56%), and IHC showed homogeneous nuclear MYB protein expression in the abluminal cells in 89% of 90 tumours with a median expression of 27% (interquartile range [IQR] 8–46%). In 62 cases where both FISH and IHC were compared, a *MYB::NFIB* fusion was detected in 38 tumours (61%), of which 37 expressed MYB with a median staining of 30% (IQR 12–56%). This expression was significantly higher (p=0.02) than the median of 6% (IQR 4–30%) noted in non-translocated tumours. Establishing a cut-off of 60% MYB expression for fusion positivity achieved 100% specificity and 100% positive predictive value within the study cohort. This finding highlights the promise of MYB IHC as a reliable and quick surrogate for FISH in predicting *MYB::NFIB* fusion status, improving accessibility and cost-efficiency.[6] The fusion detection rates and MYB IHC results reported in this study align with and expand upon those published in previous research.[17,20–22]

No significant correlation was found between MYB expression and clinicopathological parameters, yet a slight rise in median MYB expression was recorded with increasing solid tumour growth. Previous studies, such as those by West et al.[17] and Mitani et al.[20], reported trends towards higher recurrence rates and specific tumour characteristics associated with the *MYB::NFIB* translocation, though these observations were not statistically significant or consistent. This reinforces the conclusion that MYB expression is not a reliable prognostic marker for disease progression or treatment guidance. However, challenges remain in its broader applicability as concerns arise regarding the generalizability of the 60% cut-off to routine practice. This is especially relevant given the differential diagnosis of salivary gland neoplasms, such as myoepithelial carcinoma, polymorphous adenocarcinoma, basaloid squamous cell carcinomas, and basal cell adeno(carcino)mas, some of which may show weak or focal MYB antibody reactivity.[17,23] Xu et al.'s[21] findings of MYB expression in non-AdCC tumours (9%) highlight the diagnostic challenge, particularly in cases where expression falls below the threshold. Furthermore, variability in staining protocols, interpretation thresholds, and tumour heterogeneity complicates its application outside controlled study settings.[17] Exploring *MYB*-related molecular pathways could additionally provide insights into other regulatory mechanisms affecting MYB expression and its impact on tumour behaviour. For example, understanding how *MYB*-driven gene expression influences AdCC's invasive properties might reveal therapeutic targets that could mitigate the aggressive features associated with high *MYB::NFIB* fusion-positive tumours. Moreover, while *MYB* fusion status has not yet been linked to treatment outcomes, prospective studies could evaluate whether *MYB::NFIB* fusion-positive patients respond differently to specific therapies, such as IGF1R inhibitors, which have proven effective in some *MYB*-driven cancers.[24] Future studies should aim to refine cut-off values, validate their applicability in diverse clinical settings, and explore complementary biomarkers to better predict disease behaviour and recurrence risk.

In this context, CXCR4 has emerged as a promising candidate due to its role in tumour cell migration, metastasis, and recurrence. **Chapter 3** investigates CXCR4 expression in 66 AdCC cases, offering new insights into its utility as a prognostic tool.[25,26] IHC revealed that intracellular CXCR4 expression was uniform across tumour cells with limited spatial variability. It was present in 81% of primary AdCC samples, with a median expression level of 29% (IQR 1–70%), aligning with findings from smaller studies on this topic.[18,27,28] CXCR4 expression was significantly higher in primary tumours that recurred compared to those that did not (median 60%; IQR 33–72% vs 12%; IQR 1–70%; Kruskal-Wallis p=0.01). Following dichotomization, tumours with high CXCR4 expression above

25% were significantly associated with perineural growth (p=0.02) and bone invasion (p=0.03). In a multivariate Cox proportional hazards model, high CXCR4 expression indicated a 7.2-fold higher risk of recurrence (hazard ratio [HR] 7.2, 95% confidence interval [CI] 1.5–72.4, p=0.04). As expected, postoperative radiotherapy did improve recurrence-free survival (RFS) significantly (HR 25.1, 95% CI 1.9–339.9, p=0.03). The model incorporating CXCR4 expression is more predictive than one based solely on established prognostic factors, such as growth pattern, resection margins, perineural growth, and bone invasion (Harrell's C-statistic 0.73 vs 0.80). A solid growth pattern in this study showed a clear tendency towards worse RFS in univariate analysis, but statistical significance was not reached, in contrast to the literature.[1–3,9,15,16,29] Conversely, our larger PSMA expression study, detailed in Chapter 4, provided a strong association between solid growth and reduced RFS (p=0.02).

The metastatic spread of tumours is thought to be driven by CXCR4, which facilitates tumour cell migration along CXCL12 gradients found in typical metastatic sites for AdCC, such as the lungs, liver, and bone.[26,27,30,31] Despite this, no correlation was determined between high CXCR4 expression and the development of distant metastases, although a higher expression of CXCR4 was observed in tumours that metastasized (49% vs 23%). The lack of statistical significance, similar to that noted with the growth pattern and RFS, may be attributed to the small sample size in this study and the relatively short follow-up period. The CXCL12/CXCR4 axis may contribute to bone invasion by mediating osteolysis through stimulation of osteoclast precursors, highlighting its possible role in promoting local aggressiveness.[32] However, neither perineural growth nor bone invasion was associated with locoregional recurrence, consistent with existing literature.[2] Interestingly, inflammation at the tumour border may upregulate CXCL12, conceivably driving recurrences in high CXCR4-expressing tumours. This mirrors findings in inflammatory conditions like Sjögren's syndrome, where reactive salivary gland epithelial cells show increased CXCL12 expression.[18,33,34] These findings emphasize the potential value of incorporating CXCR4 into clinical workflow to identify high-risk AdCC patients who could benefit from intensive surveillance and tailored treatments to mitigate recurrence risk.

The implications of CXCR4 as a prognostic and therapeutic biomarker in AdCC offer promising directions for future research. Prospective studies involving larger patient cohorts and longer follow-up are needed to validate its role in predicting metastasis. Antagonist drug AMD3100 and multiple other anti-CXCR4 peptides, antibodies and low-molecular weight agents have been investigated and proved to inhibit or delay cancer progression in various tumour sites, and furthermore improved sensitization of tumour cells to conventional chemotherapy for combined treatment.[26,30,35] Radiolabelled

CXCR4-ligands have now been developed for PET-specific imaging, which also makes these targets suitable for future radionuclide treatment.[36,37] Expanded research is necessary to delineate whether CXCR4 expression in AdCC is preserved in recurrent and distant tissues, and whether primary, recurrent and/or distant AdCC tumour sites can be depicted on CXCR4-targeted PET/CT.

Renowned for its critical role in prostate cancer, PSMA has gained recognition as a versatile biomarker in oncology, serving as both a diagnostic tool and a therapeutic target.[38–40]. **Chapter 4** examines PSMA protein expression across primary, recurrent, and distant AdCC tumours from 110 patients, exploring its relevance to clinical outcomes. This chapter sheds light on PSMA's involvement in tumour biology and its potential application as a theranostic tool in AdCC management. PSMA was expressed in 94% of primary AdCC tumours, with a median of 31% positive tumour cells (IQR 15–60%). Recurrent and metastatic AdCC samples showed PSMA expression in 80% and 90% of cases, with median expression levels of 60% (IQR 30–90%) and 23% (IQR 10–55%), respectively. Compared to their corresponding primary tumours (median 40%; IQR 15–70%), PSMA expression showed a non-significant trend of increasing in recurrences and decreasing in distant metastases. PSMA expression displayed limited spatial and temporal variability, making it a consistent target across tumour stages. Nevertheless, primary tumour expression could not reliably predict levels in recurrences or metastases, limiting its utility as a prognostic marker. This highlights the heterogeneity of PSMA expression during tumour evolution, especially in the proportion of positive cells.

PSMA expression in AdCC was not correlated with pathological stage, tumour grade, or disease progression. However, significant associations were identified with tumour subsite and bone invasion. Tumours originating from the minor salivary glands exhibited a lower PSMA expression than those from the major salivary glands (21% vs 50%; $p<0.01$), and tumours with bone invasion had a lower expression than those without (17% vs 39%; $p=0.04$). Notably, tumour subsite and bone invasion were strongly correlated, possibly introducing confounding, as nearly all bone-invasive tumours originated in the minor salivary glands. Using a dichotomized cut-off of 10% PSMA expression, patients with ≤10% PSMA expression had significantly worse RFS over 10 years (HR 3.0; 95% CI 1.1–8.5, $p=0.04$). This low-expression group was predominantly composed of tumours located in the nasal cavity, nasopharynx, or maxillary sinus—subsites tied to poorer prognoses. Other strong predictors of worse RFS included solid tumours (HR 3.7; 95% CI 1.3–11.2, $p=0.02$) and the absence of postoperative radiotherapy (HR 5.1; 95% CI 1.2–17.5,

p=0.02). Despite these associations, no relation was found between PSMA expression and other clinical parameters such as overall survival, disease-specific survival, or metastasis-free survival. Furthermore, the additive predictive value of PSMA for RFS was minimal, as indicated by Harrell's C-statistic (increase from 0.79 to 0.81). These findings, alongside the earlier discussed prognostic limitations, reduce its applicability as a universal prognostic marker.

Analogous to prostate cancer, AdCC demonstrates PSMA expression primarily in epithelial tumour cells. In our study, PSMA expression appeared in a granular pattern, either within the cytoplasm or concentrated at the luminal side of the cell membrane, a description later confirmed by another study.[41] In contrast, other malignancies often show PSMA expression in the endothelial cells of tumour-associated neovasculature.[38,42,43] This shared pattern underscores a similar epithelial localization of PSMA in these two tumour types, distinguishing them from other malignancies. However, notable differences exist. High PSMA expression in prostate cancer correlates with aggressive tumour features and poorer survival outcomes, but no such associations were found in AdCC.[38,44] Instead, an inverse pattern was identified, where lower PSMA expression led to poorer RFS. This unexpected finding suggests a fundamentally different role for PSMA in AdCC compared to prostate cancer and may reflect unique tumour behaviour. Studies in prostate cancer reported that PSMA activates the AKT and MAPK pathways to drive proliferation and survival, whereas in AdCC, epigenetic silencing of PSMA during tumour progression may partially explain this inverse relation.[45–47]

Further differences include the levels and patterns of PSMA expression. In primary AdCC, 94% of tumours expressed PSMA with a median of 31% positive cells (IQR 15–60%), whereas primary prostate cancer tumours revealed a more heterogeneous expression, with an average of 53 ± 32% positive cells.[38,44] In metastases, the disparity becomes even more pronounced: metastatic prostate cancer shows extensive PSMA expression in regional lymph nodes (72 ± 36%) and distant metastases (92 ± 10%), whereas metastatic AdCC exhibits significantly lower expression, with a median of 23% positive cells (IQR 10–55%). In normal tissues, PSMA expression also differs. Normal prostate tissue demonstrates PSMA positivity in 100% of samples (77 ± 32% positive cells), though with lower staining intensity than prostate tumour tissue.[38,44] By contrast, PSMA expression was detected in 59% of normal salivary gland samples, primarily in mucous gland cells, reflected by a higher percentage of positive cells in minor salivary glands compared to major salivary glands.[41] Despite the variation in PSMA expression between prostate cancer and AdCC, the consistent and unambiguous expression of PSMA across primary, recurrent, and metastatic AdCC underscores its promise for targeted imaging and therapies.

In conclusion, PART A of this thesis advances the understanding of biomarkers in AdCC, highlighting their diagnostic, prognostic, and therapeutic potential through an integrated approach that enhances clinical decision-making and supports personalized medicine.

Nonetheless, these chapters acknowledge several limitations. First, although the cohort sizes are substantial for this rare malignancy, they become small after dichotomization. This affects both the statistical significance and the generalizability of findings, particularly for CXCR4 and PSMA as a prognostic marker. For some patients, the relatively short follow-up periods may have limited the ability to capture associations with long-term survival metrics. This is relevant in AdCC, where slow tumour growth and delayed-onset distant metastases present common challenges to effective prognostic evaluation.[1] Second, variability in staining protocols and interpretation thresholds for MYB, CXCR4, and PSMA IHC introduces plausible biases. To mitigate this, standardizing methodologies across centres is critical to achieve consistent and reproducible results in future investigations. Third, the exploratory nature of multiple correlation analyses increases the risk of false-positive findings. While these insights offer valuable hypotheses for further research, confirmatory studies with rigorous statistical corrections are needed to establish their clinical relevance.[48]

Looking ahead, integrating biomarkers such as MYB, CXCR4, and PSMA into routine clinical workflows holds meaningful promise for improving AdCC management. For MYB, refining diagnostic thresholds and identifying complementary molecular markers could enhance diagnostic accuracy in complex differential diagnoses. In addition, MYB poses unique therapeutic challenges. As a transcription factor, *MYB* is inherently difficult to target directly, and current strategies must instead focus on its downstream pathways or related regulatory networks.[49] CXCR4, given its associations with recurrence risk and bone invasion, is an interesting target for novel therapeutic interventions, including CXCR4 inhibitors and radiolabelled CXCR4 ligands.[36,37] Similarly, PSMA offers considerable prospects for theranostic applications.

PART B: TARGETED DIAGNOSTICS

The consistent expression of PSMA in AdCC, combined with its limited presence in normal tissues apart from salivary and prostate glands, underscores its potential as a target for diagnostic imaging in salivary gland tumours. PSMA PET/CT, already established in prostate cancer diagnostics and guiding theranostic strategies, provides a non-invasive approach to visualizing PSMA expression in vivo.[39,41] It may play a role

in detecting both primary and metastatic AdCC lesions that express PSMA, as well as in selecting patients who could benefit from targeted radionuclide therapy such as Lutetium-177-PSMA.[19,40,50,51] Because PSMA protein expression varies between primary tumours, recurrences, and distant metastases in AdCC, and PSMA PET/CT offers in-vivo targeting capabilities, this imaging modality may provide additive and complementary value over PSMA IHC in selecting patients for therapy. To maximize its utility, a thorough understanding of physiological PSMA uptake in normal salivary and seromucous glands is critical for distinguishing pathological uptake from baseline activity.[52,53]

Chapter 5 maps the physiological uptake of ^{68}Ga-PSMA PET/CT across 30 patients, examining major and minor head and neck glands. Among the major glands, the parotid and submandibular glands demonstrated the highest uptake, with mean maximum standardized uptake values (SUV_{max}) of 12.3 ± 3.9 (range 5.2–22.9) and 11.7 ± 3.5 (range 6.0–22.2), respectively. The sublingual glands depicted lower but measurable uptake, similar to minor salivary and seromucous glands. Uptake varied across glandular tissues, with intraindividual differences in SUV_{max} ranging from 9.0% in the submandibular glands to 18.1% in the sublingual glands. Maximum differences reached 41.7% in the sublingual glands and 48.2% in the lacrimal glands. The high and uniform tracer accumulation in major salivary glands contrasts with the variability observed in minor glands. Recognizing these distinctions is crucial for differentiating tumour-associated uptake from naturally elevated physiological uptake. Moreover, the lacrimal glands exhibit tracer accumulation comparable to that of salivary and seromucous glands, although the current understanding of PSMA expression patterns and their function in lacrimal gland cells remains insufficient.[54] The anatomical atlas of PSMA uptake presented in this study, along with detailed reference ranges, provides a foundation for improving diagnostic accuracy, reducing false-positive findings, and enhancing the clinical utility of PSMA PET/CT in salivary gland malignancies. The diagnostic capabilities of PSMA PET/CT may also enable more precise and effective treatment strategies for AdCC. Accurate mapping of PSMA uptake allows for the sparing of critical salivary gland regions during radiotherapy, including previously unrecognized minor gland sites. This approach not only reduces the risk of xerostomia, xerophthalmia, and swallowing difficulties, preserving patients' quality of life, but also provides greater flexibility in radiotherapy optimization for glandular regions devoid of substantial uptake. Despite its promise, certain limitations warrant attention. For example, the lower SUV_{max} values observed in minor salivary glands likely reflect differences in gland volume. Whether these differences correspond to biological variations —such

as fewer specific cells per volume— remains unclear. Additionally, the limited spatial resolution of current PET/CT scanners may introduce partial volume errors, leading to underestimation of tracer uptake in small structures like minor salivary and seromucous glands.[55] Advances in PET/CT imaging, such as integrating metabolic prognosticators to assess tumour heterogeneity and predict treatment response, could further refine and personalize management strategies, ultimately improving disease control.[56–60]

Chapter 6 explores this capability as the first study to evaluate ^{68}Ga-PSMA-HBED-CC PET/CT (PSMA PET/CT) in a cohort of nine patients with a history of AdCC, focusing on its clinical relevance in detecting recurrent or metastatic disease, as well as its correlation with PSMA IHC. Patients were restaged using PSMA PET/CT due to clinically suspected local recurrence or distant metastasis. The cohort included four men and five women, with a mean age at diagnosis of 51 years. Local recurrence occurred in six cases, at a median of 2.8 years (IQR 2.1–7.6 years) from the time of initial diagnosis. Eight patients developed distant metastases, with a mean onset time of 5.8 years (± 4.1 years; range, 0–12.5 years). PSMA PET/CT successfully visualized all sites of local recurrence and distant metastases. Four scans depicted tracer accumulation indicative of residual or recurrent AdCC, and eight scans revealed uptake in areas consistent with known distant metastases, of which four showed progression. Further, three scans identified tracer uptake in four newly suspected metastatic lesions. These findings are supported by a recent study, which highlighted the superior tumour detection and upstaging capabilities of PSMA PET/CT over CT in salivary gland malignancies.[61] The median SUV_{max} for local recurrent AdCC was 2.52 (IQR 2.41–5.95), whereas the median SUV_{max} for distant metastatic AdCC was higher, at 4.01 (IQR 2.66–8.71). Normal tissue uptake was observed with median SUV_{max} values of 10.94 (IQR 9.01–15.55) in the parotid gland, 3.83 (IQR 2.99–4.88) in the liver, and 23.76 (IQR 15.00–35.00) in the kidneys. It is noteworthy that all patients had received adjuvant radiotherapy on the primary tumour, which may have negatively influenced PSMA-ligand uptake measured with PSMA PET/CT.

Three patients underwent ^{18}F-FDG PET/CT imaging within three months of their PSMA PET/CT scans, allowing for a direct comparison of both scans. Each modality demonstrated distinct strengths in imaging AdCC. Although FDG PET/CT remains a cornerstone for staging head and neck cancers, its sensitivity in AdCC is limited due to the typically lower FDG uptake in these tumours as opposed to e.g. squamous cell carcinoma. Furthermore, physiological FDG uptake in salivary glands can be influenced by inflammatory processes, potentially masking the primary tumour or causing false positives. Moreover, low FDG uptake in the primary tumour may not reliably rule

out distant metastases in the case of a negative FDG PET/CT. Comparative studies confirm that FDG PET/CT has sensitivity similar to conventional CT for detecting primary AdCC, but is superior in identifying nodal and distant metastases.[1,8,62] In our study, PSMA PET/CT matched the sensitivity of FDG PET/CT, outperforming it in detecting distant metastases and lesions obscured by physiological uptake or high localized FDG metabolism, especially in cases of local recurrence such as near the skull base. Immunohistochemistry further supported these findings by confirming PSMA expression in all tissue samples corresponding to areas of PSMA-ligand uptake observed on PET/CT, including primary tumours, local recurrences, and distant metastases. These results align with recent studies on this topic.[19,63,64] The percentage of tumour cells expressing PSMA ranged from 5% to 90%, with a median of 30% (IQR 15–70%). Despite some heterogeneity caused by tumour-specific upregulation or downregulation of PSMA, all matched primary, recurrent, and metastatic samples consistently demonstrated either positive or negative PSMA expression.

However, discrepancies between PSMA protein expression and PSMA PET/CT were noted. For instance, histopathologically confirmed peritoneal metastases and a suspected liver metastasis did not show PSMA-ligand uptake on PET/CT. The absence of tracer uptake in these metastases may be due to levels being equal to or below the background physiological PSMA uptake in these tissues.[39] Second, pulmonary nodules identified as suspicious on CT —but cytologically not confirmed as malignant— measured five millimetre or less in diameter and did not exhibit ligand uptake either. If these nodules were indeed metastases, their invisibility on PSMA PET/CT could be attributed to insufficient tracer uptake combined with the limited spatial resolution of PET imaging. This limitation affects the detection of small tumour volumes and is well-documented in FDG PET/CT.[55] Notably, no FDG uptake was depicted in the pulmonary or peritoneal metastases as well. Other inconsistencies may arise from the biological variability of AdCC, microenvironmental factors such as reduced vascularization and elevated interstitial pressure, and specific tracer kinetics in slow-growing tumours.[65] Nevertheless, integrating PSMA PET/CT findings with histopathological data is essential for optimizing diagnostic accuracy and minimizing the risk of underdiagnosis. Although they share targeting mechanisms, the relation between PSMA tissue-level expression and in vivo imaging remains insufficiently understood and requires additional clarification. Several other limitations of PSMA PET/CT must be addressed to refine its clinical utility. The physiological uptake of PSMA in normal salivary glands and other non-prostatic tissues, analogous to FDG PET/CT, increases the risk of misinterpretation as tumour activity, posing a substantial challenge to diagnostic interpretation. This issue is relevant in primary tumours and

recurrent disease, becoming even more pronounced in deep-seated regions like the skull base, nasopharynx, or deep parotid tissues, where biopsy access is limited.[39] Prior treatments, including (stereotactic) radiotherapy, may further complicate the interpretation of PSMA PET/CT by obscuring the distinction between viable tumour tissue and post-treatment effects, as demonstrated in Chapter 6.[66,67] The robust reference guide with an anatomical atlas presented in Chapter 5 may help to overcome some of these issues.

More research is required to validate these findings in larger cohorts and to investigate imaging performance in non-malignant areas, for instance in autoimmune diseases such as sarcoidosis and Sjögren's syndrome.[68,69] In parallel, a promising alternative imaging modality, ^{68}Ga-FAPI PET/CT, is being explored, which targets fibroblast activation protein (FAP) in cancer-associated fibroblasts. Similar to PSMA PET/CT it depicts high uptake in AdCC as confirmed by histopathology. By visualizing stromal components of the tumour microenvironment, ^{68}Ga-FAPI PET/CT may address the limitations of PSMA PET/CT, particularly in cases of low or heterogeneous PSMA expression. Further studies are needed to establish its role in the diagnostic workflow of AdCC.[70]

In conclusion, the complimentary use of PSMA PET/CT and IHC, as outlined in PART B of this thesis, provides valuable diagnostic capabilities for visualizing AdCC disease progression, recurrences, and distant metastases. In addition, it achieves diagnostic reliability at least comparable to FDG PET/CT when physiological background uptake is appropriately accounted for during interpretation.[64] Our findings are supported by a recent systematic review, which highlights the promising role of PSMA-targeted PET/CT as both a diagnostic and therapeutic tool.[71]

To accelerate the clinical adoption of PSMA PET/CT, several areas for improvement can be explored. The potential advantages of ^{18}F-PSMA PET/CT over ^{68}Ga-PSMA PET/CT, such as greater specificity and enhanced tumour-to-background contrast, warrant side-by-side investigation to establish its added value.[72] Additionally, examining the prognostic significance of SUV_{max} thresholds for both radioisotopes could provide predictive values for tumour activity. Advancing these approaches through optimized imaging protocols, radiotracer refinement, and the incorporation of complementary diagnostic techniques may broaden the applicability of PSMA PET/CT, particularly for AdCC, and extend its use to other salivary gland tumours.

PART C: TARGETED THERAPY

The combined results of Chapters 4, 5, and 6 provide a compelling rationale for adopting theranostics to transform the therapeutic landscape for AdCC. Radioligand therapy (RLT) utilizes PSMA-targeting molecules conjugated with beta emitters and gamma photons, integrating diagnostic imaging and targeted treatment by enabling precise delivery of therapy to tumour cells and real-time tracking of the radiolabelled molecules within the body. Mirroring its well-established success in metastatic castration-resistant prostate cancer, recurrent or metastatic AdCC patients may also benefit from RLT, with PSMA PET/CT facilitating their selection.[40,50,51]

Chapter 7 evaluates the feasibility of this personalized, image-guided treatment by introducing ^{177}Lu-PSMA-617 as a last-resort palliative treatment for patients with advanced salivary gland tumours, for whom all conventional treatment options have failed. Six patients underwent PSMA RLT, including four with AdCC. Tumours originated in the parotid, oral cavity (hard palate and cheek mucosa), and submandibular glands. At treatment initiation, two had locoregional recurrence and four had distant metastases. Two patients completed all scheduled four cycles, four discontinued due to tumour progression, side effects or demotivation. The therapy was generally well tolerated, with mild to moderate side effects such as fatigue, nausea, and xerostomia. Xerophthalmia was not spontaneously reported by patients and was not explicitly assessed. One patient experienced grade 3 thrombocytopenia, prompting treatment discontinuation, underscoring the need for careful patient selection and monitoring for hematologic toxicity. Pre-treatment tumour targeting was moderate (mean SUV_{max} 8.2, range 3.5–12.5), with PSMA tissue expression in neoplastic cells ranging from 5% to 95%, without a clear correlation between SUV_{max} and protein expression. Clinical benefits initially emerged in patients with higher PSMA expression; however, this did not translate into sustained disease stabilization, reflecting response heterogeneity. The palliative impact was more pronounced, with four patients experiencing relief from pain, dyspnoea, and fatigue within weeks of starting treatment. Despite these symptomatic improvements, objective radiological responses were modest. The best results were achieved in two AdCC patients: one attained a partial response with a 30% SUV_{max} reduction and disease stabilization for 10 months, while another demonstrated stable disease for six months. Three patients experienced disease progression following initial symptom relief. No treatment-related deaths occurred. Median survival was six months following treatment initiation, with one patient remaining alive 36 months post-treatment. Regardless of the small sample size, this study supports the rationale for PSMA-targeted RLT as a valuable palliative option for salivary gland cancers when standard treatments fail. Our findings

are strongly supported by two recent case series, which reported consistent results and drew analogous conclusions.[61,73] However, the retrospective, single-centre design and lack of a control group limit the ability to assign these effects solely to ^{177}Lu-PSMA therapy or to assess its efficacy against prior palliative treatments. Prospective, multi-centre controlled clinical trials are needed to validate the therapeutic benefit of RLT in this patient population.

When evaluating ^{177}Lu-PSMA therapy in salivary gland tumours versus prostate cancer, symptomatic relief was demonstrated in a similar proportion of patients, with an equivalent side effect profile.[51] The use of validated quality-of-life questionnaires in prostate cancer revealed pain reduction (≥1 point on the Brief Pain Inventory) and improved global health scores (≥10 points increase in EORTC QLQ-C30) in nearly half of the patients after two cycles.[40,74] However, in prostate cancer radiological response rates are notably higher. Up to 10% of patients achieve a complete response, and pooled meta-analyses present partial response in 37%, stable disease in 38%, and progressive disease in 25% of the patients.[40,75] This discrepancy may be attributed to the lower PSMA-ligand uptake in salivary gland tumours (mean SUV_{max} 8.2) compared to prostate cancer lesions (mean SUV_{max} 13.3), likely affecting tumour targeting.[76] Furthermore, only two patients in our study completed all four intended cycles, whereas prostate cancer trials documented a median of five cycles per patient, which may have influenced treatment efficacy.[40,77] When optimal PSMA uptake and treatment adherence are attained, ^{177}Lu-PSMA therapy has demonstrated significant gains in both progression-free and overall survival in prostate cancer, underscoring the potential of this therapy.[77]

The lower PSMA-ligand uptake observed in AdCC suggests that higher doses or more frequent treatment cycles may be required to obtain better therapeutic outcomes. To optimize and increase tumour targeting, research should focus on the alpha-emitter ^{225}Ac-PSMA-617, which offers major advantages over conventional beta-emitting ^{177}Lu-PSMA-617. Alpha particles differ from beta particles in both their physical and biological effects. Unlike beta radiation, which travels several millimetres, alpha radiation travels only a few cell diameters (less than 100 μm) but delivers notably higher linear energy transfer, causing more severe double-strand DNA breaks that overcome radioresistance. By contrast, beta radiation induces less complex DNA damage (single-strand breaks).[78,79] AdCC could specifically benefit from this therapy as PSMA is expressed within the neoplastic epithelial cells, unlike other malignancies where PSMA is primarily localized in the neovasculature.[42,43] One of the key benefits of ^{225}Ac-PSMA-617 over ^{177}Lu-PSMA-617 is its ability to target low to moderate PSMA-expressing tumours. This is accomplished through the aforementioned direct high-linear energy

transfer radiation delivery to target cells, unlike the crossfire effect required by ^{177}Lu, which relies on PSMA density for sufficient exposure. Although alpha radiation offers precise targeting, it also increases the risk of off-target effects, with a significant impact on salivary tissues with high PSMA expression. This may lead to irreversible xerostomia or xerophthalmia, prompting the development of protective strategies to mitigate salivary and lacrimal gland toxicity. These include the use of monosodium glutamate, which competes with PSMA-targeting molecules, and glutamate receptor antagonists like kynurenic acid, both of which have been effective in reducing off-target uptake in preclinical studies. Cooling techniques, personalized dosimetry, and optimized fractionated dosing protocols may further minimize salivary gland damage while balancing efficacy and toxicity.[80] Given these developments, ^{225}Ac-PSMA-617 offers theoretically promising perspectives for future AdCC treatment. However, no clinical studies have yet been conducted on salivary gland tumours. For now, even though ^{177}Lu-PSMA therapy has not resulted in a complete or long-term response, its palliative benefits outlined in this chapter emphasize its value as a last-resort treatment for advanced AdCC patients. The demonstrated symptom relief and disease stabilization provided meaningful improvements in quality of life for patients at this final stage of their disease, generally with acceptable side effects. When all other conventional therapies have been exhausted, we recommend performing a ^{68}Ga-PSMA PET/CT to assess PSMA tumour targeting to determine patient eligibility for ^{177}Lu-PSMA treatment.

OVERALL CONCLUSION

This thesis advances the diagnosis, prognostication and treatment of AdCC through biomarker-driven diagnostics, PSMA-targeted imaging, and targeted radionuclide therapy. By focusing on MYB, CXCR4, and PSMA as molecular targets, it offers novel approaches for disease characterization, staging, and therapeutic intervention. MYB IHC enhanced diagnostic accuracy, providing a fast, accessible, and reliable alternative to detect *MYB::NFIB* fusions. CXCR4 aided prognostication by identifying patients at higher risk of recurrence, facilitating personalized follow-up plans. The consistent expression of PSMA in primary, recurrent, and metastatic AdCC enabled both visualization with ^{68}Ga-PSMA PET/CT and targeted delivery of ^{177}Lu-PSMA radionuclides. Mapping the physiological uptake of PSMA-ligand in salivary and seromucous glands generated essential reference data for PET/CT interpretation, improving precise staging and radiotherapy planning. PSMA PET/CT demonstrated superior detection of recurrences and metastases over FDG PET/CT, particularly in

areas with high physiological FDG metabolic activity. The implementation of ^{177}Lu-PSMA radionuclide therapy validated its feasibility in advanced AdCC, providing symptom relief and disease stabilization. This theranostic solution addresses an urgent clinical need and offers new hope for patients without alternative treatment options. To conclude, this thesis establishes a new paradigm in biomarker-driven strategies for AdCC, driving the shift towards personalized care. It lays the foundation for future innovations in the diagnosis, treatment, and optimization of quality of life for patients with this rare and challenging-to-treat malignancy.

REFERENCES

1. Coca-Pelaz A, Rodrigo JP, Bradley PJ, et al. Adenoid cystic carcinoma of the head and neck - An update. Oral Oncol. 2015;51(7):652-661.
2. Jang S, Patel PN, Kimple RJ, McCulloch TM. Clinical Outcomes and Prognostic Factors of Adenoid Cystic Carcinoma of the Head and Neck. Anticancer Res. 2017;37(6):3045-3052.
3. Spiro RH, Huvos AG, Strong EW. Adenoid cystic carcinoma of salivary origin. A clinicopathologic study of 242 cases. Am J Surg. 1974;128(4):512-520.
4. Hellquist H, Skalova A. Adenoid Cystic Carcinoma. In: Histopathology of the Salivary Glands. Springer Berlin Heidelberg; 2014:221-260.
5. Perzin KH, Gullane P, Clairmont AC. Adenoid cystic carcinomas arising in salivary glands: a correlation of histologic features and clinical course. Cancer. 1978;42(1):265-282.
6. Jacobs TW, Gown AM, Yaziji H, Barnes MJ, Schnitt SJ. Comparison of fluorescence in situ hybridization and immunohistochemistry for the evaluation of HER-2/neu in breast cancer. J Clin Oncol. 1999;17(7):1974-1982.
7. Freling N, Crippa F, Maroldi R. Staging and follow-up of high-grade malignant salivary gland tumours: The role of traditional versus functional imaging approaches - A review. Oral Oncol. 2016;60:157-166.
8. Jung JH, Lee SW, Son SH, et al. Clinical impact of (18) F-FDG positron emission tomography/CT on adenoid cystic carcinoma of the head and neck. Head Neck. 2017;39(3):447-455.
9. Van Weert S, Bloemena E, Van Der Waal I, et al. Adenoid cystic carcinoma of the head and neck: a single-center analysis of 105 consecutive cases over a 30-year period. Oral Oncol. 2013;49(8):824-829.
10. Alfieri S, Granata R, Bergamini C, et al. Systemic therapy in metastatic salivary gland carcinomas: A pathology-driven paradigm? Oral Oncol. 2017;66:58-63.
11. Atallah S, Marc M, Schernberg A, et al. Beyond Surgical Treatment in Adenoid Cystic Carcinoma of the Head and Neck: A Literature Review. Cancer Manag Res. 2022;14:1879-1890.
12. Onaga R, Enokida T, Ito K, et al. Combination chemotherapy with taxane and platinum in patients with salivary gland carcinoma: a retrospective study of docetaxel plus cisplatin and paclitaxel plus carboplatin. Front Oncol. 2023;13:1185198
13. Kacew AJ, Hanna GJ. Systemic and Targeted Therapies in Adenoid Cystic Carcinoma. Curr Treat Options Oncol. 2023;24(1):45-60.
14. Zhou J, Zhao G, Wang S, Li N. Systemic therapy in the management of metastatic or locally recurrent adenoid cystic carcinoma of the salivary glands: a systematic review of the last decade. Br J Cancer. 2024 131:6. 2024;131(6):1021-1031.
15. Huang M, Ma D, Sun K, Yu G, Guo C, Gao F. Factors influencing survival rate in adenoid cystic carcinoma of the salivary glands. Int J Oral Maxillofac Surg. 1997;26(6):435-439.
16. Bjørndal K, Krogdahl A, Therkildsen MH, et al. Salivary gland carcinoma in Denmark 1990-2005: A national study of incidence, site and histology. Results of the Danish Head and Neck Cancer Group (DAHANCA). Oral Oncol. 2011;47(7):677-682.
17. West RB, Kong C, Clarke N, et al. MYB expression and translocation in adenoid cystic carcinomas and other salivary gland tumors with clinicopathologic correlation. Am J Surg Pathol. 2011;35(1):92-99.
18. Zushi Y, Noguchi K, Hashitani S, et al. Relations among expression of CXCR4, histological patterns, and metastatic potential in adenoid cystic carcinoma of the head and neck. Int J Oncol. 2008;33(6):1133-1139.

19. de Keizer B, Krijger GC, Ververs FT, van Es RJJ, de Bree R, Willems S. 68Ga-PSMA PET-CT Imaging of Metastatic Adenoid Cystic Carcinoma. Nucl Med Mol Imaging. 2017;51(4):360-361.
20. Mitani Y, Li J, Rao PH, et al. Comprehensive analysis of the MYB-NFIB gene fusion in salivary adenoid cystic carcinoma: Incidence, variability, and clinicopathologic significance. Clin Cancer Res. 2010;16(19):4722-4731.
21. Xu B, Drill E, Ho AAAAA, et al. Predictors of Outcome in Adenoid Cystic Carcinoma of Salivary Glands: A Clinicopathologic Study With Correlation Between MYB Fusion and Protein Expression. Am J Surg Pathol. 2017;41(10):1422-1432.
22. von Holstein SL, Fehr A, Persson M, et al. Adenoid cystic carcinoma of the lacrimal gland: MYB gene activation, genomic imbalances, and clinical characteristics. Ophthalmology. 2013;120(10):2130-2138.
23. Brill LB, Kanner WA, Fehr A, et al. Analysis of MYB expression and MYB-NFIB gene fusions in adenoid cystic carcinoma and other salivary neoplasms. Mod Pathol. 2011 24:9. 2011;24(9):1169-1176.
24. Andersson MK, Afshari MK, Andren Y, et al. Targeting the Oncogenic Transcriptional Regulator MYB in Adenoid Cystic Carcinoma by Inhibition of IGF1R/AKT Signaling. J Natl Cancer Inst. 2017;109(9).
25. Zlotnik A, Yoshie O. The Chemokine Superfamily Revisited. Immunity. 2012;36(5):705-712.
26. Vandercappellen J, Van Damme J, Struyf S. The role of CXC chemokines and their receptors in cancer. Cancer Lett. 2008;267(2):226-244.
27. Muller A, Sonkoly E, Eulert C, et al. Chemokine receptors in head and neck cancer: Association with metastatic spread and regulation during chemotherapy. Int J Cancer. 2006;118(9):2147-2157.
28. Phattarataratip E, Dhanuthai K. Expression of C-X-C motif chemokine receptors 4 and 7 in salivary gland neoplasms. Arch Oral Biol. 2017;83:136-144.
29. Zhang CY, Xia RH, Han J, et al. Adenoid cystic carcinoma of the head and neck: Clinicopathologic analysis of 218 cases in a Chinese population. Oral Surg Oral Med Oral Pathol Oral Radiol. 2013;115(3):368-375.
30. Domanska UM, Kruizinga RC, Nagengast WB, et al. A review on CXCR4/CXCL12 axis in oncology: No place to hide. Eur J Cancer. 2013;49(1):219-230.
31. Wang Z, Sun J, Feng Y, Tian X, Wang B, Zhou Y. Oncogenic roles and drug target of CXCR4/CXCL12 axis in lung cancer and cancer stem cell. Tumour Biol. 2016;37(7):8515-8528.
32. Coniglio SJ. Role of tumor-derived chemokines in osteolytic bone metastasis. Front Endocrinol (Lausanne). 2018;9:313.
33. Yopp AC, Shia J, Butte JM, et al. CXCR4 expression predicts patient outcome and recurrence patterns after hepatic resection for colorectal liver metastases. Ann Surg Oncol. 2012;19(Suppl 3);339–346.
34. Barone F, Bombardieri M, Rosado MM, et al. CXCL13, CCL21, and CXCL12 Expression in Salivary Glands of Patients with Sjogren's Syndrome and MALT Lymphoma: Association with Reactive and Malignant Areas of Lymphoid Organization. J Immunol.2008;180(7):5130-5140.
35. Chatterjee S, Behnam Azad B, Nimmagadda S. The intricate role of CXCR4 in cancer. Adv Cancer Res. 2014;124:31-82.
36. Gourni E, Demmer O, Schottelius M, et al. PET of CXCR4 Expression by a 68Ga-Labeled Highly Specific Targeted Contrast Agent. J Nucl Med. 2011;52(11):1803-1810.
37. Schottelius M, Osl T, Poschenrieder A, et al. [177Lu]pentixather: Comprehensive preclinical characterization of a first CXCR4-directed endoradiotherapeutic agent. Theranostics. 2017;7(9):2350-2362.

38. Wright GL, Haley C, Beckett M Lou, Schellhammer PF. Expression of prostate-specific membrane antigen in normal, benign, and malignant prostate tissues. Urol Oncol Semin Orig Investig. 1995;1(1):18-28.
39. Afshar-Oromieh A, Hetzheim H, Kratochwil C, et al. The novel theranostic PSMA-ligand PSMA-617 in the diagnosis of prostate cancer by PET/CT: biodistribution in humans, radiation dosimetry and first evaluation of tumor lesions. J Nucl Med. 2015;56(11):1697-1705.
40. Hofman MS, Violet J, Hicks RJ, et al. [177Lu]-PSMA-617 radionuclide treatment in patients with metastatic castration-resistant prostate cancer (LuPSMA trial): a single-centre, single-arm, phase 2 study. Lancet Oncol. 2018;19(6):825-833.
41. Nishida H, Kondo Y, Kusaba T, Kadowaki H, Daa T. Immunohistochemical Reactivity of Prostate-Specific Membrane Antigen in Salivary Gland Tumors. Head Neck Pathol. 2021;16(2):427.
42. Backhaus P, Noto B, Avramovic N, et al. Targeting PSMA by radioligands in non-prostate disease—current status and future perspectives. Eur J Nucl Med Mol Imaging. 2018;45(5):860-877.
43. Salas Fragomeni RA, Amir T, Sheikhbahaei S, et al. Imaging of Non-Prostate Cancers Using PSMA-Targeted Radiotracers: Rationale, Current State of the Field, and a Call to Arms. J Nucl Med. 2018;59(6):871-877
44. Ross JS, Sheehan CE, Fisher H a G, et al. Correlation of primary tumor prostate-specific membrane antigen expression with disease recurrence in prostate cancer. Clin Cancer Res. 2003;9(17):6357-6362.
45. Kaittanis C, Andreou C, Hieronymus H, et al. Prostate-specific membrane antigen cleavage of vitamin B9 stimulates oncogenic signaling through metabotropic glutamate receptors. J Exp Med. 2018;215(1):159-175.
46. Perico ME, Grasso S, Brunelli M, et al. Prostate-specific membrane antigen (PSMA) assembles a macromolecular complex regulating growth and survival of prostate cancer cells "in vitro" and correlating with progression "in vivo." Oncotarget. 2016;7(45):74189-74202.
47. Mhawech-Fauceglia P, Smiraglia DJ, Bshara W, et al. Prostate-specific membrane antigen expression is a potential prognostic marker in endometrial adenocarcinoma. Cancer Epidemiol Biomarkers Prev. 2008;17(3):571-577.
48. Rothman KJ. No adjustments are needed for multiple comparisons. Epidemiology. 1990;1(1):43-46.
49. da Silva FJ, Carvalho de Azevedo J, Ralph ACL, Pinheiro J de JV, Freitas VM, Calcagno DQ. Salivary glands adenoid cystic carcinoma: a molecular profile update and potential implications. Front Oncol. 2023;13:1191218.
50. Has Simsek D, Kuyumcu S, Agaoglu FY, Unal SN. Radionuclide Therapy With 177Lu-PSMA in a Case of Metastatic Adenoid Cystic Carcinoma of the Parotid. Clin Nucl Med. 2019;44(9):764-766.
51. Rahbar K, Ahmadzadehfar H, Kratochwil C, et al. German multicenter study investigating 177Lu-PSMA-617 radioligand therapy in advanced prostate cancer patients. J Nucl Med. 2017;85(1):85-90.
52. Afzelius P, Nielsen MY, Ewertsen C, Bloch KP. Imaging of the major salivary glands. Clin Physiol Funct Imaging. 2016;36(1):1-10.
53. La'Porte SJ, Juttla JK, Lingam RK. Imaging the Floor of the Mouth and the Sublingual Space. Radiographics. 2011;31(5):1215-1230.
54. Różycki R. Diagnostic imaging of the nasolacrimal drainage system. Part I. Radiological anatomy of lacrimal pathways. Physiology of tear secretion and tear outflow. Med Sci Monit. 2014;20:628-638.

55. Kinahan PE, Fletcher JW. Positron emission tomography-computed tomography standardized uptake values in clinical practice and assessing response to therapy. Semin Ultrasound, CT MRI. 2010;31(6):496-505.
56. Almståhl A, Alstad T, Fagerberg-Mohlin B, Carlén A FC. Explorative study on quality of life in relation to salivary secretion rate in patients with head and neck cancer treated with radiotherapy. Head Neck. 2016;38(5):782-791.
57. Gensheimer MF, Liao JJ, Garden AS, et al. Submandibular gland-sparing radiation therapy for locally advanced oropharyngeal squamous cell carcinoma: patterns of failure and xerostomia outcomes. Radiat Oncol. 2014;9(1):255.
58. Ekmekcioglu Ö, Busstra M, Klass ND, Verzijlbergen F. Bridging the Imaging Gap: PSMA PET/CT Has a High Impact on Treatment Planning in Prostate Cancer Patients with Biochemical Recurrence—A Narrative Review of the Literature. J Nucl Med. 2019;60(10):1394-1398.
59. Jang JY, Pak KJ, Yi KI, et al. Differential Prognostic Value of Metabolic Heterogeneity of Primary Tumor and Metastatic Lymph Nodes in Patients with Pharyngeal Cancer. Anticancer Res. 2017;37(10):5899-5905.
60. Chan SC, Cheng NM, Hsieh CH, et al. Multiparametric imaging using (18)F-FDG PET/CT heterogeneity parameters and functional MRI techniques: prognostic significance in patients with primary advanced oropharyngeal or hypopharyngeal squamous cell carcinoma treated with chemoradiotherapy. Oncotarget. 2017;8(37):62606-62621.
61. Civan C, Kasper S, Berliner C, et al. PSMA-Directed Imaging and Therapy of Salivary Gland Tumors: A Single-Center Retrospective Study. J Nucl Med. 2023;64(3):372-378.
62. Lonneux M, Hamoir M, Reychler H, et al. Positron emission tomography with [18F] fluorodeoxyglucose improves staging and patient management in patients with head and neck squamous cell carcinoma: a multicenter prospective study. J Clin Oncol. 2010;28(7):1190-1195.
63. Lütje S, Sauerwein W, Lauenstein T, Bockisch A, Poeppel TD. In Vivo Visualization of Prostate-Specific Membrane Antigen in Adenoid Cystic Carcinoma of the Salivary Gland. Clin Nucl Med. 2016;41(6):476-477.
64. Shamim SA, Kumar N, Arora G, et al. Comparison of 68Ga-PSMA-HBED-CC and 18F-FDG PET/CT in the Evaluation of Adenoid Cystic Carcinoma-A Prospective Study. Clin Nucl Med. 2023;48(11):E509-E515.
65. Wang X, Zhang X, Zhang X, et al. Design, preclinical evaluation, and first-in-human PET study of [68Ga]Ga-PSFA-01: a PSMA/FAP heterobivalent tracer. Eur J Nucl Med Mol Imaging. 2025;52(3):1166-1176.
66. Hotta M, Nguyen K, Thin P, et al. Kinetics and patterns of PSMA PET uptake after radiation therapy for prostate cancer: a single center retrospective study. J Nucl Med. 2022;63(Suppl 2):3041.
67. Onal C, Guler OC, Torun N, et al. Impact of definitive radiotherapy on metabolic response measured with 68Ga-PSMA-PET/CT in patients with intermediate-risk prostate cancer. Prostate. 2024 84(15):1366-1374.
68. De Galiza Barbosa F, Queiroz MA, Nunes RF, et al. Nonprostatic diseases on PSMA PET imaging: A spectrum of benign and malignant findings. Cancer Imaging. 2020;20(1):1-23.
69. Avcu A, Oksuzoglu K, Kissa TN, et al. AB0833 THE USE OF F-18 FDG PET/CT AND Ga-68 PSMA PET/CT IN THE EVALUATION OF SALIVARY GLANDS IN SJÖGREN'S SYNDROME. Ann Rheum Dis. 2024;83(Suppl 1):1713-1714.
70. Röhrich M, Syed M, Liew DP, et al. 68Ga-FAPI-PET/CT improves diagnostic staging and radiotherapy planning of adenoid cystic carcinomas – Imaging analysis and histological validation. Radiother Oncol. 2021;160(7)192-201.

71. Rizzo A, Albano D, Elisei F, et al. The Potential Role of PSMA-Targeted PET in Salivary Gland Malignancies: An Updated Systematic Review. Diagnostics (Basel). 2024;14(14):1516.
72. Yu W, Zhao M, Deng Y, et al. Meta-analysis of 18 F-PSMA-1007 PET/CT, 18 F-FDG PET/CT, and 68Ga-PSMA PET/CT in diagnostic efficacy of prostate Cancer. Cancer Imaging. 2023;23(1):1-11.
73. Trautwein NF, Brendlin A, Reischl G, et al. PSMA-Guided Imaging and Therapy of Advanced Adenoid Cystic Carcinomas and Other Salivary Gland Carcinomas. Cancers (Basel). 2024;16(22):3843.
74. Fendler WP, Reinhardt S, Ilhan H, et al. Preliminary experience with dosimetry, response and patient reported outcome after 177Lu-PSMA-617 therapy for metastatic castration-resistant prostate cancer. Oncotarget. 2017;8(2):3581-3590.
75. Yadav MP, Ballal S, Sahoo RK, Dwivedi SN, Bal C. Radioligand therapy with 177Lu-PSMA for metastatic castration-resistant prostate cancer: A systematic review and meta-analysis. Am J Roentgenol. 2019;213(2):275-285.
76. Afshar-Oromieh A, Avtzi E, Giesel FL, et al. The diagnostic value of PET/CT imaging with the 68Ga-labelled PSMA ligand HBED-CC in the diagnosis of recurrent prostate cancer. Eur J Nucl Med Mol Imaging. 2015;42(2):197-209.
77. Sartor O, de Bono J, Chi K, et al. Lutetium-177-PSMA-617 for Metastatic Castration-Resistant Prostate Cancer. N Engl J Med. 2021;385(12):1091-1103.
78. Kratochwil C, Bruchertseifer F, Rathke H, et al. Targeted Alpha Therapy of mCRPC with (225)Actinium-PSMA-617: Dosimetry estimate and empirical dose finding. J Nucl Med. 2017;58(10):1624-1631
79. Belli ML, Sarnelli A, Mezzenga E, et al. Targeted Alpha Therapy in mCRPC (Metastatic Castration-Resistant Prostate Cancer) Patients: Predictive Dosimetry and Toxicity Modeling of 225Ac-PSMA (Prostate-Specific Membrane Antigen). Front Oncol. 2020;10:531660.
80. Heynickx N, Segers C, Coolkens A, Baatout S, Vermeulen K. Characterization of Non-Specific Uptake and Retention Mechanisms of [177Lu]Lu-PSMA-617 in the Salivary Glands. Pharmaceuticals. 2023;16(5):692.

Nederlandse samenvatting

Adenoid cysteus carcinoom (AdCC) is een van de meest agressieve speekselkliertumoren, gekenmerkt door een complexe pathologie en een onvoorspelbare klinische presentatie. Het behandelen van deze ziekte vereist een multidisciplinaire benadering voor diagnostiek, therapiekeuze en het voorspellen van de ziekte-uitkomst. Het optimaliseren van de huidige technieken vormt een cruciale stap om de vooruitzichten voor deze patiënten te verbeteren.[1–4]

AdCC is verantwoordelijk voor 20–35% van alle kwaadaardige speekselkliertumoren, met een jaarlijkse incidentie van 2 tot 3 per miljoen inwoners. De ziekte treft vooral mensen in hun vijfde en zesde decennium, met een lichte voorkeur voor vrouwen.[1–4]

De diagnostiek bestaat uit klinisch, histopathologisch en beeldvormend onderzoek. Hoewel histopathologie de basis vormt voor het stellen van de diagnose, kan dit lastig zijn op kleine biopten vanwege overlappende kenmerken met andere speekselkliertumoren, blijkens uit het hoge herzieningspercentage van 14% tot 29% na volledige tumorexcisie.[1,5] Moleculaire diagnostiek speelt een steeds belangrijkere rol in de diagnostiek, bijvoorbeeld met de identificatie van de *MYB::NFIB*-fusie, die in ongeveer 50% van de gevallen voorkomt.[1,6] Histologisch worden drie groeipatronen onderscheiden: tubulair, cribriform en solide. Het tubulaire patroon heeft de beste prognose, het solide patroon wordt geassocieerd met een agressief beloop.[5,7] Andere factoren die de prognose negatief beïnvloeden zijn: gevorderd tumorstadium; oorsprong uit kleine speekselklieren; onvoldoende chirurgische marge en (peri)neurale invasie.[1–4,8,9]

MRI en CT worden gebruikt ter beeldvorming van de lokale uitbreiding van de tumor, terwijl PET/CT vooral dient voor het detecteren van afstandsmetastasen. Door de lage FDG-opname in AdCC kunnen recidieven en metastasen echter lastig te beoordelen zijn.[10,11]

De primaire behandeling van AdCC is chirurgisch en gericht op volledige tumorresectie met negatieve snijvlakken, bijna altijd gevolgd door radiotherapie ter verkleining van het risico op een lokaal recidief.[1,2] Na de initiële behandeling is bij patiënten met gevorderde ziekte een lokaal recidief niet zeldzaam en lastig te behandelen door eerdere chirurgie en radiotherapie. Daarnaast ontwikkelt tot 40% van de patiënten langzaam progressieve long- of botmetastasen binnen vijf jaar na de diagnose. Systemische behandelingen, doorgaans chemotherapie en immunotherapie, hebben over het algemeen beperkt effect.[12–14]

De overlevingskansen zijn de afgelopen decennia aanzienlijk toegenomen. Locoregionale controle is gestegen van ongeveer 36% naar meer dan 80% vijf jaar na het stellen van de diagnose, terwijl ziektevrije overleving verbeterde van 31% naar meer dan 65%.[2,3,8,9] Hoewel deze vooruitgang bemoedigend is, blijven er uitdagingen

bestaan op het gebied van diepe (irresectabele) recidieven en metastasen. Dit proefschrift richt zich op het verkennen en valideren van nieuwe aangrijpingspunten voor zowel diagnostiek als behandeling door het combineren van histopathologie, geavanceerde beeldvorming en doelgerichte therapie. Het doel is om hiermee bij te dragen aan een beter begrip van de ziekte, nauwkeurigere diagnostiek en effectievere geïndividualiseerde behandelmethoden voor patiënten met AdCC, uiteindelijk leidend tot betere overleving en kwaliteit van leven.

Deel A (Hoofdstukken 2, 3 en 4) onderzoekt drie biomarkers in AdCC —cellulair myeloblastose-gen (*MYB*), chemokine receptor type 4 (CXCR4) en prostaat-specifiek membraan antigeen (PSMA)— in hun rol in het identificeren van AdCC, voorspellen van ziekteprogressie en hun potentieel als doelwit voor gerichte beeldvorming en therapie.
Deel B (Hoofdstukken 5 en 6) richt zich op PSMA in de diagnostiek met als doel het verfijnen van de stadiëring van AdCC. Eerst wordt het normale opnamepatroon van PSMA-ligand op PET/CT in kaart gebracht, gevolgd door de eerste toepassing van PSMA PET/CT in combinatie met immunohistochemie bij AdCC.
Deel C (Hoofdstuk 7) introduceert PSMA-gerichte radioligandtherapie (PSMA-RLT), dat mogelijk nieuwe behandelopties biedt voor patiënten met speekselkliertumoren waarvoor conventionele behandelingen niet effectief zijn gebleken.

DEEL A: BIOMARKERS IN ADENOID CYSTEUS CARCINOOM

Om de betrouwbaarheid van het stellen van de diagnose AdCC te verbeteren, onderzoekt **Hoofdstuk 2** de detectie van de fusie tussen het *MYB*-gen en het nuclear factor I B-type (*NFIB*)-gen, die ontstaat als gevolg van translocatie t(6;9)(q22–23;p23–24). Deze *MYB::NFIB*-translocatie activeert een fusie-eiwit dat oncogene processen stimuleert, zoals een langere overleving van cellen, ongecontroleerde celproliferatie en verminderde apoptose, en wordt beschouwd als pathognomonisch voor AdCC.[1,6] Overexpressie van MYB kan echter ook optreden zonder deze fusie, vermoedelijk door andere *MYB*-herschikkingen of alternatieve routes.[15,16] Voor de detectie van de *MYB::NFIB*-translocatie wordt vaak fluorescentie in situ hybridisatie (FISH) gebruikt met een *break apart probe*. Ondanks dat FISH zeer specifiek is, is het duur en complex. Immunohistochemie (IHC) biedt daarentegen een sneller en kostenefficiënter alternatief, waardoor het geschikter is voor routinematig gebruik.[17,18] Honderdtien patiënten met AdCC werden geanalyseerd, waarbij de *MYB::NFIB*-fusie in 56% van de 90 tumoren met behulp van FISH werd geïdentificeerd. IHC toonde in 89% homogene nucleaire MYB-expressie in abluminale cellen, met een mediane expressie van 27% (interkwartielrange [IQR] 8–46%). Bij 62 gevallen waarin zowel FISH als IHC werden vergeleken, werd in 38 tumoren (61%) een *MYB::NFIB*-fusie gedetecteerd, waarvan 37 MYB-expressie lieten zien met een mediane aankleuring van 30% (IQR 12–56%). Deze expressie was significant hoger (p=0,02) dan de mediane expressie van 6% (IQR 4–30%) die werd waargenomen in tumoren zonder de translocatie. Het vaststellen van een afkapwaarde van 60% MYB-expressie voor fusiepositiviteit resulteerde in een specificiteit en positief voorspellende waarde van 100%. Deze resultaten bevestigen dat MYB IHC een betrouwbaar, snel en kostenefficiënt alternatief is voor FISH bij het voorspellen van de *MYB::NFIB*-fusiestatus.[18] Hoewel geen correlatie werd gevonden met klinisch-pathologische parameters komen de bevindingen overeen met eerder onderzoek en bouwen hierop voort.[6,16,19,20]

Naast deze veelbelovende resultaten noemt de studie ook enkele beperkingen in de toepasbaarheid van IHC. De generaliseerbaarheid van de 60%-afkapwaarde naar de klinische praktijk is een uitdaging, met name bij de diagnostiek van speekselkliertumoren met overlappende kenmerken, zoals myoepitheliaal carcinoom, polymorf adenocarcinoom en basaloïd plaveiselcelcarcinoom, waarvan sommige zwakke of focale MYB-reactiviteit kunnen vertonen. Daarnaast bemoeilijken variaties in kleuring, afkapwaarden en tumorheterogeniteit het gebruik van IHC buiten de gecontroleerde setting.[6,21] Verder onderzoek naar *MYB*-gerelateerde moleculaire

pathways kan waardevolle inzichten bieden in de invloed van MYB-expressie op tumorgedrag en kan mogelijke nieuwe (therapeutische) doelwitten opleveren. Tot nu toe is de *MYB*-fusiestatus nog niet direct gekoppeld aan therapierespons, maar toekomstige studies kunnen onderzoeken of patiënten met deze fusie baat hebben bij therapieën zoals IGF1R-remmers, die in bepaalde *MYB*-gedreven tumoren al effectief zijn gebleken.[22]

Hoofdstuk 3 richt zich op chemokines vanwege hun cruciale rol in het immuunsysteem en hun betrokkenheid bij celregulering, inclusief apoptose en mitogenese, met daaruitvolgende essentiële functies in hematopoëse, tumorgroei en metastasering.[23,24] De focus ligt specifiek op CXCR4, een chemokinereceptor die chemokine ligand 12 (CXCL12) bindt en onder andere een sleutelrol vervult in de embryonale ontwikkeling en immuuncelverkeer. CXCR4 komt tot overexpressie in meer dan 20 tumortypen, met inbegrip van AdCC, en wordt beschouwd als een veelbelovend diagnostisch en therapeutisch doelwit.[25,26] Verhoogde CXCR4-expressie wordt vaak geassocieerd met een toegenomen risico op lokaal recidief en afstandsmetastasen, doordat het angiogenese stimuleert en tumorcellen via hun CXCR4-receptoren gericht aantrekt naar CXCL12-rijke metastatische locaties waaronder lymfeklieren, longen en lever.[24–27] Antagonisten zoals AMD3100, evenals anti-CXCR4-peptiden en -antistoffen, kunnen tumorgroei remmen.[26–29] Bovendien bieden recent ontwikkelde CXCR4-liganden nieuwe opties voor PET-specifieke beeldvorming en toekomstige radioligandtherapie.[30,31]
Immunohistochemische CXCR4-expressie werd onderzocht in 66 AdCC-tumoren. Eenentachtig procent van de primaire tumoren toonde uniforme expressie, met mediaan 29% positieve cellen (IQR 1–70%), consistent met eerdere studies.[25,29,32] Primaire tumoren die recidiveerden hadden significant hogere CXCR4-expressie dan tumoren zonder recidief (mediaan 60%; IQR 33–72% versus 12%; IQR 1–70%; KW p=0,01). In onze studie werd geen correlatie gevonden tussen hoge CXCR4-expressie en het optreden van afstandsmetastasen, hoewel er wel een trend zichtbaar was: 49% expressie in metastatische tumoren tegenover 23% in niet-metastatische tumoren. De beperkte studiepopulatie en de korte follow-upduur kunnen het uitblijven van een duidelijk verband wellicht verklaren.
Tumoren met CXCR4-expressie boven de 25% waren significant geassocieerd met perineurale groei en botinvasie (p=0,02 en p=0,03) en gingen gepaard met een 7,2-voudig verhoogd risico op tumorrecidief (hazard ratio [HR] 7,2, 95% betrouwbaarheidsinterval [CI] 1,5–72,4, p=0,04), onafhankelijk van andere klinisch-pathologische factoren. Zoals verwacht verbeterde postoperatieve radiotherapie de recidiefvrije overleving (RFS) aanzienlijk (HR 25,1; 95% CI 1,9–339,9; p=0,03).

Een solide groeipatroon, vaak geassocieerd met slechtere overleving, liet in deze studie slechts een trend zien en was niet significant gerelateerd aan een hogere recidiefkans.[1–4,8,9,33] Onze grotere studie naar PSMA-expressie, beschreven in Hoofdstuk 4, bevestigde deze associatie echter wel (p=0,02). De CXCL12/CXCR4-as lijkt botinvasie te bevorderen door osteolyse te induceren via stimulatie van osteoclastvoorlopers.[34] Perineurale groei en botinvasie waren zelf niet gerelateerd aan locoregionaal recidief, wat consistent is met bestaande literatuur.[2] Deze bevindingen onderstrepen de waarde van CXCR4 in het identificeren van AdCC-patiënten met een hoog risico, die baat kunnen hebben bij aangepaste behandelingen en intensieve follow-up. CXCR4 heeft aanzienlijke potentie als prognostische en therapeutische biomarker in AdCC, met bewezen effectiviteit van CXCR4-remmers bij het remmen van tumorgroei, het versterken van chemogevoeligheid in combinatietherapieën, en veelbelovende toepassingen van radioactief gelabelde CXCR4-liganden voor PET/CT-beeldvorming en radionuclidetherapie.[26-28,30,31]

PSMA-eiwitexpressie wordt onderzocht in **Hoofdstuk 4** en betreft een type II transmembraan glycoproteïne dat oorspronkelijk werd ontdekt in zowel benigne en maligne prostaatweefsel. Het staat bekend om zijn cruciale rol in diagnostiek en therapie bij prostaatkanker en is daarmee een belangrijke oncologische biomarker.[35-40] PSMA is voornamelijk gelokaliseerd in het cytoplasma en op het apicale oppervlak van epitheelcellen die de prostaatgangen bekleden. Tijdens dysplastische en maligne transformatie verplaatst het zich naar het luminale oppervlak van de afvoergangen, wat de toegenomen expressie verklaart. Het correleert met tumorgraad en -stadium en derhalve een slechte prognose.[38,41–43] Hoewel PSMA oorspronkelijk als prostaat-specifiek werd beschouwd, komt het ook tot expressie in andere weefsels, waaronder de nieren, het zenuwstelsel, de dunne darm, het ductale borstepitheel en subtypen van schwannoom en blaaskanker. Daarnaast wordt het aangetroffen in het neovasculaire endotheel van diverse solide tumoren, wat wijst op een mogelijke rol in tumor-geassocieerde angiogenese.[42,44–46] In speekselklieren bevindt PSMA zich voornamelijk in het cytoplasma van secretoire acinaire cellen, terwijl het niet tot expressie komt in afvoergangcellen.[47,48] In tegenstelling tot prostaat-specifiek antigeen (PSA) kan PSMA niet worden gebruikt als tumormarker op basis van bloedonderzoek.[49,50] Een case-report uit ons instituut en een tweede studie suggereerden PSMA-expressie in AdCC.[51,52] Dit vormde de aanleiding voor het huidige onderzoek naar PSMA-eiwitexpressie in 110 primaire, recidiverende en metastatische AdCC-tumoren. PSMA-expressie werd aangetoond in 94% van de primaire AdCC-samples (mediaan 31% positieve cellen; IQR 15–60%), 80% van de recidieven (mediaan 60%; IQR 30–90%) en 90% van de metastasen

(mediaan 23%; IQR 10–55%). Vergeleken met de corresponderende primaire tumoren (mediaan 40%; IQR 15–70%) liet PSMA-expressie een niet-significante trend zien van toename in recidieven en afname in afstandsmetastasen. Deze heterogeniteit beperkt de betrouwbaarheid van PSMA als prognostische marker voor het voorspellen van expressie in recidieven of metastasen. De expressie correleerde niet met pathologisch stadium, tumorgraad of ziekteprogressie, maar wel met tumorlokalisatie en botinvasie. Lagere PSMA-expressie werd waargenomen in tumoren van kleine speekselklieren (21% vs. 50%; p<0,01) en in tumoren met botinvasie (17% vs. 39%; p=0,04). Tumorlokalisatie en botinvasie waren sterk gecorreleerd, omdat botinvasieve tumoren vrijwel altijd afkomstig waren uit kleine speekselklieren.

Na dichotomisatie bleek dat patiënten met een PSMA-expressie van ≤10% een slechtere recidiefvrije overleving (RFS) over 10 jaar hadden (HR 3,0; 95% CI 1,1–8,5; p=0,04). Deze tumoren waren voornamelijk gelokaliseerd in de neusholte, nasofarynx of sinus maxillaris, lokalisaties die geassocieerd zijn met een ongunstigere prognose. Andere voorspellers van een lagere RFS waren tumoren met een solide groeiwijze (HR 3,7; 95% CI 1,3–11,2; p=0,02) en het niet toedienen van postoperatieve radiotherapie (HR 5,1; 95% CI 1,2–17,5; p=0,02). De aanvullende voorspellende waarde van PSMA voor RFS was echter minimaal, blijkens uit Harrell's *C-statistic*, die slechts toenam van 0,79 naar 0,81. PSMA-expressie correleerde niet met andere klinische parameters zoals algemene overleving, ziekte-specifieke overleving of metastasevrije overleving.

PSMA-expressie in AdCC werd, net als in prostaatkanker, voornamelijk waargenomen in epitheliale tumorcellen, in een korrelig patroon binnen het cytoplasma of geconcentreerd aan de luminale zijde van de celmembraan.[53] Hiermee onderscheidt AdCC zich van andere maligniteiten waarin PSMA vaker tot expressie komt in endotheelcellen van tumor-geassocieerde vaatnieuwvorming.[38,54,55] Een belangrijk verschil is echter dat hoge PSMA-expressie in prostaatkanker samenhangt met agressieve tumorkenmerken en een slechtere overleving, terwijl in AdCC een omgekeerde relatie werd gevonden, vermoedelijk door epigenetische onderdrukking tijdens tumorprogressie.[38,43,56] Daarnaast verschillen de expressiepatronen: primaire prostaatkankertumoren worden beschreven als meer heterogeen, met gemiddeld 53 ± 32% positieve cellen, tegenover een mediaan van 31% in AdCC. In prostaatkanker-metastasen is dit percentage nog veel hoger met 92 ± 10% aankleurende cellen, vergeleken met een mediaan van 23% in AdCC. Alle benigne prostaatmonsters zijn tevens PSMA-reactief, met een gemiddelde van 77 ± 32% positieve cellen, zij het met een lagere kleuringintensiteit dan in prostaatkankertumoren. In normaal speekselklierweefsel werd PSMA-expressie aangetroffen in 59% van de monsters, voornamelijk in muceuze kliercellen, met een

hogere expressie in kleine speekselklieren dan in grote.[38,43,53] Ondanks deze verschillen benadrukt de consistente PSMA-expressie in AdCC het potentieel voor *targeted* diagnostiek en therapie.

In conclusie toont DEEL A van dit proefschrift aan dat de onderzochte biomarkers belangrijke diagnostische en prognostische waarde hebben en mogelijkheden bieden voor therapeutische toepassingen bij AdCC. De studies hebben echter beperkingen, zoals kleine cohorten (na dichotomisering), variabiliteit in kleuringprotocollen en korte follow-upduur, wat de noodzaak onderstreept van gestandaardiseerde methodologieën en vervolgonderzoek met robuuste validatie.[57] Deze inzichten zullen bijdragen aan het optimaliseren en personaliseren van de AdCC-zorg.

DEEL B: DOELGERICHTE DIAGNOSTIEK

De anatomie van speekselklieren vormt een uitdaging voor diagnostische beeldvorming, vooral bij het beoordelen van tumorinvasie. Hoewel CT en MRI effectief zijn voor het visualiseren van de parotideale- en submandibulaire klieren, is de detectie van de sublinguale en kleine speekselklieren beperkt. Dit is te wijten aan hun omvang en het geringe contrast met omliggend weefsel, waardoor deze klieren vaak alleen duidelijk zichtbaar zijn bij tumorgroei.[58–61] De consistente expressie van PSMA in AdCC, gecombineerd met de minimale expressie in andere weefsels —behoudens de speekselklieren en prostaat— benadrukt het potentieel als doelwit voor gerichte beeldvorming. De ontwikkeling van PSMA PET/CT met radionucliden ^{68}Ga en ^{18}F biedt een niet-invasieve methode om PSMA-expressie in vivo zichtbaar te maken en wordt inmiddels beschouwd als een beproefd theranostisch hulpmiddel bij prostaatkanker. Moleculen zoals ^{68}Ga-PSMA-HBED-CC kenmerken zich door een korte halfwaardetijd in het bloed, laag levermetabolisme en hoge opname in PSMA-exprimerende weefsels.[39,46,53,62] Aangezien ^{68}Ga-HBED-CC naast lever, milt, darmen en nieren ook wordt opgenomen in de speeksel- en traanklieren, kan het een rol spelen bij het detecteren van primaire en metastatische AdCC-laesies met PSMA-expressie en bij de selectie van patiënten voor doelgerichte radionuclidetherapie met Lutetium-177-PSMA.[39,40,52,63,64] Daarnaast biedt het mogelijk aanvullende en complementaire waarde ten opzichte van PSMA IHC, mede door de variatie in PSMA-expressie tussen primaire AdCC-tumoren, recidieven en metastasen. Een goed begrip van fysiologische PSMA-ligandopname in normale speeksel- en seromuceuze klieren is essentieel om pathologische opname te onderscheiden van fysiologische (achtergrond)activiteit.[60,65]

Hoofdstuk 5 brengt bij 30 patiënten de fysiologische opname van ^{68}Ga-PSMA PET/CT in speeksel- en seromuceuze klieren in kaart. De hoogste opname werd gezien in de parotideale en submandibulaire klieren (gemiddelde SUV_{max} respectievelijk 12,3 ± 3,9 en 11,7 ± 3,5), terwijl de sublinguale en kleine speeksel- en seromuceuze klieren lagere waarden toonden. De uniforme traceraccumulatie in grote speekselklieren contrasteert met de variabiliteit in kleine klieren, die het grootst is in de sublinguale (41,7%) en traanklieren (48,2%). Daarnaast vertonen de traanklieren traceropname die vergelijkbaar is met die van speeksel- en seromuceuze klieren, maar de betekenis hiervan is nog nauwelijks onderzocht.[66]

De in deze studie gepresenteerde anatomische atlas van PSMA-ligandopname met referentiekader vormt een basis voor het verfijnen van de diagnostische nauwkeurigheid en het verminderen van fout-positieve bevindingen. Daarnaast kan het de klinische toepasbaarheid van PSMA PET/CT bij speekselkliertumoren vergroten en vermoedelijk ondersteunen bij therapeutische interventies. Tijdens radiotherapie kunnen kritieke speekselkliergebieden, inclusief eerder niet-herkende kleine klieren, worden gespaard, wat het risico op xerostomie, xeroftalmie en slikproblemen vermindert en de kwaliteit van leven behoudt. Klierregio's zonder substantiële opname hoeven daarentegen niet zozeer te worden gespaard, wat meer flexibiliteit biedt bij de optimalisatie van radiotherapie.

Hoewel PSMA PET/CT veel potentie biedt, zijn er beperkingen, met name in de compacte structuren. Lagere SUV_{max}-waarden in kleine speekselklieren, waarschijnlijk verband houdend met volumetrische verschillen of biologische variaties, evenals de beperkte ruimtelijke resolutie van PET/CT-scanners, kunnen leiden tot een onderschatting van traceropname.[67] Verdere ontwikkelingen in PET/CT-beeldvorming, waaronder het integreren van metabole prognostische waarden om tumorheterogeniteit te beoordelen en de behandelrespons te voorspellen, moeten de behandelstrategieën verder verfijnen en personaliseren, wat uiteindelijk zal bijdragen aan een verbeterde ziektecontrole.[68–72]

Hoofdstuk 6 onderzoekt als eerste studie de klinische relevantie van ^{68}Ga-PSMA-HBED-CC PET/CT en de correlatie met PSMA IHC bij de detectie van recidief of metastatisch AdCC. Negen patiënten met een gemiddelde leeftijd van 51 jaar, die klinisch verdacht werden van progressie van hun AdCC, ondergingen een PSMA PET/CT ter herstadiëring. Alle bekende recidieven en metastasen toonden traceropname, waarvan in vier patiënten de metastasen progressie lieten zien. Bij drie patiënten werden in totaal vier nieuwe metastasen geïdentificeerd. Deze bevindingen worden ondersteund door een recente vergelijkende studie die de geoptimaliseerde tumordetectie en stadiëring van PSMA PET/CT ten opzichte van CT bij speekselkliermaligniteiten benadrukte.[73]

De mediane SUV_{max} voor lokaal recidief AdCC was 2,52 (IQR 2,41–5,95), en voor metastasen 4,01 (IQR 2,66–8,71). De referentiewaarden voor SUV_{max} in normale weefsels waren als volgt: parotis 10,94 (IQR 9,01–15,55), lever 3,83 (IQR 2,99–4,88) en nieren 23,76 (IQR 15,00–35,00). Alle patiënten waren overigens adjuvant behandeld met radiotherapie op de primaire tumor, wat de PSMA-ligandopname gemeten met PSMA PET/CT wellicht negatief heeft beïnvloed.

Drie patiënten ondergingen een PSMA PET/CT en een ^{18}F-FDG PET/CT binnen een tijdsinterval van drie maanden, waardoor directe vergelijking mogelijk was. FDG PET/CT, een veelgebruikte modaliteit in het stadiëren van hoofd-halskanker, heeft bij AdCC echter een beperkte sensitiviteit door de doorgaans lage FDG-opname in deze tumoren ten opzichte van onder andere plaveiselcelcarcinoom. Inflammatoire processen in speekselklieren kunnen de fysiologische opname versterken, wat het risico op fout-positieven vergroot of tumoren zelfs kan maskeren. Verder sluit bij een lage FDG-opname in de primaire tumor een negatieve FDG PET/CT metastasen niet altijd betrouwbaar uit. Vergelijkende studies bevestigen dit beeld: FDG PET/CT heeft eenzelfde sensitiviteit als conventionele CT voor het detecteren van primaire AdCC, maar is superieur in het identificeren van lymfeklier- en afstandsmetastasen.[1,11,74] In lijn met recente literatuur toonde onze studie dat PSMA PET/CT overeenkomstige sensitiviteit heeft als FDG PET/CT, maar met name beter presteert bij het detecteren van recidieven die gemaskeerd worden door fysiologische opname of lokaal toegenomen FDG-metabolisme, bijvoorbeeld nabij de schedelbasis. Immunohistochemie bevestigde concordante PSMA-expressie in weefselmonsters van primaire tumoren, lokale recidieven en metastasen in gebieden met PSMA-ligandopname op de PET/CT. Het percentage PSMA-exprimerende tumorcellen varieerde van 5% tot 90%, met een mediane expressie van 30% (IQR 15–70%).[51,52,75] De discrepanties tussen PSMA-eiwitexpressie en PSMA PET/CT kunnen worden verklaard door tracerwaarden die gelijk zijn aan of lager liggen dan de fysiologische achtergrondopname, of door onvoldoende traceropname als gevolg van de beperkte resolutie van PET/CT bij kleine afwijkingen, een bekende beperking die uitgebreid is beschreven bij FDG PET/CT.[39,67] Andere verschillen kunnen voortkomen uit de biologische variabiliteit van AdCC, factoren in de tumormicro-omgeving zoals verminderde vascularisatie en verhoogde interstitiële druk, en specifieke tracerkinetiek in langzaam groeiende tumoren.[76] Het integreren van PSMA PET/CT-resultaten met histopathologische data is daarom essentieel om de diagnostische nauwkeurigheid voor AdCC te verbeteren. Ondanks het gedeelde *target* blijft de relatie tussen PSMA-expressie op weefselniveau en in vivo beeldvorming onvoldoende begrepen en vraagt om verdere verduidelijking.

PSMA PET/CT kent enkele beperkingen die de klinische toepasbaarheid bemoeilijken. Fysiologische PSMA-ligandopname in normale speekselklieren en andere niet-prostaatweefsels vergroot het risico op foutieve interpretatie als tumoractiviteit, overeenkomstig met FDG PET/CT. Dit probleem is relevant bij primaire tumoren en diepe recidieven bijvoorbeeld nabij de schedelbasis, nasofarynx of diepe kwab van de parotis, waar een biopsie lastig is.[39] Eerdere behandelingen, meestal (stereotactische) radiotherapie, bemoeilijken de interpretatie door het vertroebeld onderscheid tussen tumorweefsel en post-therapeutische effecten, zoals besproken in Hoofdstuk 6.[77,78] De anatomische atlas uit Hoofdstuk 5 biedt deels een oplossing, maar nieuw onderzoek is nodig om deze bevindingen in grotere cohorten te valideren en om de traceropname in niet-tumoreuze gebieden, onder andere bij auto-immuunziekten als sarcoïdose en Sjögren, beter te begrijpen.[79,80] Inmiddels wordt ^{68}Ga-FAPI PET/CT onderzocht als een veelbelovende alternatieve beeldvormingstechniek, die fibroblast-activerend eiwit (FAP) in tumor-geassocieerde fibroblasten kan visualiseren. Net als PSMA PET/CT toont het een hoge ligandopname in AdCC, hetgeen tevens bevestigd wordt door histopathologie. Door stromale componenten van de tumormicro-omgeving in beeld te brengen, biedt ^{68}Ga-FAPI PET/CT mogelijk een alternatief bij tumoren met lage of heterogene PSMA-expressie.[81]

Concluderend beschrijft DEEL B van dit proefschrift de complementaire waarde van PSMA PET/CT en IHC bij het diagnosticeren en monitoren van AdCC ziekteprogressie, recidieven en metastasen, met een betrouwbaarheid minstens gelijkwaardig aan FDG PET/CT, mits fysiologische opname correct wordt geïnterpreteerd.[75,82] Toekomstig onderzoek kan zich richten op de voordelen van ^{18}F-PSMA PET/CT boven ^{68}Ga-PSMA PET/CT, met name de grotere specificiteit en verhoogde tumor-tot-achtergrond ratio.[83] Daarnaast zou het verder uitdiepen van de SUV_{max}-drempelwaarden van beide radiotracers tumoractiviteit kunnen gaan voorspellen. Het verbeteren van beeldvorming, het verfijnen van radiotracers en het integreren van aanvullende diagnostische methoden zal de toepasbaarheid van PSMA PET/CT bij AdCC vergroten en allicht uitbreiden naar andere speekselkliertumoren.

DEEL C: DOELGERICHTE THERAPIE

Radiogelabelde PSMA-liganden bieden een veelbelovende therapie voor tumoren die PSMA tot expressie brengen, doordat het radioactieve ligand zich specifiek bindt aan PSMA op tumorcellen. Lutetium-177 is een voorbeeld van zo'n isotoop, dat zowel bèta-straling uitzendt om tumorcellen van binnenuit te bestralen, als gammastraling

waarmee de opname van de tracer in het lichaam gelijktijdig kan worden gevolgd.[84] Palliatieve behandeling met ^{177}Lu-PSMA bij prostaatkanker leidde bij patiënten met hoge PSMA-ligandopname op PET/CT tot een biochemische respons in 97% van de gevallen, tegen minimale bijwerkingen. Toevoeging van ^{177}Lu-PSMA-therapie aan de standaardbehandeling verhoogde de mediane progressievrije overleving van 3,4 naar 8,7 maanden en de totale overleving van 11,3 naar 15,3 maanden.[40,85]

Gezien het succes bij prostaatkanker gecombineerd met de intracellulaire expressie van PSMA in speekselkliertumorcellen en de opname ervan op PSMA PET/CT, onderzocht **Hoofdstuk 7** het gebruik van ^{177}Lu-PSMA-617 als ultimum remedium voor palliatieve therapie bij AdCC, wanneer alle andere behandelopties zijn uitgeput.

Zes patiënten ondergingen PSMA-RLT: vier met AdCC, één met een mucoepidermoïd carcinoom en één met een ongedifferentieerd carcinoom. De tumoren waren gelokaliseerd in de parotis, mondholte (palatum durum en wangmucosa) en submandibulaire speekselklier. Twee patiënten voltooiden alle vier cycli, terwijl vier voortijdig stopten vanwege tumorprogressie, bijwerkingen of demotivatie. Eén patiënt ontwikkelde graad 3 trombocytopenie, anderen ervoeren mildere bijwerkingen waaronder vermoeidheid, misselijkheid en xerostomie. Bij aanvang van de behandeling hadden twee patiënten een locoregionaal recidief en vier patiënten afstandsmetastasen. De tumor-*targeting* was matig (gemiddelde SUV_{max} 8,2), met PSMA-expressie variërend van 5% tot 95%, zonder correlatie tussen SUV_{max} en eiwitexpressie. Vier patiënten rapporteerden binnen weken verlichting van symptomen zoals een afname van pijn, kortademigheid en vermoeidheid. Hogere PSMA-expressie leek aanvankelijk te leiden tot een beter klinisch effect, desalniettemin vertaalde dit zich niet in (langdurige) ziektecontrole of betere radiologische respons. De beste resultaten werden behaald bij twee AdCC-patiënten: één had een partiële respons (30% SUV_{max}-reductie) en 10 maanden stabiele ziekte, en de ander stabiele ziekte gedurende zes maanden. Drie patiënten ervoeren progressie ondanks initiële symptoomverlichting. De mediane overleving was zes maanden, één patiënt was 36 maanden na behandeling nog in leven. Ondanks de kleine groep toont deze studie het potentieel van PSMA-RLT als palliatieve behandeling voor speekselkliertumoren wanneer standaardtherapieën falen, en de resultaten worden ondersteund door twee recente case-reports.[73,86] Echter, de retrospectieve, single-center opzet en het ontbreken van een controlegroep beperken de kans om de effecten exclusief toe te schrijven aan ^{177}Lu-PSMA-therapie en bemoeilijken een vergelijking met eerdere palliatieve behandelingen. Grootschalige, prospectieve multicenter studies zijn nodig om het therapeutische voordeel en de klinische waarde van PSMA-RLT definitief vast te stellen.

Bij ^{177}Lu-PSMA-therapie voor speekselkliertumoren en prostaatkanker werden overeenkomstige symptoomverlichting en bijwerkingen waargenomen, maar de radiologische respons is aanzienlijk hoger bij prostaatkanker. Tot 10% van de patiënten met prostaatkanker bereikt een complete respons, en meta-analyses rapporteren een partiële respons in 37%, stabiele ziekte in 38% en progressieve ziekte in 25%.[40,87] Dit verschil kan worden verklaard door de lagere PSMA-ligandopname bij speekselkliertumoren (gemiddelde SUV_{max} 8,2) vergeleken met prostaatkankerlaesies (gemiddelde SUV_{max} 13,3).[88] Bovendien voltooiden slechts twee patiënten in onze studie alle vier cycli, terwijl prostaatkankeronderzoek een mediaan van vijf cycli rapporteerde, wat wellicht de effectiviteit zou kunnen beïnvloeden.[40,85] De significante toename in zowel progressievrije als algehele overleving bij prostaatkanker benadrukken wel de potentiële waarde van deze therapie en onderstrepen het belang van streven naar optimale PSMA-ligandopname en voldoende behandelingscycli.[85] Bij AdCC is dit uitdagender vanwege de lagere PSMA-expressie, maar doordat PSMA wordt geëxprimeerd in de neoplastische epitheelcellen, in tegenstelling tot de neovasculatuur bij andere maligniteiten, biedt ^{225}Ac-PSMA-617 mogelijk een oplossing. Deze alfa-*emitter* kan tumoren met lage tot matige PSMA-expressie vermoedelijk effectiever *targeten* door een hogere lineaire energietransfer, die leidt tot complexere DNA-schade als dubbelstrengsbreuken, wat radioresistentie kan doorbreken.[54,55,89,90] Hoewel alfastraling preciezer werkt, verhoogt het ook het risico op bijwerkingen in speekselklieren met hoge PSMA-expressie, wat kan leiden tot onomkeerbare xerostomie of xeroftalmie. Beschermende maatregelen, bijvoorbeeld glutamaat-antagonisten, koeling en fractionele dosering, zijn essentieel om toxiciteit te verminderen en de effectiviteit te optimaliseren.[91] Theoretisch lijkt ^{225}Ac-PSMA-617 veelbelovend voor de behandeling van AdCC, maar er zijn momenteel nog geen klinische studies uitgevoerd bij speekselkliertumoren. Voor nu heeft ^{177}Lu-PSMA-therapie bij speekselkliertumoren, en AdCC in het bijzonder, geen complete of langdurige respons opgeleverd, maar de palliatieve waarde blijkt uit toegenomen kwaliteit van leven door symptoomverlichting en beperkte ziektestabilisatie in de laatste levensfase. Bij uitgeputte behandelmogelijkheden wordt een ^{68}Ga-PSMA PET/CT aanbevolen om de geschiktheid voor ^{177}Lu-PSMA-therapie te beoordelen.

SLOTCONCLUSIE

Dit proefschrift bevordert de diagnostiek, prognostiek en behandeling van AdCC door het exploreren van biomarkers, PSMA-gerichte beeldvorming en gerichte radionuclidentherapie. MYB IHC optimaliseert de diagnostische nauwkeurigheid als een snelle, toegankelijke methode om *MYB::NFIB*-fusies te detecteren. CXCR4 dient als prognostische marker om patiënten met een hoger recidiefrisico te identificeren. Consistente PSMA-expressie in primair, recidiverend en gemetastaseerd AdCC maakt zowel nauwkeurige visualisatie met ^{68}Ga-PSMA PET/CT als gerichte ^{177}Lu-PSMA-therapie mogelijk. PSMA PET/CT levert essentiële referentiegegevens voor de stadiëring van AdCC en wellicht andere speekselkliertumoren, en toont betere detectie van recidieven en metastasen in vergelijking met FDG PET/CT. De implementatie van ^{177}Lu-PSMA-therapie bevestigt de haalbaarheid van deze theranostische aanpak in gevorderd AdCC, met symptoomverlichting en ziektecontrole als resultaat en biedt hoop voor patiënten zonder alternatieve behandelopties. Concluderend introduceert dit proefschrift een nieuw paradigma in biomarker-gestuurde benaderingen voor AdCC, dat een belangrijke stap vormt richting meer gepersonaliseerde zorg. Het legt de basis voor toekomstige innovaties in diagnostiek en behandeling, en daarmee voor verbetering van zowel de ziekte-uitkomst als de kwaliteit van leven van patiënten met deze zeldzame en moeilijk te behandelen maligniteit.

REFERENTIES

1. Coca-Pelaz A, Rodrigo JP, Bradley PJ, et al. Adenoid cystic carcinoma of the head and neck - An update. Oral Oncol. 2015;51(7):652-661.
2. Jang S, Patel PN, Kimple RJ, McCulloch TM. Clinical Outcomes and Prognostic Factors of Adenoid Cystic Carcinoma of the Head and Neck. Anticancer Res. 2017;37(6):3045-3052.
3. Spiro RH, Huvos AG, Strong EW. Adenoid cystic carcinoma of salivary origin. A clinicopathologic study of 242 cases. Am J Surg. 1974;128(4):512-520.
4. Bjørndal K, Krogdahl A, Therkildsen MH, et al. Salivary gland carcinoma in Denmark 1990-2005: A national study of incidence, site and histology. Results of the Danish Head and Neck Cancer Group (DAHANCA). Oral Oncol. 2011;47(7):677-682.
5. Hellquist H, Skalova A. Adenoid Cystic Carcinoma. In: Histopathology of the Salivary Glands. Springer Berlin Heidelberg; 2014:221-260.
6. West RB, Kong C, Clarke N, et al. MYB expression and translocation in adenoid cystic carcinomas and other salivary gland tumors with clinicopathologic correlation. Am J Surg Pathol. 2011;35(1):92-99.
7. Perzin KH, Gullane P, Clairmont AC. Adenoid cystic carcinomas arising in salivary glands: a correlation of histologic features and clinical course. Cancer. 1978;42(1):265-282.
8. Huang M, Ma D, Sun K, Yu G, Guo C, Gao F. Factors influencing survival rate in adenoid cystic carcinoma of the salivary glands. Int J Oral Maxillofac Surg. 1997;26(6):435-439.
9. Van Weert S, Bloemena E, Van Der Waal I, et al. Adenoid cystic carcinoma of the head and neck: a single-center analysis of 105 consecutive cases over a 30-year period. Oral Oncol. 2013;49(8):824-829.
10. Freling N, Crippa F, Maroldi R. Staging and follow-up of high-grade malignant salivary gland tumours: The role of traditional versus functional imaging approaches - A review. Oral Oncol. 2016;60:157-166.
11. Jung JH, Lee SW, Son SH, et al. Clinical impact of (18) F-FDG positron emission tomography/CT on adenoid cystic carcinoma of the head and neck. Head Neck. 2017;39(3):447-455.
12. Alfieri S, Granata R, Bergamini C, et al. Systemic therapy in metastatic salivary gland carcinomas: A pathology-driven paradigm? Oral Oncol. 2017;66:58-63.
13. Laurie SA, Ho AL, Fury MG, Sherman E, Pfister DG. Systemic therapy in the management of metastatic or locally recurrent adenoid cystic carcinoma of the salivary glands: a systematic review. Lancet Oncol. 2011;12(8):815-824.
14. Locati LD, Perrone F, Losa M, et al. Treatment relevant target immunophenotyping of 139 salivary gland carcinomas (SGCs). Oral Oncol. 2009;45(11):986-990.
15. Persson M, Andersson MK, Mitani Y, et al. Rearrangements, Expression, and Clinical Significance of MYB and MYBL1 in Adenoid Cystic Carcinoma: A Multi-Institutional Study. Cancers (Basel). 2022;14(15):3691.
16. Mitani Y, Li J, Rao PH, et al. Comprehensive analysis of the MYB-NFIB gene fusion in salivary adenoid cystic carcinoma: Incidence, variability, and clinicopathologic significance. Clin Cancer Res. 2010;16(19):4722-4731.
17. Rettig EM, Tan M, Ling S, et al. MYB rearrangement and clinicopathologic characteristics in head and neck adenoid cystic carcinoma. Laryngoscope. 2015;125(9):E292-E299.
18. Jacobs TW, Gown AM, Yaziji H, Barnes MJ, Schnitt SJ. Comparison of fluorescence in situ hybridization and immunohistochemistry for the evaluation of HER-2/neu in breast cancer. J Clin Oncol. 1999;17(7):1974-1982.

19. Xu B, Drill E, Ho AAAAA, et al. Predictors of Outcome in Adenoid Cystic Carcinoma of Salivary Glands: A Clinicopathologic Study With Correlation Between MYB Fusion and Protein Expression. Am J Surg Pathol. 2017;41(10):1422-1432.
20. S.L. VH, A. F, M. P, et al. Adenoid cystic carcinoma of the lacrimal gland: MYB gene activation, genomic imbalances, and clinical characteristics. Ophthalmology. 2013;120(10):2130-2138.
21. Brill LB, Kanner WA, Fehr A, et al. Analysis of MYB expression and MYB-NFIB gene fusions in adenoid cystic carcinoma and other salivary neoplasms. Mod Pathol. 2011;24(9):1169-1176.
22. Andersson MK, Afshari MK, Andren Y, et al. Targeting the Oncogenic Transcriptional Regulator MYB in Adenoid Cystic Carcinoma by Inhibition of IGF1R/AKT Signaling. J Natl Cancer Inst. 2017;109(9).
23. Zlotnik A, Yoshie O. The Chemokine Superfamily Revisited. Immunity. 2012;36(5):705-712.
24. Wang Z, Sun J, Feng Y, Tian X, Wang B, Zhou Y. Oncogenic roles and drug target of CXCR4/CXCL12 axis in lung cancer and cancer stem cell. Tumour Biol. 2016;37(7):8515-8528.
25. Zushi Y, Noguchi K, Hashitani S, et al. Relations among expression of CXCR4, histological patterns, and metastatic potential in adenoid cystic carcinoma of the head and neck. Int J Oncol. 2008;33(6):1133-1139.
26. Domanska UM, Kruizinga RC, Nagengast WB, et al. A review on CXCR4/CXCL12 axis in oncology: No place to hide. Eur J Cancer. 2013;49(1):219-230.
27. Vandercappellen J, Van Damme J, Struyf S. The role of CXC chemokines and their receptors in cancer. Cancer Lett. 2008;267(2):226-244.
28. Chatterjee S, Behnam Azad B, Nimmagadda S. The intricate role of CXCR4 in cancer. Adv Cancer Res. 2014;124:31-82.
29. Muller A, Sonkoly E, Eulert C, et al. Chemokine receptors in head and neck cancer: Association with metastatic spread and regulation during chemotherapy. Int J Cancer. 2006;118(9):2147-2157.
30. Gourni E, Demmer O, Schottelius M, et al. PET of CXCR4 Expression by a 68Ga-Labeled Highly Specific Targeted Contrast Agent. J Nucl Med. 2011;52(11):1803-1810.
31. Schottelius M, Osl T, Poschenrieder A, et al. [177Lu]pentixather: Comprehensive preclinical characterization of a first CXCR4-directed endoradiotherapeutic agent. Theranostics. 2017;7(9):2350-2362.
32. Phattarataratip E, Dhanuthai K. Expression of C-X-C motif chemokine receptors 4 and 7 in salivary gland neoplasms. Arch Oral Biol. 2017;83:136-144.
33. Zhang CY, Xia RH, Han J, et al. Adenoid cystic carcinoma of the head and neck: Clinicopathologic analysis of 218 cases in a Chinese population. Oral Surg Oral Med Oral Pathol Oral Radiol. 2013;115(3):368-375.
34. Coniglio SJ. Role of tumor-derived chemokines in osteolytic bone metastasis. Front Endocrinol (Lausanne). 2018;9:313.
35. Horoszewicz JS, Kawinsky E MG. Monoclonal antibodies to a new antigenic marker in epithelial prostatic cells and serum of prostatic cancer patients. Anticancer Res. 1987;7(5B):927-935.
36. Lopes AD, Davis WL, Rosenstraus MJ, Uveges AJ, Gilman SC. Immunohistochemical and Pharmacokinetic Characterization of the Site-specific Immunoconjugate CYT-356 Derived from Antiprostate Monoclonal Antibody 7E11-C5. Cancer Res. 1990;50(19):6423-6429.
37. Israeli RS, Powell CT, Fair WR, Heston WD. Molecular cloning of a complementary DNA encoding a prostate-specific membrane antigen. Cancer Res. 1993;53(2):227-230.
38. Wright GL, Haley C, Beckett M Lou, Schellhammer PF. Expression of prostate-specific membrane antigen in normal, benign, and malignant prostate tissues. Urol Oncol Semin Orig Investig. 1995;1(1):18-28.

39. Afshar-Oromieh A, Hetzheim H, Kratochwil C, et al. The novel theranostic PSMA-ligand PSMA-617 in the diagnosis of prostate cancer by PET/CT: biodistribution in humans, radiation dosimetry and first evaluation of tumor lesions. J Nucl Med. 2015;56(11):1697-1705.
40. Hofman MS, Violet J, Hicks RJ, et al. [177Lu]-PSMA-617 radionuclide treatment in patients with metastatic castration-resistant prostate cancer (LuPSMA trial): a single-centre, single-arm, phase 2 study. Lancet Oncol. 2018;19(6):825-833.
41. Madu CO, Lu Y. Novel diagnostic biomarkers for prostate cancer. J Cancer. 2010;1:150-177.
42. Ristau BT, O'Keefe DS, Bacich DJ. The prostate-specific membrane antigen: Lessons and current clinical implications from 20 years of research. Urol Oncol Semin Orig Investig. 2014;32(3):272-279.
43. Ross JS, Sheehan CE, Fisher H a G, et al. Correlation of primary tumor prostate-specific membrane antigen expression with disease recurrence in prostate cancer. Clin Cancer Res. 2003;9(17):6357-6362.
44. Chang SS, Reuter VE, Heston WDW, Bander NH, Grauer LS, Gaudin PB. Five Different Anti-Prostate-specific Membrane Antigen (PSMA) Antibodies Confirm PSMA Expression in Tumor-associated Neovasculature. Cancer Res. 1999;59(13):3192-3198.
45. Silver DA, Pellicer I, Fair WR, Heston WD, Cordon-Cardo C. Prostate-specific membrane antigen expression in normal and malignant human tissues. Am Assoc Cancer Res. 1997;3(1):81-85.
46. Mease RC, Foss CA, Pomper MG. PET imaging in prostate cancer: focus on prostate-specific membrane antigen. Curr Top Med Chem. 2013;13(8):951-962.
47. Troyer JK, Beckett ML, Wright GL. Detection and characterization of the prostate-specific membrane antigen (PSMA) in tissue extracts and body fluids. Int J Cancer. 1995;62(5):552-558.
48. Wolf P, Freudenberg N, Bühler P, et al. Three conformational antibodies specific for different PSMA epitopes are promising diagnostic and therapeutic tools for prostate cancer. Prostate. 2010;70(5):562-569.
49. Levesque M, Hu H, D'Costa M, Diamandis EP. Prostate-specific antigen expression by various tumors. J Clin Lab Anal. 1995;9(2):123-128.
50. Chang SS. Overview of prostate-specific membrane antigen. Rev Urol. 2004;6(Suppl 10):S13-S18.
51. Lütje S, Sauerwein W, Lauenstein T, Bockisch A, Poeppel TD. In Vivo Visualization of Prostate-Specific Membrane Antigen in Adenoid Cystic Carcinoma of the Salivary Gland. Clin Nucl Med. 2016;41(6):476-477.
52. de Keizer B, Krijger GC, Ververs FT, van Es RJJ, de Bree R, Willems S. 68Ga-PSMA PET-CT Imaging of Metastatic Adenoid Cystic Carcinoma. Nucl Med Mol Imaging. 2017;51(4):360-361.
53. Nishida H, Kondo Y, Kusaba T, Kadowaki H, Daa T. Immunohistochemical Reactivity of Prostate-Specific Membrane Antigen in Salivary Gland Tumors. Head Neck Pathol. 2021;16(2):427.
54. Backhaus P, Noto B, Avramovic N, et al. Targeting PSMA by radioligands in non-prostate disease—current status and future perspectives. Eur J Nucl Med Mol Imaging. 2018;45(5):860-877.
55. Salas Fragomeni RA, Amir T, Sheikhbahaei S, et al. Imaging of Non-Prostate Cancers Using PSMA-Targeted Radiotracers: Rationale, Current State of the Field, and a Call to Arms. J Nucl Med. 2018;59(6):871-877.

56. Mhawech-Fauceglia P, Smiraglia DJ, Bshara W, et al. Prostate-specific membrane antigen expression is a potential prognostic marker in endometrial adenocarcinoma. Cancer Epidemiol Biomarkers Prev. 2008;17(3):571-577.
57. Rothman KJ. No adjustments are needed for multiple comparisons. Epidemiology. 1990;1(1):43-46.
58. Bailey B, Calhoun K. Head and Neck Surgery Otolaryngology, Vol 1. 3rd ed. Lippincot Williams&Wilkins.; 2001.
59. Hand AR, Pathmanathan D, Field RB. Morphological features of the minor salivary glands. Arch Oral Biol. 1999;44(Suppl 1):S3-S10.
60. Afzelius P, Nielsen MY, Ewertsen C, Bloch KP. Imaging of the major salivary glands. Clin Physiol Funct Imaging. 2016;36(1):1-10.
61. Wang X dong, Meng L jiao, Hou T ting, Zheng C, Huang S hui. Frequency and Distribution Pattern of Minor Salivary Gland Tumors in a Northeastern Chinese Population: A Retrospective Study of 485 Patients. J Oral Maxillofac Surg. 2015;73(1):81-91.
62. Lütje S, Heskamp S, Cornelissen AS, et al. PSMA Ligands for Radionuclide Imaging and Therapy of Prostate Cancer: Clinical Status. Theranostics. 2015;5(12):1388-1401.
63. Has Simsek D, Kuyumcu S, Agaoglu FY, Unal SN. Radionuclide Therapy With 177Lu-PSMA in a Case of Metastatic Adenoid Cystic Carcinoma of the Parotid. Clin Nucl Med. 2019;44(9):764-766.
64. Rahbar K, Ahmadzadehfar H, Kratochwil C, et al. German multicenter study investigating 177Lu-PSMA-617 radioligand therapy in advanced prostate cancer patients. J Nucl Med. 2017;85(1):85-90.
65. La'Porte SJ, Juttla JK, Lingam RK. Imaging the Floor of the Mouth and the Sublingual Space. Radiographics. 2011;31(5):1215-1230.
66. Różycki R. Diagnostic imaging of the nasolacrimal drainage system. Part I. Radiological anatomy of lacrimal pathways. Physiology of tear secretion and tear outflow. Med Sci Monit. 2014;20:628-638.
67. Kinahan PE, Fletcher JW. Positron emission tomography-computed tomography standardized uptake values in clinical practice and assessing response to therapy. Semin Ultrasound, CT MRI. 2010;31(6):496-505.
68. Almståhl A, Alstad T, Fagerberg-Mohlin B, Carlén A FC. Explorative study on quality of life in relation to salivary secretion rate in patients with head and neck cancer treated with radiotherapy. Head Neck. 2016;38(5):782-791.
69. Gensheimer MF, Liao JJ, Garden AS, et al. Submandibular gland-sparing radiation therapy for locally advanced oropharyngeal squamous cell carcinoma: patterns of failure and xerostomia outcomes. Radiat Oncol. 2014;9(1):255.
70. Ekmekcioglu Ö, Busstra M, Klass ND, Verzijlbergen F. Bridging the Imaging Gap: PSMA PET/CT Has a High Impact on Treatment Planning in Prostate Cancer Patients with Biochemical Recurrence—A Narrative Review of the Literature. J Nucl Med. 2019;60(10):1394-1398.
71. Jang JY, Pak KJ, Yi KI, et al. Differential Prognostic Value of Metabolic Heterogeneity of Primary Tumor and Metastatic Lymph Nodes in Patients with Pharyngeal Cancer. Anticancer Res. 2017;37(10):5899-5905.
72. Chan SC, Cheng NM, Hsieh CH, et al. Multiparametric imaging using (18)F-FDG PET/CT heterogeneity parameters and functional MRI techniques: prognostic significance in patients with primary advanced oropharyngeal or hypopharyngeal squamous cell carcinoma treated with chemoradiotherapy. Oncotarget. 2017;8(37):62606-62621.

73. Civan C, Kasper S, Berliner C, et al. PSMA-Directed Imaging and Therapy of Salivary Gland Tumors: A Single-Center Retrospective Study. J Nucl Med. 2023;64(3):372-378.
74. Lonneux M, Hamoir M, Reychler H, et al. Positron emission tomography with [18F] fluorodeoxyglucose improves staging and patient management in patients with head and neck squamous cell carcinoma: a multicenter prospective study. J Clin Oncol. 2010;28(7):1190-1195.
75. Shamim SA, Kumar N, Arora G, et al. Comparison of 68Ga-PSMA-HBED-CC and 18F-FDG PET/CT in the Evaluation of Adenoid Cystic Carcinoma-A Prospective Study. Clin Nucl Med. 2023;48(11):E509-E515.
76. Wang X, Zhang X, Zhang X, et al. Design, preclinical evaluation, and first-in-human PET study of [68Ga]Ga-PSFA-01: a PSMA/FAP heterobivalent tracer. Eur J Nucl Med Mol Imaging. 2025;52(3):1166-1176.
77. Hotta M, Nguyen K, Thin P, et al. Kinetics and patterns of PSMA PET uptake after radiation therapy for prostate cancer: a single center retrospective study. J Nucl Med. 2022;63(Suppl 2):3041.
78. Onal C, Guler OC, Torun N, et al. Impact of definitive radiotherapy on metabolic response measured with 68Ga-PSMA-PET/CT in patients with intermediate-risk prostate cancer. Prostate. 2024;84(15):1366-1374.
79. De Galiza Barbosa F, Queiroz MA, Nunes RF, et al. Nonprostatic diseases on PSMA PET imaging: A spectrum of benign and malignant findings. Cancer Imaging. 2020;20(1):1-23.
80. Avcu A, Oksuzoglu K, Kissa TN, et al. AB0833 THE USE OF F-18 FDG PET/CT AND Ga-68 PSMA PET/CT IN THE EVALUATION OF SALIVARY GLANDS IN SJÖGREN'S SYNDROME. Ann Rheum Dis. 2024;83(Suppl 1):1713-1714.
81. Röhrich M, Syed M, Liew DP, et al. 68Ga-FAPI-PET/CT improves diagnostic staging and radiotherapy planning of adenoid cystic carcinomas – Imaging analysis and histological validation. Radiother Oncol. 2021;160:192-201.
82. Rizzo A, Albano D, Elisei F, et al. The Potential Role of PSMA-Targeted PET in Salivary Gland Malignancies: An Updated Systematic Review. Diagnostics (Basel). 2024;14(14):1516.
83. Yu W, Zhao M, Deng Y, et al. Meta-analysis of 18 F-PSMA-1007 PET/CT, 18 F-FDG PET/CT, and 68Ga-PSMA PET/CT in diagnostic efficacy of prostate Cancer. Cancer Imaging. 2023;23(1):1-11.
84. Parlak Y, Mutevellzade G, Sezgln C, Goksoy D, Gumuser G, Saylt E. EFFECTIVE HALF-LIFE, EXCRETION AND RADIATION EXPOSURE OF 177LU-PSMA. Radiat Prot Dosimetry. 2023;199(10):1090-1095.
85. Sartor O, de Bono J, Chi K, et al. Lutetium-177-PSMA-617 for Metastatic Castration-Resistant Prostate Cancer. N Engl J Med. 2021;385(12)1091-1103.
86. Trautwein NF, Brendlin A, Reischl G, et al. PSMA-Guided Imaging and Therapy of Advanced Adenoid Cystic Carcinomas and Other Salivary Gland Carcinomas. Cancers (Basel). 2024;16(22):3843.
87. Yadav MP, Ballal S, Sahoo RK, Dwivedi SN, Bal C. Radioligand therapy with 177Lu-PSMA for metastatic castration-resistant prostate cancer: A systematic review and meta-analysis. Am J Roentgenol. 2019;213(2):275-285.
88. Afshar-Oromieh A, Avtzi E, Giesel FL, et al. The diagnostic value of PET/CT imaging with the 68Ga-labelled PSMA ligand HBED-CC in the diagnosis of recurrent prostate cancer. Eur J Nucl Med Mol Imaging. 2015;42(2):197-209.

89. Kratochwil C, Bruchertseifer F, Rathke H, et al. Targeted Alpha Therapy of mCRPC with (225)Actinium-PSMA-617: Dosimetry estimate and empirical dose finding. J Nucl Med. 2017;58(10):1624-1631.
90. Belli ML, Sarnelli A, Mezzenga E, et al. Targeted Alpha Therapy in mCRPC (Metastatic Castration-Resistant Prostate Cancer) Patients: Predictive Dosimetry and Toxicity Modeling of 225Ac-PSMA (Prostate-Specific Membrane Antigen). Front Oncol. 2020;10:531660.
91. Heynickx N, Segers C, Coolkens A, Baatout S, Vermeulen K. Characterization of Non-Specific Uptake and Retention Mechanisms of [177Lu]Lu-PSMA-617 in the Salivary Glands. Pharmaceuticals. 2023;16(5):692.

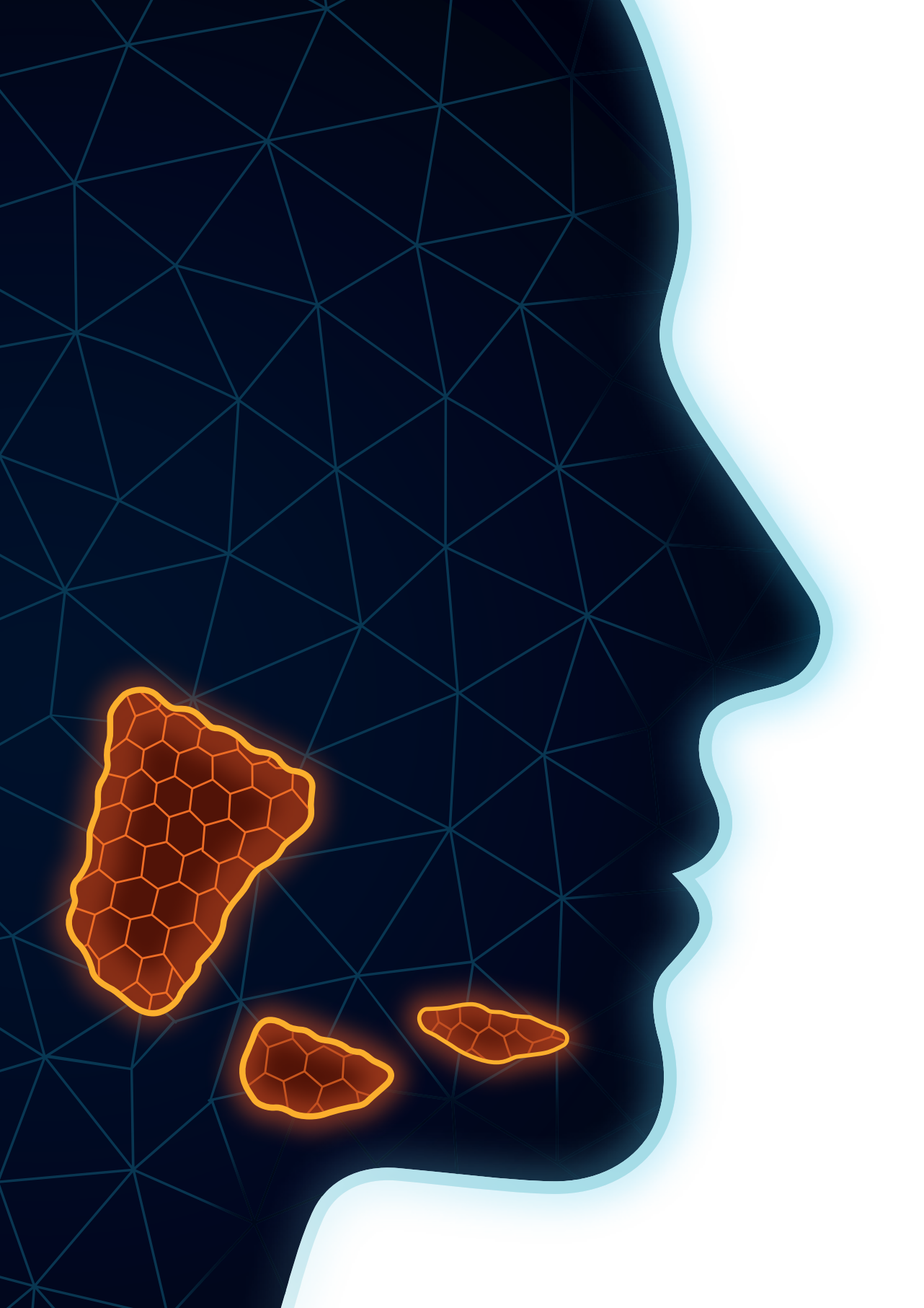

APPENDICES

List of publications

Dankwoord

About the author

LIST OF PUBLICATIONS

* included as chapter in this thesis

Surgical Complications for Oral Cavity Cancer: Evaluating Hospital Performance
HD van Oorschot, JA Hardillo, RJJ van Es, GB van den Broek, RP Takes, GB Halmos, DVC de Jel, R Dirven, M Lacko, LAA Vaassen, JJ Hendrickx, MAE Oomens, H Ghaeminia, JC Jansen, A Vesseur, R Bun, LQ Schwandt, CA Krabbe, TJW Klein Nulent, RJ Klijn, AJM van Bemmel, RJ Baatenburg de Jong.
Laryngoscope. 2025. Online ahead of print. doi: 10.1002/lary.32033.

*MYB immunohistochemistry as a predictor of *MYB::NFIB* fusion in the diagnosis of adenoid cystic carcinoma of the head and neck
TJW Klein Nulent, RJJ van Es, GE Breimer, MH Valstar, LA Smit, CM Speksnijder, R de Bree, SM Willems.
Oral Surg Oral Med Oral Pathol Oral Radiol. 2024;138(6):772-780. doi: 10.1016/j.oooo.2024.08.006.

Nationwide clinical practice variation for reconstructive surgery following oral cavity cancer from the Dutch Head and Neck Audit: are we all doing the same?
DVC de Jel, HD van Oorschot, PCA Meijer, LE Smeele, DA Young-Afat, HA Rakhorst; Dutch Head and Neck Audit group.
Br J Oral Maxillofac Surg. 2025;63(3):195-202. doi: 10.1016/j.bjoms.2024.10.232.

*First experiences with ^{177}Lu-PSMA-617 therapy for recurrent or metastatic salivary gland cancer
TJW Klein Nulent, RJJ van Es, SM Willems, AJAT Braat, LA Devriese, R de Bree, B de Keizer.
EJNMMI Res. 2021;11(1):126. doi: 10.1186/s13550-021-00866-8.

The tubarial glands paper: A starting point. A reply to comments
MH Valstar, BS de Bakker, RJHM Steenbakkers, KH de Jong, LA Smit, TJW Klein Nulent, RJJ van Es, I Hofland, B de Keizer, B Jasperse, AJM Balm, A van der Schaaf, JA Langendijk, LE Smeele, WV Vogel.
Radiother Oncol. 2021;154:308-311. doi: 10.1016/j.radonc.2020.12.001.

The tubarial salivary glands: A potential new organ at risk for radiotherapy
MH Valstar, BS de Bakker, RJHM Steenbakkers, KH de Jong, LA Smit, TJW Klein Nulent, RJJ van Es, I Hofland, B de Keizer, B Jasperse, AJM Balm, A van der Schaaf, JA Langendijk, LE Smeele, WV Vogel.
Radiother Oncol. 2021;154:292-298. doi: 10.1016/j.radonc.2020.09.034.

Assessment of tumour depth in early tongue cancer: Accuracy of MRI and intraoral ultrasound
R Noorlag, TJW Klein Nulent, VEJ Delwel, FA Pameijer, SM Willems, R de Bree, RJJ van Es.
Oral Oncol. 2020;110:104895. doi: 10.1016/j.oraloncology.2020.104895.

*High CXCR4 expression in adenoid cystic carcinoma of the head and neck is associated with increased risk of locoregional recurrence
TJW Klein Nulent, RJJ van Es, MH Valstar, LE Smeele, LA Smit, R Klein Gunnewiek, NPA Zuithoff, B de Keizer, R de Bree, SM Willems.
J Clin Pathol. 2020;73(8):476-482. doi: 10.1136/jclinpath-2019-206273.

*Prostate-specific membrane antigen (PSMA) expression in adenoid cystic carcinoma of the head and neck
TJW Klein Nulent, MH Valstar, LA Smit, LE Smeele, NPA Zuithoff, B de Keizer, R de Bree, RJJ van Es, SM Willems.
BMC Cancer. 2020;20(1):519. doi: 10.1186/s12885-020-06847-9.

*Physiologic distribution of PSMA-ligand in salivary glands and seromucous glands of the head and neck on PET/CT
TJW Klein Nulent, MH Valstar, B de Keizer, SM Willems, LA Smit, A Al-Mamgani, LE Smeele, RJJ van Es, R de Bree, WV Vogel.
Oral Surg Oral Med Oral Pathol Oral Radiol. 2018;125(5):478-486. doi: 10.1016/j.oooo.2018.01.011.

Intraoral ultrasonography to measure tumor thickness of oral cancer: A systematic review and meta-analysis
TJW Klein Nulent, R Noorlag, EM Van Cann, FA Pameijer, SM Willems, A Yesuratnam, AJWP Rosenberg, R de Bree, RJJ van Es.
Oral Oncol. 2018;77:29-36. doi: 10.1016/j.oraloncology.2017.12.007.

*Prostate-specific membrane antigen PET imaging and immunohistochemistry in adenoid cystic carcinoma – a preliminary analysis

TJW Klein Nulent, RJJ van Es, GC Krijger, R de Bree, SM Willems, B de Keizer.

Eur J Nucl Med Mol Imaging. 2017;44(10):1614-1621. doi: 10.1007/s00259-017-3737-x.

Cannabinoid receptor-2 immunoreactivity is associated with survival in squamous cell carcinoma of the head and neck

TJW Klein Nulent, PJ van Diest, P van der Groep, FKJ Leusink, CL Kruitwagen, R Koole, EM Van Cann.

Br J Oral Maxillofac Surg. 2013;51(7):604-609. doi: 10.1016/j.bjoms.2013.03.015.

DANKWOORD

Na een promotietraject van ongeveer tien jaar ben ik veel mensen dank verschuldigd. Deze reis had ik nooit alleen kunnen voltooien; de steun, inspiratie en samenwerking van velen hebben dit mogelijk gemaakt. Ik wil dan ook iedereen die hieraan heeft bijgedragen van harte bedanken.

ABOUT THE AUTHOR

Thomas Klein Nulent studied Medicine at Utrecht University. He developed an early interest in Oral and Maxillofacial Surgery during his medical training and began research in this field at the University Medical Center Utrecht (UMCU), which led to his first scientific publication.

After earning his medical degree in 2010, he worked as a surgical resident (not in training) and subsequently pursued a Dentistry degree at Radboud University Nijmegen, graduating in 2014.

In 2013, he started his specialist training in Maxillofacial Surgery at UMCU, where he combined clinical training with research in head and neck oncology.

His PhD research originated from a unique clinical case that evolved into a structured research project in collaboration with the departments of Head and Neck Surgical Oncology, Pathology and Radiology and Nuclear Medicine at UMCU.

After completing his specialist training in 2017, he undertook a clinical fellowship in Maxillofacial Head and Neck Oncology at UMCU from 2018 to 2020. He currently practises as a Maxillofacial Surgeon and Head and Neck Oncologist at Haaglanden Medical Centre in The Hague.